

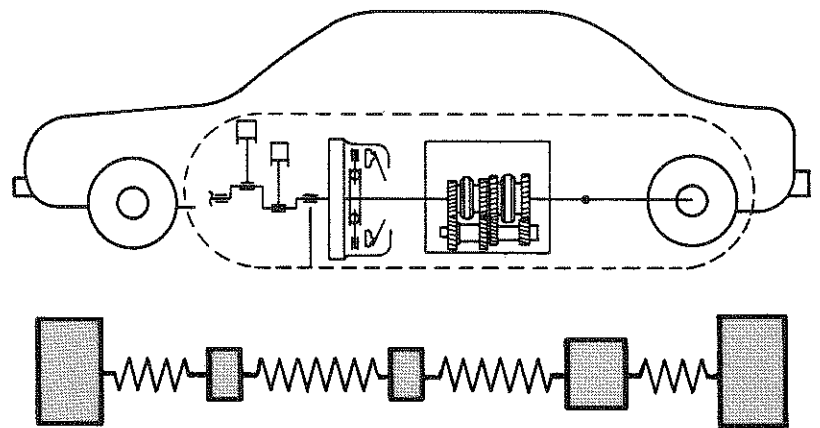


4th International Symposium  
Baden-Baden  
April 20, 1990



Torsional Vibrations in the Drive Train

# Torsional Vibrations in the Drive Train

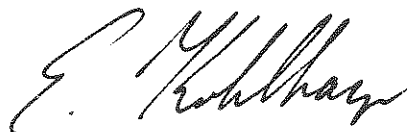


## Foreword

*The 4th LuK Clutch Symposium launches the celebration of LuK Bühl's 25th anniversary. The tradition of presenting professional symposia reflects an important segment of LuK history. It demonstrates the efforts of LuK engineers to expand their horizons beyond their day-to-day concerns by formulating general principles based on their knowledge, and ultimately gaining superior insight into their work.*

*This effort does not represent an end in itself. On the contrary, we are motivated by a desire to provide our partners in the automotive industry with the theoretical background from which they can draw practical, applicable daily solutions.*

*We are all pleased with the recognition that LuK has received for this effort from both science and industry. It is a necessary inspiration for our work in the future.*



*Dr.-Ing. Ernst H. Kohlhage*  
President

## Table of Contents

Torsional Vibrations in the Drive Train of Motor Vehicles	
Principle Considerations . . . . .	5 – 28
Torsional Vibrations in Tractor Drive Trains	
Damping Options . . . . .	29 – 54
Development of the Super-Long-Travel Dual Mass Flywheel	55 – 80
Torque Control Isolation	
The Smart Clutch . . . . .	81 – 107
Clutch Chatter . . . . .	109 – 124
Torsional Vibration Isolation in the Drive Train	
An Evaluative Study . . . . .	125 – 146

# **Torsional Vibrations in the Drive Train of Motor Vehicles Principle Considerations**

Dr.-Ing. **Wolfgang Reik**

Today more and more attention is being paid to torsional drive line vibrations. For one thing, modern automotive design is producing stronger excitation. Secondly, drive trains that have been optimized for weight and efficiency are highly sensitive to excitation. This situation results in a number of comfort problems. Gear rattle and boom, particularly in low speed ranges that are desirable for fuel efficiency, pose an annoying problem. Besides this, tip-in/back-out reactions can take all the fun out of driving. These low-frequency torsional vibrations are also known by the descriptive term "Bonanza" or bucking bronco effect.

Traditionally, torsional vibrations have been studied primarily from the standpoint of reducing noise and improving comfort. However, one must also bear in mind that this kind of drive train vibration, and resonance in particular, can generate loads that far exceed the maximum engine torque. Rapid tip-ins generate short-term loads that may equal up to twice the engine torque. In such cases, the clutch can even slip temporarily. Given current emphasis on drive train weight optimization and cost reduction, avoiding these torque peaks will certainly become more important in the future [1].

## **Excitation of Torsional Vibration in Motor Vehicle Drive Trains**

Many sources of excitation must be considered with respect to torsional vibrations. Figure 1 lists major causes, without claiming to be all-inclusive. The main source is engine irregularity resulting from the ignition cycle. This basic excitation in the motor vehicle drive train is the subject of almost all the following presentations. Irregular ignition or even misfiring can also lead to serious vibration problems, but these factors will not be treated in this series of presentations because they can usually be eliminated by optimizing ignition itself.

Driver-induced torque changes can generate the dreaded "Bonanza" effect.

ENGINE	IGNITION IRREGULAR IGNITION TORQUE CHANGE
CLUTCH	CHATTER
TORSION DAMPER	PERIODIC CHANGE IN DAMPING CHARACTERISTIC
TRANSMISSION	GEAR MESHING GEAR PITCH ERROR TORQUE SPIKES DUE TO SHIFTS
CRANKSHAFTS	BENDING ANGLE
TIRES	ROAD SURFACE CONDITION

**Figure 1:**

Sources of torsional vibration excitation in a motor vehicle drive train

A chattering clutch can also become an additional source of vibration. The physical principles affecting this phenomenon will be the subject of a separate presentation.

Axial displacement between the engine and the transmission input shaft can lead to additional radial loads that cause changes in the damping characteristic synchronous to the engine speed. This generates an associated excitation.

Gear meshing and gear pitch error in the transmission itself can also excite torsional vibrations [2]. In automatic transmissions, gear shifts can have an effect similar to a change in engine torque.

Drive shafts with bending angles can also be a source of excitation [3]. Irregular road surfaces are capable of exciting the drive train, as can tire slippage resulting from changes in friction coefficients between the tire and the road surface.

### **Engine Irregularity**

The main source of excitation for torsional vibrations is discrete engine ignition [4]. It is also the primary cause of low-speed gear rattle and boom. The following discussion deals with the basic principles involved in this phenomenon.

Torque at the crankshaft is a periodic function of time or – to use the terminology favored by the engine specialists – a function of the crankshaft angle. This torque curve is plotted as a function of time and is determined by the gas forces in the cylinder, by the geometry of the crank drive, and by the acceleration moments of the crank drive and its changing mass moments of inertia during one rotation [5, 6].

Significant mass forces only occur at higher speeds, at which point they can even become dominant. Because gear rattle and boom occur primarily at low engine speeds, inertial forces are negligible for these observations. This results in the very simple torque relation shown in Figure 2 below.

According to this equation, the time-dependent torque acting on the crankshaft is the product of the piston displacement, a geometry factor dependent on the angle of the crankshaft and the pressure curve of the cylinder. The graph shown at the bottom of Figure 2 illustrates this principle for one cylinder. In a four stroke engine, this curve is repeated twice per revolution.

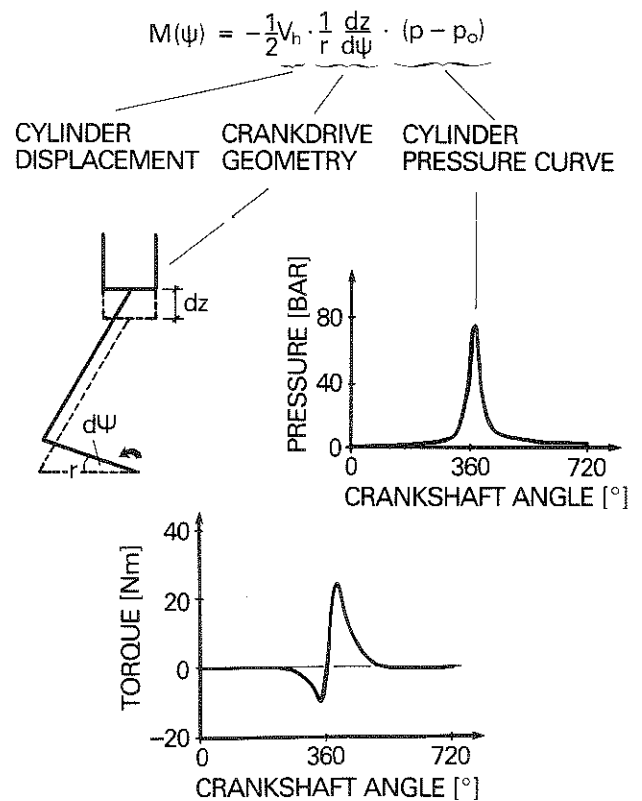


**Figure 2:**  
Engine excitation due to gas forces

For four, five, six or eight cylinder engines, the characteristic curve for each individual cylinder as shown in Figure 2 must be superimposed according to the appropriate phase angle in order to obtain the total engine characteristic. As an example, Figure 3 shows the torque curves for a four, a six and an eight cylinder engine, each with identical piston displacements.

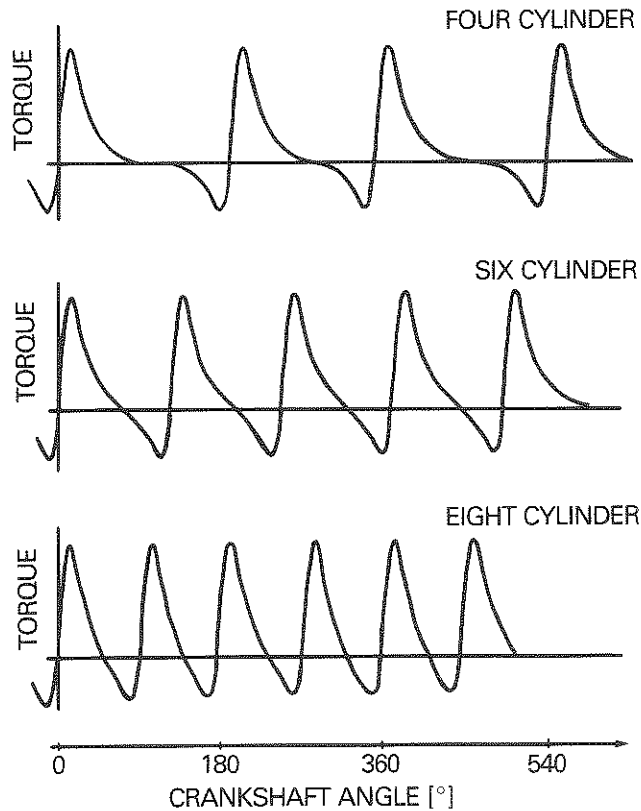


**Figure 3:**  
Crankshaft torque due to gas forces

Engines with higher numbers of cylinders have several advantages. Total cylinder displacement is distributed over several cylinders. This reduces piston displacement and the resulting excitation per cylinder accordingly. Furthermore, excitation occurs at a higher frequency. As we will demonstrate later, this simplifies torsion damper tuning.

Figure 2 showed that the torque curve is proportionate to piston displacement per cylinder. It follows then that Figure 4 shows the measured values for the positive and negative torque peaks plotted with respect to the piston displacement of one cylinder operating under full

load. The measurements were conducted in a speed range starting from about 1,500 rpm. Figure 4 includes data for both gasoline and diesel engines with four, six and eight cylinders. As one would expect from the equation shown in Figure 2, the measured values for full load actually do cluster around straight lines passing through the point of origin.

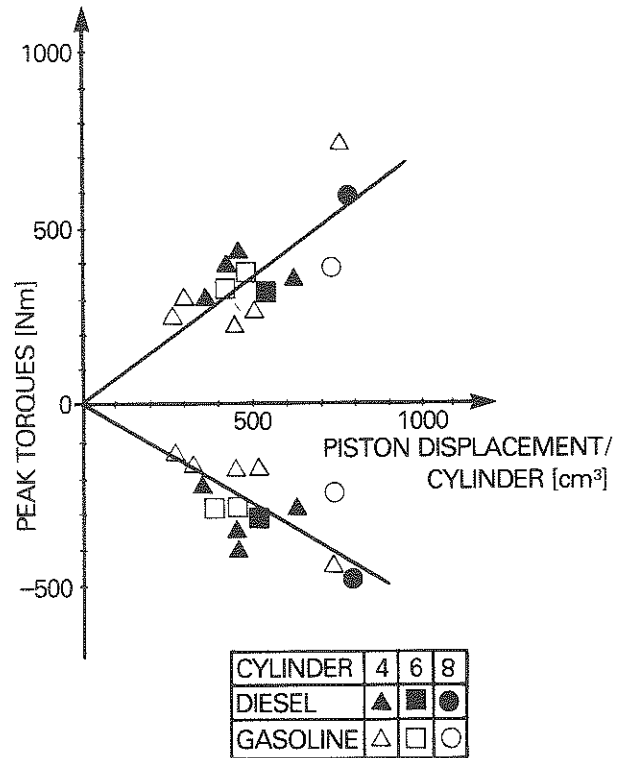


**Figure 4:**  
Peak crankshaft torques  
– full load –

Peak torque magnitude by itself does not reveal anything about engine irregularity. This value is determined based on the mass moment of inertia  $J_m$  of the crankshaft together with components such as the flywheel and the clutch, which are rigidly attached to it. The angular acceleration  $\dot{\omega}_m$  is determined using the equation:

$$M = J_m \cdot \dot{\omega}_m$$

This value exhibits an almost constant amplitude at the low speeds we are interested in. The curve for the angular velocity or the speed as a function of time can be plotted using integration:

$$\omega_m = \int \dot{\omega}_m dt$$



Given the information summarized in Figure 4, we can predict engine excitation under full load with a fair degree of accuracy. Moreover, it is possible to make comparisons between different engines and their degrees of irregularity.

However, in idle mode, the torques acting on the crankshaft do not present such a uniform picture (Figure 5).

Only the torque spikes for diesel engines are proportionate to the piston displacement of a cylinder. In the case of gasoline engines, they are much lower and they do not reveal any clearcut relationship.

Comparison of Figures 4 and 5 reveals that excitation torques under full load are similar for gasoline and diesel engines, while significant differences appear in idle mode.

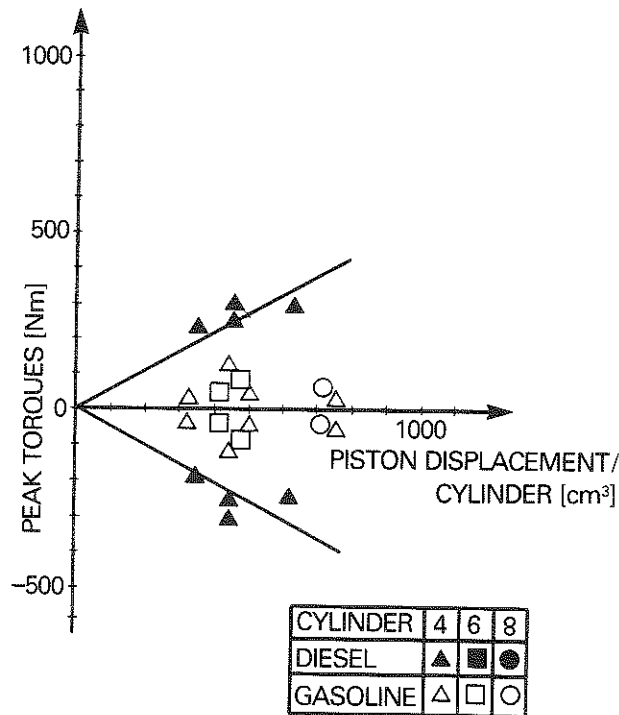


**Figure 5:**  
Peak crankshaft torques  
– idle mode –

## The Motor Vehicle Drive Train Viewed as a Torsional Vibration System

A motor vehicle drive train represents a torsional vibration system [7 – 10]. It can be roughly described as a chain of rotating inertias and torsion springs. Let us disregard the fact that the gear sets generate reaction forces on the transmission case, which is attached to the body via a more or less elastic suspension. Now we can even assume that we are dealing with a linear chain as shown in Figure 6. For purposes of clarity, we will try to get by with as few different rotating inertias and torsion springs as possible. Figure 6 illustrates the transition from a chain consisting of five rotating inertias (engine, transmission, differential, wheel and vehicle) to a chain having only three rotating inertias (engine, transmission and vehicle) [11].

This kind of simple model provides adequate information for many vibration problems. Of course, it is important to emphasize that it cannot be used to illustrate all drive train problems.

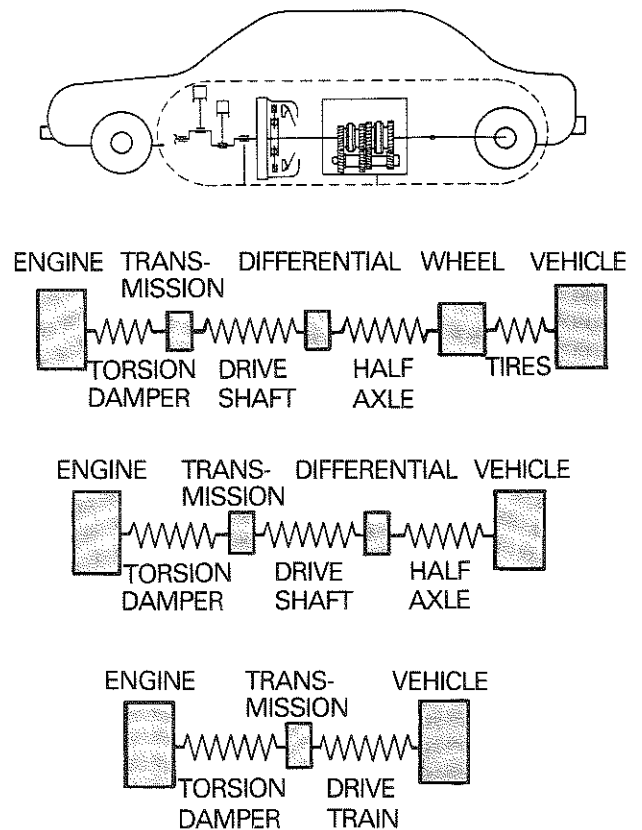


**Figure 6:**  
Analytical model for vehicle  
drive train vibrations

Anyone who has ever performed vibration calculations will welcome a simple model. It is extremely difficult to come by the necessary data for rotating inertias and spring rates and to represent the results in an easy, understandable form.

This kind of procedure always poses the danger of over simplification and associated significant errors or even false assertions. Consequently, the formulation of a model must always be accompanied by actually measuring torsional vibrations.

Figure 7 shows the possible vibration modes for a simple three-mass vibration system [12].

During the "surging" vibration mode, the engine vibrates essentially in opposition to the vehicle. The transmission is close to a vibration node and consequently only vibrates at a low amplitude. This vibration mode occurs in conjunction with vehicle surging, for instance during tip-in. Depending on the vehicle model and the selected gear, natural frequencies associated with surging range from 2 – 5 Hz, occasionally even higher.

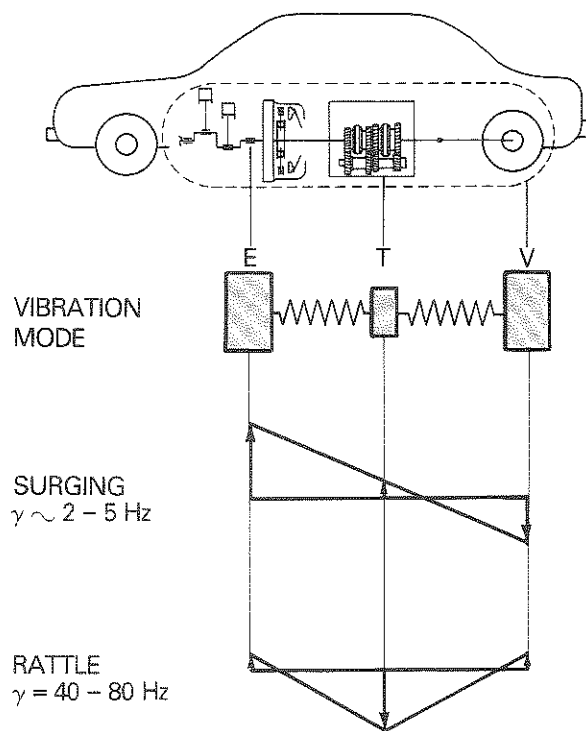


**Figure 7:**  
Vibration modes for a three-mass vibration system

In the case of "rattle," the transmission vibrates at high amplitudes. Natural frequencies of 40 – 80 Hz are typical. This vibration mode occurs in the case of gear rattle.

### Resonance Speed

Whenever engine irregularity excites the drive train vibration system, resonance can occur if the excitation frequency equals the natural frequency.

Figure 8 shows the resonance curve for a single inertia vibration system, with its typical resonance peak. Excitation frequencies are proportional to speed. Consequently, the graphing format shown in Figure 9, where excitation frequency is shown as a function of speed, is appropriate for our purposes. Because four cylinder engines feature two ignition cycles per revolution, they primarily excite vibrations of the 2nd order. This 2nd order vibration is represented in the heavy straight line passing through the origin.

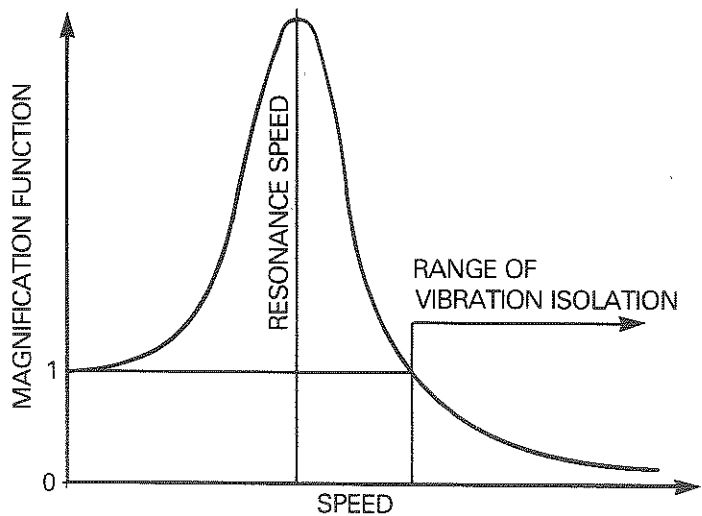


Figure 8 Resonance curve for simple oscillator

Because engine excitation is not sinusoidal, additional high frequency components must occur in the excitation, but their intensity generally decreases with increased frequency. High frequency components also exhibit a fixed ratio to the engine speed. The 4th and 6th order vibrations are plotted on the graph as well. In the event of irregular ignition, the 1st or 0.5th order can also occur. All these orders are represented by straight lines with different slopes.

Figure 9 also shows the natural frequencies for a passenger car for "rattle" and "surging" in gears 1 – 5. Of course, since the natural frequencies are not dependent on speed, they result in horizontal lines.

Resonance can – but does not have to – occur at each intersection point. The numerous possible resonance points provide a picture of complex drive train vibration behavior.

Rattle vibration is excited primarily by the 2nd and the 4th order. Associated resonance speeds typically occur in the range between about 700 and 2,000 rpm. The lower the selected gear, the higher these speeds. Surging vibration can actually only be excited by engine irregularity of the 0.5th order and then only in higher gears. Excitation in this vibration mode usually occurs as broad-band excitation resulting from a tip-in/back-out jerk.

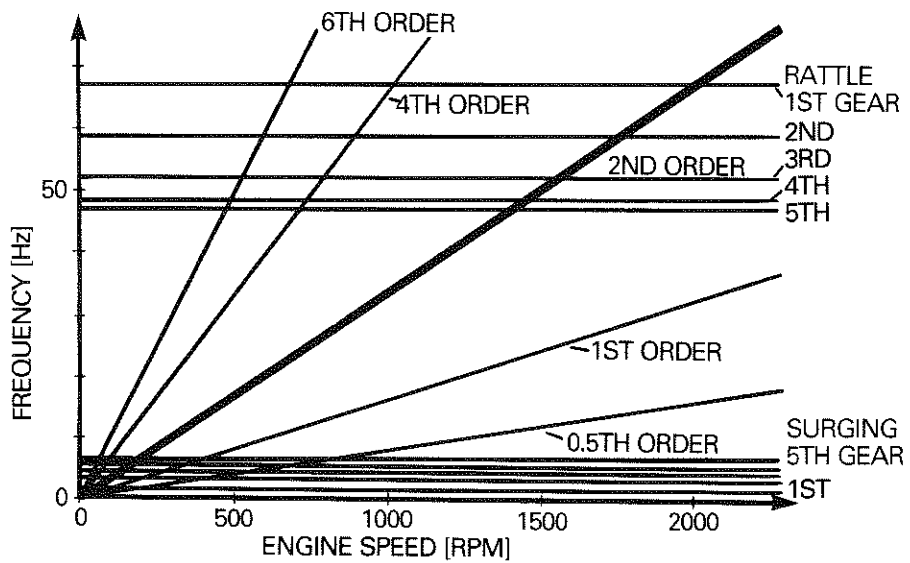


**Figure 9** Excitation frequencies as a function of engine speed for a four cylinder engine

## Isolation of Torsional Vibration

In theory, there are several options for modifying the vibration performance of a motor vehicle drive train in order to reduce undesirable torsional vibrations. Unfortunately, however, compelling engineering considerations prevent us from changing most of the components making up the drive train. Therefore, with the exception of the flywheel mass, it is hardly possible to change the mass moments of inertia involved in the system. Nor is it readily feasible to alter the spring rates (stiffness) of the tires, half axles and drive shafts. Consequently, as shown in Figure 10, the only actual option left to target for positive change is the connection between the engine and the transmission.

An appropriately damped, torsionally elastic coupling – in other words, a torsion damper – can be used to shift the resonance speeds, damp resonance amplitudes, and in some cases, even achieve genuine vibration isolation.

Generally speaking, gear rattle in drive, coast and idle modes requires different torsional elasticity and damping characteristics. Consequently, most torsion dampers include precisely tuned multi-stage characteristic curves, with each stage optimized individually for their respective load ranges (Figure 10).

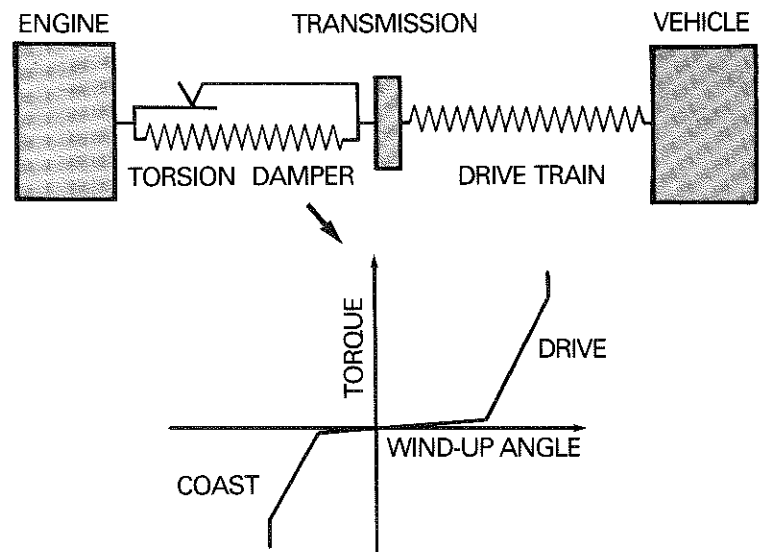


**Figure 10** Torsion damper characteristic curve in analytical model

Based on a calculated example, Figure 11 illustrates how vibration performance can be influenced by changing torsional spring rate and damping. The individual sections of the matrix graph each show the vibration amplitude of the engine and the transmission speed plotted as a function of the mean engine speed. Engine speed is plotted as a solid line, and transmission speed as a broken line. Each section was based on the calculation for a torsion damper with different frictional hysteresis and torsional spring rate. The torsional spring rate increases along the horizontal axis, and hysteresis increases on the vertical axis. The graph in the upper right-hand section reveals that at a torsional spring rate of  $20 \text{ Nm/}^\circ$  without frictional hysteresis, we encounter several high amplitude resonance points. At about 1,600 rpm there is a 2nd order resonance caused by the main engine excitation. The 4th order resonance occurs at about 800 rpm, which is attributable to the first engine harmonic. An additional 2nd order resonance occurs between these two values, but is associated with a different vibration form. Vibration isolation does not occur until we reach the speed range above natural frequency in the 2,000 rpm range.

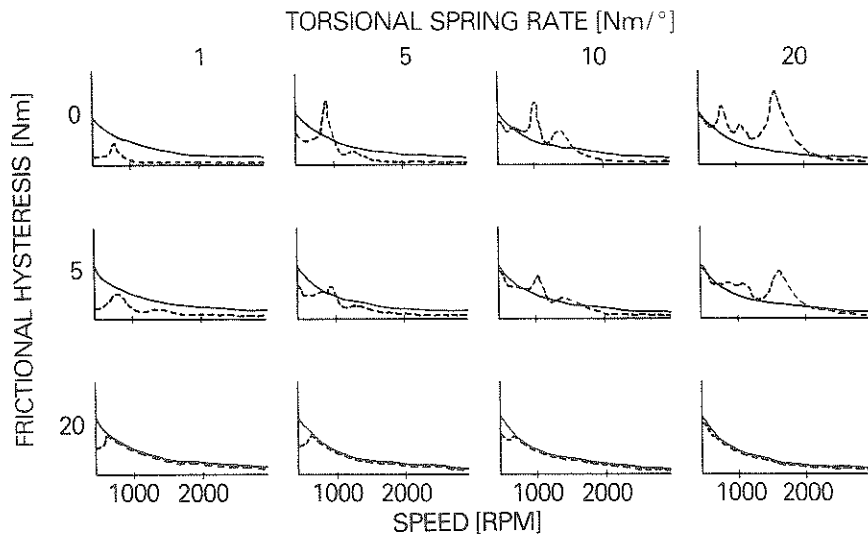


**Figure 11** Effect of torsional spring rate and frictional hysteresis on the resonance curve of a four-cylinder passenger car engine

If we reduce the torsional spring rate, we can shift the resonances to lower speeds and introduce the vibration isolation range sooner. At very low torsional spring rates of about  $1 \text{ Nm}/^\circ$ , the vibration amplitude also decreases significantly in the resonance range. With this design, the very flexible coupling hardly passes any vibrations at all through to the rest of the drive train. This would constitute the ideal torsion damper. Unfortunately, however, it is impossible to accommodate this kind of flat spring rate in the space available for installing the clutch.

Modern long-travel clutch disc designs such as those being developed at LuK can achieve about  $10 \text{ Nm}/^\circ$  in passenger car engines with moderate torque ratings. Consequently, we must reduce resonance amplitude by introducing carefully defined damping. And this is achieved at the cost of vibration isolation in the range above natural frequency (Figure 11, bottom). With high hysteresis values, the torsion damper exhibits increasingly rigid performance.

The matrix in Figure 11 clearly shows that it is impossible to achieve vibration isolation in drive mode over the entire speed range using an elastic coupling such as a conventional torsion damper. As a result, torsion damper tuning always represents a compromise. Low hysteresis results in high resonance amplitudes at low speeds and good vibration isolation at high speeds, whereas high hysteresis leads to rigid performance. If a satisfactory compromise proves impossible, other vibration damping procedures must be adopted, such as a dual mass flywheel, a torque control isolation system (TCI) or a hydrodynamic coupling.

### **Torsion Measurement System**

It has already been pointed out that modelling drive train vibration analysis poses the risk of incorrect projections. Sometimes systems are oversimplified when defining the analytical model, or mass moments of inertia, spring rates and damping factors do not accurately reflect the system. For instance, transmission damping factors cannot be determined directly at all, but have to be established by comparing vibration measurement with vibration calculations. The resulting damping factor must be varied in the calculations until the calculated results agree with measured results with respect to amplitude and phase. The damping value derived in this way is then introduced into the final calculation.

Therefore it is very important to measure torsional vibrations. Calculation and measurement go hand in hand and are mutually interdependent.



For this reason, LuK has for many years considered it essential to have access to appropriate modelling procedures and measurement capability as well. It is particularly important that measuring equipment be easy to use and produce quick results because tuning vehicles are generally only available for brief periods.

Because no appropriate measuring equipment was available off the shelf, LuK has worked together with AFT, a LuK affiliate, to develop a mobile torsional vibration measuring computer. This system uses simple sensors and very user-friendly software and provides immediate output of almost all important information needed for analysis of torsional vibration systems.

Figure 12 shows a block diagram of this measuring computer. The standard measurement is recorded using special magneto-resistive sensors that recognize rotational direction as well as vibration. These sensors provide digital measurement of the time elapsed between successive gear teeth on the flywheel and in the transmission. It is also possible to implement other measuring points, such as on the differential gear.

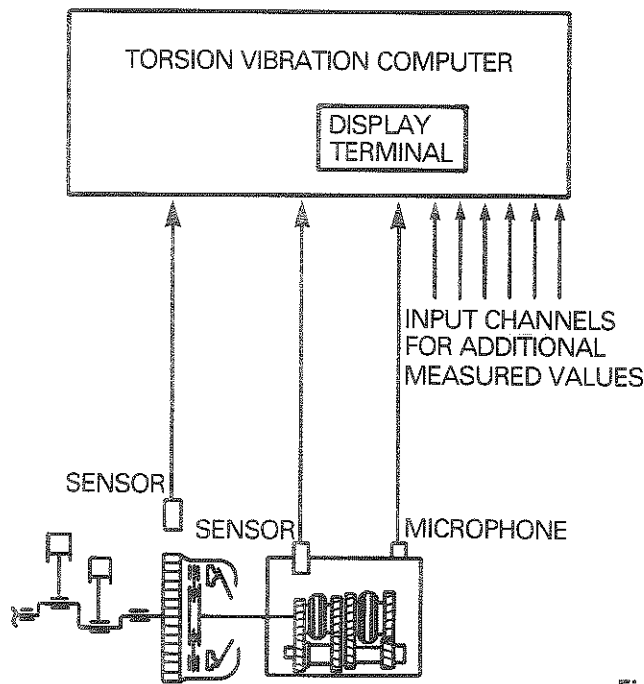


Figure 12 Measuring computer

A sensor measures structure-borne noise at an appropriate point on the transmission. A custom-designed electronic evaluation circuit provides high time resolution of structure-borne noise intensity.

Additional input channels can be used to gather data on temperatures, acceleration, throttle position, clutch travel, etc. High resolution, high scanning rate analog-digital converters are used for this purpose.

Measured values can be checked directly on the computer display in the vehicle. A 20 MB hard disk drive stores data for further evaluation.

After speed data has been collected in the vehicle, they are processed at a stationary work station. This routine produces the angular acceleration values that are critical for calculation purposes and calculates the engine and transmission vibration angles that are superimposed on the average speed.

LuK has developed an evaluation algorithm for determining the relative torsional angle between the engine and the transmission. This program provides precise data on torsion damper movement and function. Consequently, in most cases it is possible to get by without measuring drive train torque.

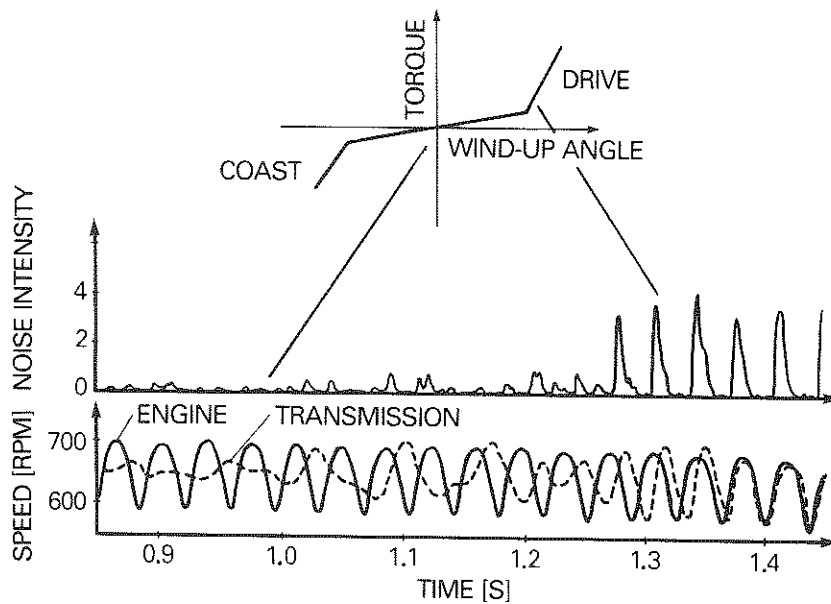
All measured and calculated curves can be displayed synchronous to noise intensity and the output from other AD channels.

The following examples illustrate the system's capability.

### **Sample Applications for the Torsion Measuring Computer**

Figure 13 shows a measurement made in idle mode.

At the beginning of the measurement interval, the torsion damper vibrates in the idle stage with good vibration isolation and no gear rattle. During measurement, the test driver pulls slightly on the gear shift lever in order to increase transmission drag torque. As a result, the torsion damper operating point migrates into the steep main stage. This eliminates the good vibration isolation and the transmission starts to rattle. As shown in the measured noise intensity curves, precisely one noise impulse is generated on the positive flank of the transmission speed curve for each engine excitation oscillation. In this case, the noise is generated while the input shaft accelerates after a slow-down phase. During this slow-down phase, the free-wheeling gears accelerate ahead of the input shaft.



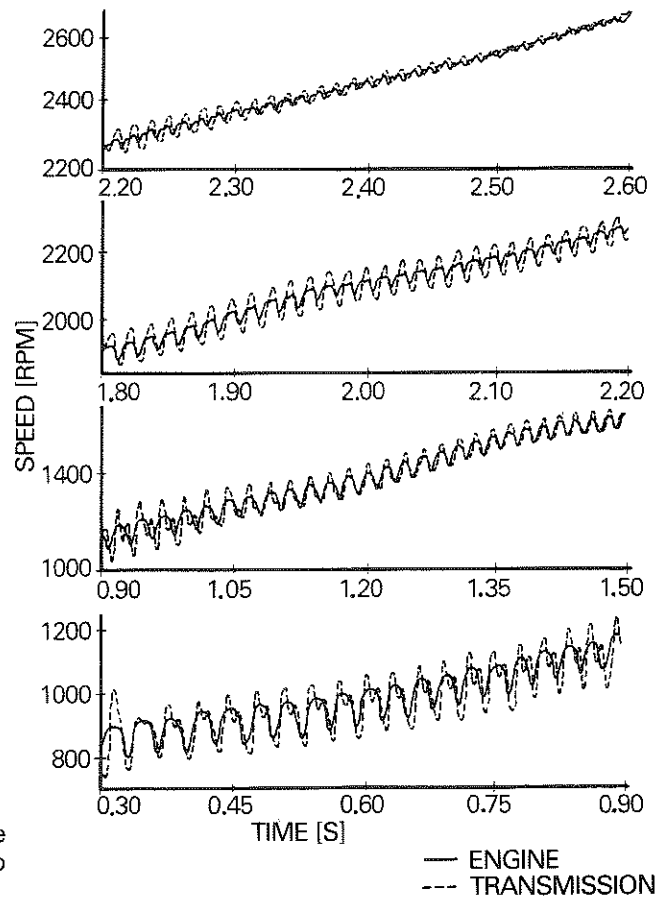
**Figure 13** Changes in vibration behavior during idle mode as a result of shift lever loading

Figure 14 shows a torsional vibration measurement in drive mode under full load for a four-cylinder gasoline engine.

The graph is divided into four sections, representing the speed range 850 to 2,500 rpm. First we can clearly see the 4th order resonance at 1,000 rpm, at which point the transmission input shaft vibrates at twice the basic combustion frequency. At about 2,000 rpm, the 2nd order is extremely evident. In the intermediate resonance range, peak vibrations are somewhat lower at the transmission input shaft. As has been confirmed in many tests, gear rattle increases as angular acceleration at the transmission input shaft increases. For this reason, both resonance points can also be recognized subjectively in the form of pronounced rattle.

Figure 15 shows a tip-in/back-out procedure in which torsion damper torsional rotation was plotted throughout the measuring cycle.

First the driver steps down abruptly on the gas pedal. He accelerates from about 1,200 rpm to 3,200 rpm, then lets up abruptly on the gas, and the coast phase begins (bottom of Figure 15).



**Figure 14:**  
Torsional vibrations in drive mode at speeds from 850 to 2600 rpm

At the beginning of the measurement cycle, the measuring computer sets the torsion angle equal to zero. Starting from this point, all changes in torsion damper position occurring during the measuring period are calculated. In the example shown in Figure 15, the torsion damper winds about  $7^\circ$  in the drive direction when the driver steps on the gas. During acceleration, it turns an additional  $3^\circ$  as speed and, with it, engine torque, increase. Once the acceleration process is completed, the torsion damper returns to its initial position after a few surge vibrations.

Changes in the torsion damper wind-up angle can be determined with an accuracy of about  $0.1^\circ$ . This procedure uses only the information generated by the two speed sensors and is therefore as simple as possible. Complex torque measurements are usually superfluous because the torsion damper wind-up angle is directly related to a torque.

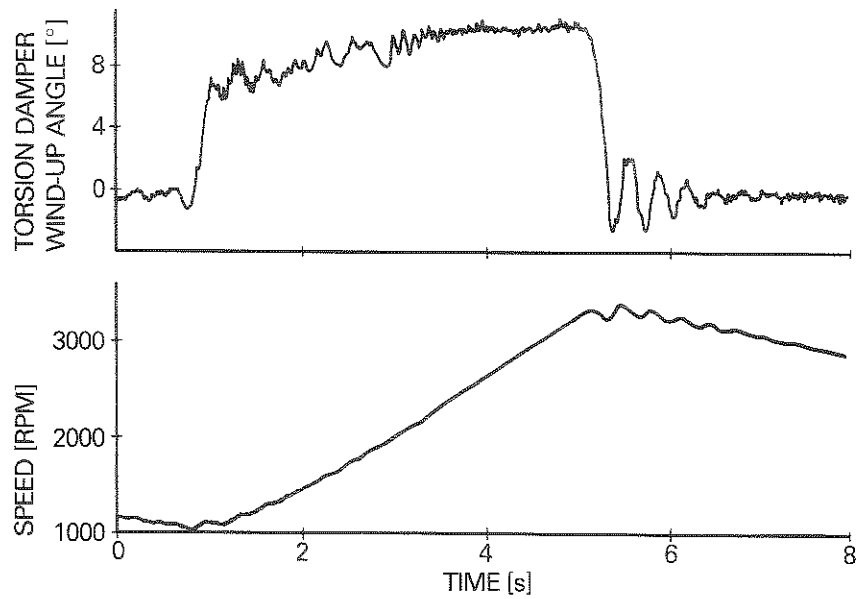


**Figure 15** Tip-in/back-out

### The Interaction between Measurement and Calculation during Tuning

Optimum torsion damper tuning requires mutual interaction of vibration measurement and calculation, as noted above. If we worked with only one of these procedures, the danger of incorrect interpretation would be too great. Measured data supports the vibration model selected. Without calculation, changes in the system parameters can never be systematically studied. Without this calculation procedure, we would probably have never been able to develop the dual mass flywheel.

The interaction between measurement and calculation during torsion damper tuning will be explained using the following examples:

A clutch disc with a well-functioning idle stage damper was installed in a passenger car. Figure 16 shows the schematic functional characteristic. However, as is frequently the case with idle-stage dampers, a short, annoying shut-off rattle occurs when the engine is shut off. LuK was supposed to improve shut-off performance without causing any deterioration in the idle stage.

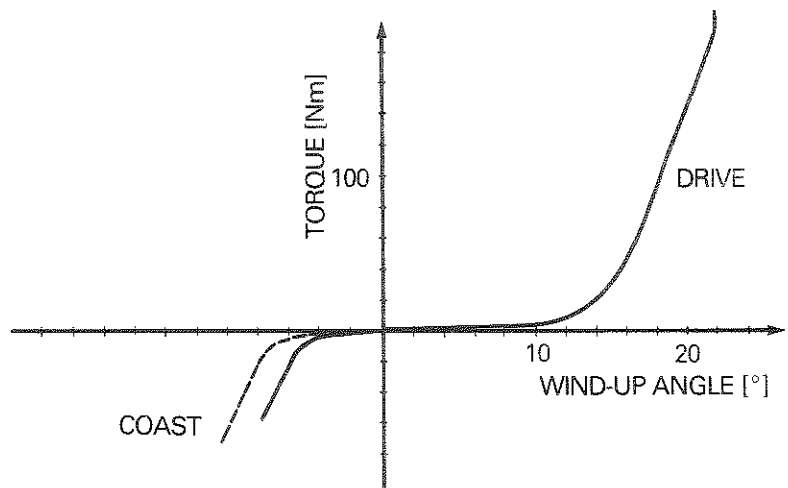


**Figure 16** Idle stage torsion damper characteristics

Initial measurement of torsional vibration behavior (Figure 17) resulted in a series of important findings. First of all, speed measurement (Graph Section C) exhibits excellent isolation at idle speed. In other words, the idle stage damper is functioning well. When the ignition is shut off, the engine decelerates at a constant rate. However, it does not stop abruptly at 0 speed, but instead continues to vibrate in the opposite direction. The measuring computer detects and displays this phenomenon. Based on the inertia of the engine, the flywheel and the clutch, we can assume a constant time-delay moment of -30 Nm, which is generated by internal engine friction.

The good vibration isolation in idle deteriorates below a speed of about 600 rpm and even turns into resonance. The transmission virtually vibrates simultaneously with the final engine vibrations. It is obvious to associate this resonance with the short transmission rattle. Noise measurement recorded in the top graph section substantiates this assumption.

It is interesting to note that strong noise peaks occur specifically when the transmission is subjected to particularly strong negative acceleration. The plotted graph (Section D) shows strong acceleration peaks in the transmission. Obviously the torsion damper is operating in the steep coast stage.

The torsion damper wind-up angle appears in Graph Section B. Vibrations of about  $16^\circ$  occur during the short resonance interval, passing through almost the entire predamper range.

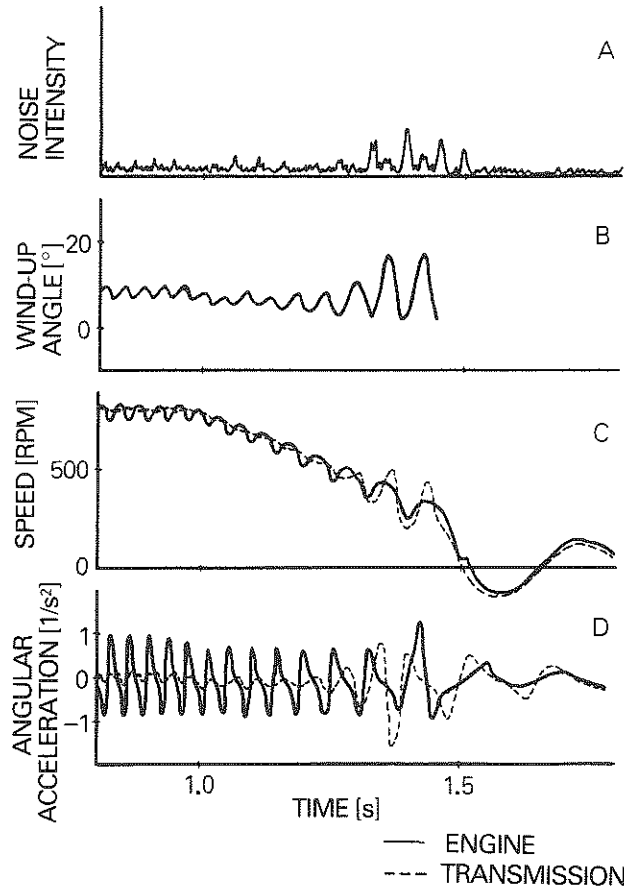


**Figure 17:**  
Measuring the shut-off procedure

We attempted a vibration simulation based on the analysis of the shut-off cycle. We consider that we have a good correlation if the amplitude and phase position of the calculation approximate the measured values, as can be seen below in Figure 18.

At this point we can conduct iterative computer calculations. And we already suspect what the problem is: the primary noise is associated with operation in the coast stage.

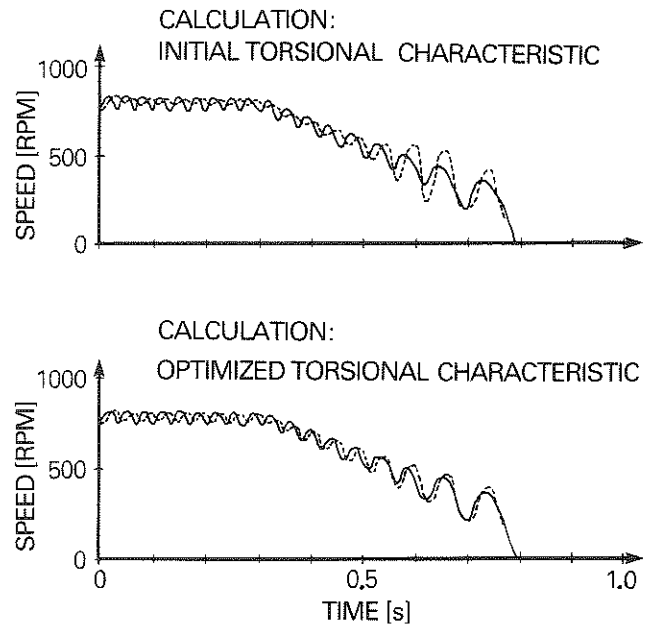


**Figure 18:** Engine shut-off calculation

— ENGINE  
 - - - TRANSMISSION

The bottom section of Figure 18 shows computer results with a reduced resonance amplitude. The coast stage – shown as a broken line in Figure 16 – is extended and an additional friction control plate added. The measured curve for this new characteristic actually shows a more favorable performance. In comparison, the top graph in Figure 19 again shows the speed curve from Figure 17. Subjective noise evaluation has improved by 3 rating points. The remaining rattle noise is no longer perceived as objectionable.

Success doesn't always come this quickly. The calculation process cannot predict what degree of vibration isolation is required in order to eliminate transmission noises. Rattle intensity depends to a great extent on the vehicle's tendency to transmit structure-borne noise, which cannot be predicted yet.

If results are unsatisfactory after the first round of tuning, vibration isolation has to be improved even further.



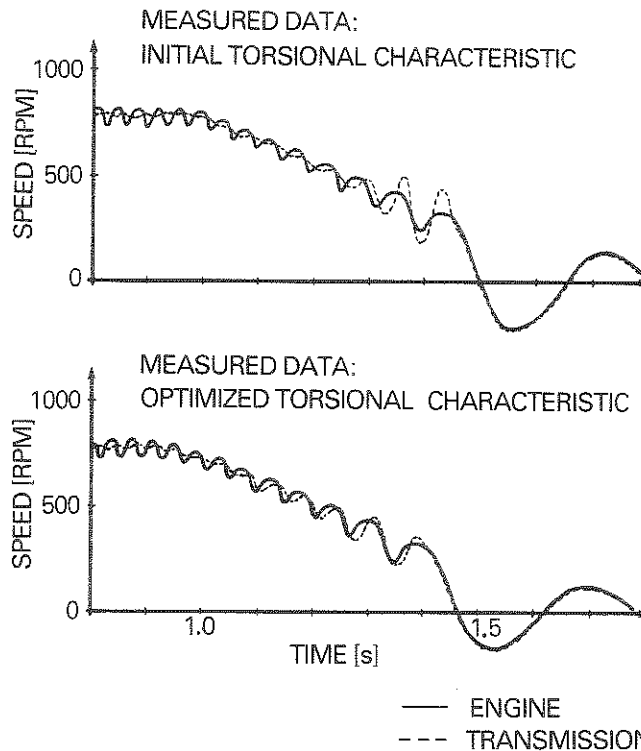


**Figure 19:**  
Engine shut-off measured data

But other areas should not be allowed to deteriorate. For instance, a characteristic that is well suited for the idle stage can cause tip-in/back-out problems. We have to reach a compromise between both vibration modes. In such cases, tuning can become a time-consuming activity, even with electronic measuring systems and computer assistance.

For many years, the measurement and calculation procedures that support our successful torsion damper tuning had to be performed in-house in our testing labs. Nevertheless, our customers in the automotive industry frequently expressed a real need to be able to perform this work in their facilities or in the field. Frequently the limited availability of prototype vehicles, coupled with secrecy requirements, necessitates outside testing capability.

LuK has responded to this need by developing our mobile tuning lab. It contains all the basic tools needed to support a well-documented tuning program:

- A torsion test stand with computer analysis capability for plotting torsion damper and dual mass flywheel characteristic data
- A break-in test stand for testing torsion damper friction control assemblies
- A measuring computer for in-vehicle acquisition of torsional vibration data
- A computer for vibration simulation
- A small workbench, complete with basic tools.

With the mobile tuning lab, it is frequently possible to solve torsional vibration problems on-site at the vehicle manufacturer's own test facilities. This means that LuK can also help in cases where a secret prototype cannot be driven off a customer's test track.

## **Summary**

The most important source of excitation for torsional vibrations in the vehicle drive train has been discussed. The main sources of excitation, gas forces in the engine, have been analyzed for low speeds, ignoring the effects of inertial forces. The alternating torques applied at the crankshaft under full load are proportional to the cylinder displacement. In idle mode, this only applies for diesel engines.

The drive train represents a vibration system with several resonance frequencies. Subjected to engine excitation, these frequencies can lead to numerous resonant speeds. With conventional clutch disc torsion dampers, it is possible to shift resonant speeds somewhat, and resulting resonances can be damped. Vibration isolation is only possible beyond speeds of about 2,000 rpm.

Measurement of the torsional vibrations causing gear rattle or boom is essential for the analysis of the problem. Measuring procedures have been described. However, to optimize torsion damper design, designers need simulation procedures in order to conduct systematic variations of system parameters. An example has been provided showing how measurement and calculation complement each other during the tuning process.

## Bibliography

- [1] Küçükay, F. and Pfau, W.  
Extrembelastungen in Personenwagenantriebssträngen [Extreme Loads in Passenger Car Drive Trains], *Automobiltechnische Zeitschrift* 91 (1989), p. 7
- [2] Küçükay, F.  
Dynamik der Zahnradgetriebe [The Dynamics of Gear Transmissions], Springer-Verlag
- [3] Chikamori, S. and Yoshikawa, N.  
Analysis of Drive Train Noise and Vibration. *Intern J. of Vehicle Design*, Vol. 2 (1981), p. 408
- [4] Hafner K. E. / Maas, H.  
Torsionsschwingungen in der Verbrennungskraftmaschine [Torsional Vibrations in Internal Combustion Engines], Springer Verlag
- [5] Maas H. / Klier, H.  
Momente und deren Ausgleich in der Verbrennungskraftmaschine [Torques and Torque Compensation in Internal Combustion Engines], Springer Verlag
- [6] Hafner, K. E. / Maas, H.  
Theorie der Triebwerksschwingungen der Verbrennungskraftmaschine [Theory of Drive Train Vibrations in Internal Combustion Engines], Springer Verlag
- [7] Wilson, K.  
Torsional Vibration Problems, Vol. 4, Chapman and Hall
- [8] Witte, L.  
Schwingungen im Antriebsstrang von Personenkraftwagen [Vibrations in Passenger Car Drive Trains], *VDI-Berichte Nr. 444* (1982), p. 77
- [9] Kaufhold, G.  
Rechenmodelle für Dreh- und Biegeschwingungen [Analytical Models for Torsional and Bending Vibrations], 1st Aachener Symposium for Vehicle and Engine Engineering 1987
- [10] Laschet, A.  
Simulation von Antriebssystemen [Simulation of Drive Systems], Springer Verlag, 1988
- [11] Reik, W.  
Torsionsschwingungen und Getriebegeräusche [Torsional Vibrations and Transmission Noises], *Automobil-Industrie* 1/87, p. 37 – 43 and LuK Clutch Symposium 1986
- [12] Klotter, K.  
Technische Schwingungslehre [Technical Vibration Theory], Vol. 1 – 3, Springer-Verlag

# Torsional Vibrations in Tractor Drive Trains

## Damping Options

Dipl. Ing. Karl Keck

Two thirds of LuK's current tractor clutch disc designs feature torsion dampers for master clutch operation, and in individual cases for PTO-drive as well. The general reason for using these torsion dampers is to eliminate annoying noises generated by torsional vibrations in the drive train.

The percentage of tractor clutch systems using torsion dampers has continued to increase over the last few years. As is the case with other types of vehicles, this is attributable to overall enhancement of total vehicle quality. In addition to improving mechanical efficiency by reducing internal friction, there can be further reasons in the specific case of tractor transmissions:

- closer ratios between the different gear stages, resulting in a greater number of components that are capable of vibrating and generating noise.
- greater overdrive transmission ratios, which proportionately magnify the irregularities of the internal combustion engine that cause vibrations.
- power-shift transmissions using the torsion damper as the connective element with the engine make, for various design reasons, special demands of the torsion damper.

LuK has kept pace with these customer demands and has over recent years invested increasing amounts of development work in torsion dampers for their tractor line.

The results of this work, which contributes as much to a general understanding of torsional vibrations in tractor drive trains as it does to the individual design problem, will be the topic of the following presentation. This discussion makes a number of comparisons to passenger car tuning because the basic problems involved and the general approach to problem solving are similar.

## The Engine as a Source of Torsional Vibration

Today's tractors usually use four-stroke diesel engine drive systems. Discontinuous fuel combustion results in irregular crankshaft torque, which fluctuates around an average value.

Figure 1 shows the torques affecting the crankshaft.

In comparison to the first presentation, the graph has been expanded to include tractor values. The peak-peak amplitude of the torque transmitted from the crankshaft to the flywheel is plotted as a function of cylinder piston displacement, both for idle mode and for operation under full load. The graph yields the following specific average values that can be used for estimating magnitudes:

- Idle mode: specific peak-peak amplitude of the torque approx.  $1000 \text{ Nm/dm}^3$
- Full load: specific peak-peak amplitude of the torque approx.  $1800 \text{ Nm/dm}^3$

Both passenger car and tractor diesel engines adhere to this basic pattern. Passenger cars have cylinder piston displacements in the range of  $0.3 - 0.6 \text{ dm}^3$ ; tractors, on the other hand, usually use cylinder piston displacements of about  $1 \text{ dm}^3$ .

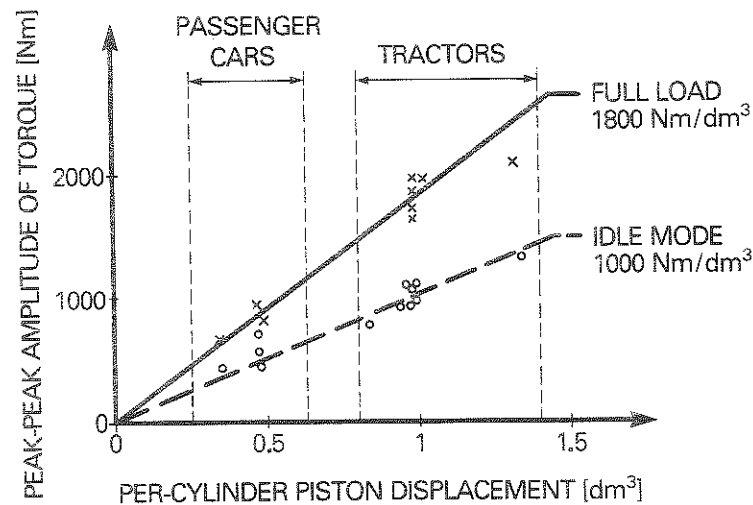
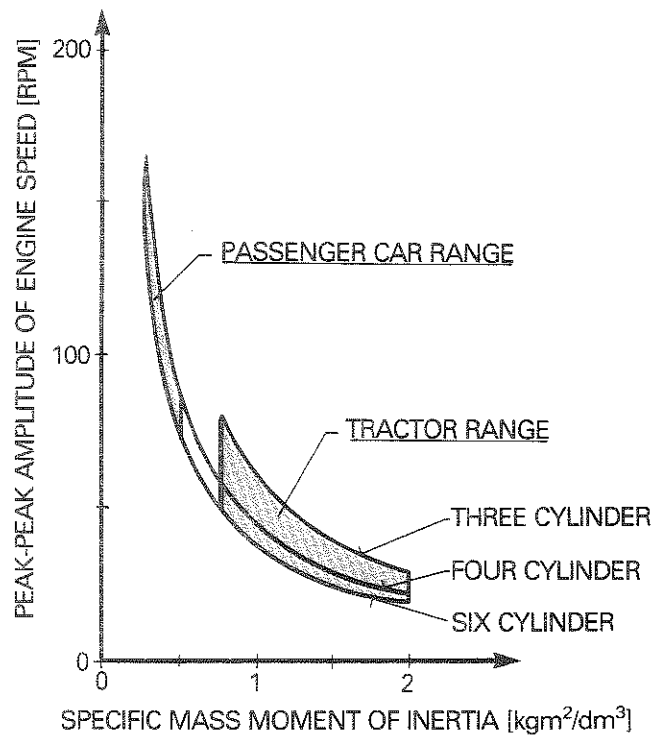


Figure 1: Torque amplitude for diesel engines

Depending on the size of the flywheel, the torque amplitude produces a specific angular acceleration amplitude and thus becomes the source of torsional vibrations. Based on this value, the number of cylinders in the engine, and the speed level, it is possible to calculate both the amplitude of the speed and the angle.

Figure 2 shows the speed amplitude for an idle speed of 700 rpm plotted as a function of the number of cylinders and the specific mass moment of inertia of the engine. In this case the specific inertia of the engine is to be understood as the total mass moment of inertia of the crankshaft drive + the flywheel + the clutch referenced to the piston displacement of the individual cylinder. The graph shows the standard ranges for tractors and passenger cars.



**Figure 2:**  
Engine speed amplitude in idle at 700 rpm

In like manner, Figure 3 shows speed amplitudes for full engine load at 1000 rpm. It is important to note the following factors:

- The specific mass moment of inertia of the engine varies relatively drastically, as does the magnitude of the torsional vibrations generated in any individual case. The graph shows speed fluctuations for the

tractor range and accounts for varying numbers of cylinders at full load. These values lie between 25 and 100 rpm, which represents a ratio of 1:4.

- Based on numerical values alone, tractor conditions are more advantageous than those for passenger cars. However, this advantage disappears immediately if a transmission features, for instance, a 2:1 overdrive transmission ratio, which is entirely possible. This means that the amplitude doubles at individual mating gears or synchronization elements.
- Under full load, the amplitude for passenger car engines averages about 3 times the magnitude of tractor engine amplitudes. However, the amplitude is lower than one would expect from a simple continuation of the curves for the tractor range. This could be attributable to the fact that passenger car diesel engines usually use indirect fuel injection.

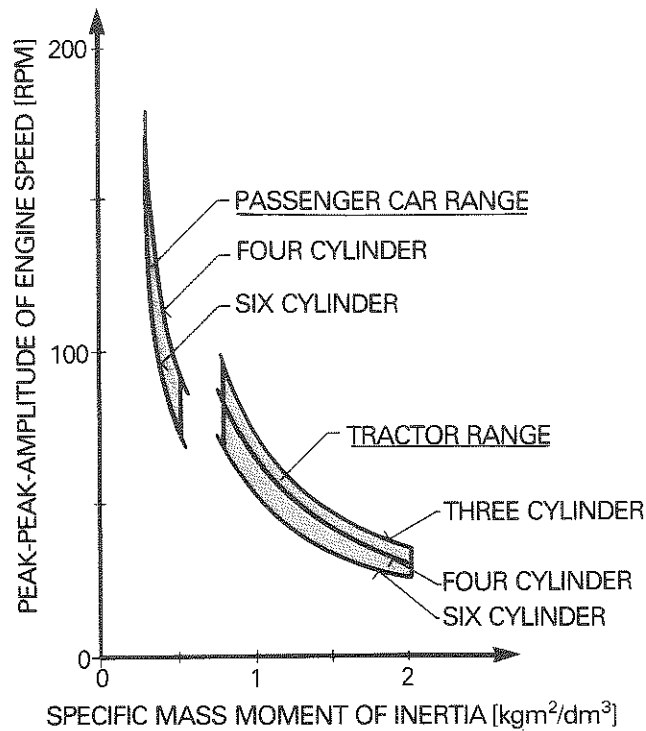


**Figure 3:**  
Engine speed amplitude under full load at 1000 rpm

## The Drive Train as a Torsional Oscillator

What do tractor transmissions look like? Depending on desired vehicle speeds ranging from approximately 1 to 25 mph, these transmissions must reduce nominal engine speeds of, for instance, 2,400 rpm at ratios of 1:20 to 1:400, working with drive wheels approximately 1.75 m in diameter. The highest transmission ratio of 1:400 requires a sequence of at least 4 reduction stages. To cover the ratio spread of 1:20 in steps of 1.2, approximately 16 gear sets are required.

Transmissions of this type are approximately 1 – 2 m long. Transmission input torques for 30 to 200 hp engines average between 100 and 800 Nm.

The number of reduction stages and gears allow numerous design options, which we have in production and which make it impossible to generalize tractor transmissions.

The following discussion will deal with torsional vibration problems and concrete numerical values for the simplest possible type of transmission. Figure 4 illustrates this kind of transmission in schematic form. The illustration shows the 4 reduction stages, specifically:

- speed section
- range section
- differential
- final drive ratio

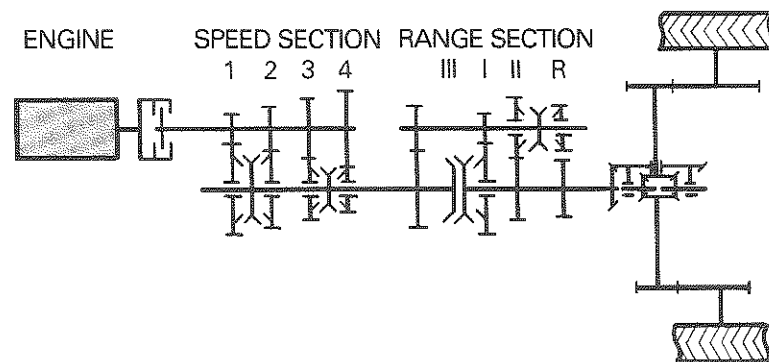


Figure 4: Block diagram for a simple tractor transmission (12/4)



There are four transmission gear reduction ratios in the first stage and another four in the second stage, including one reverse gear. This yields twelve forward and four reverse gears. For clarity's sake, not all components are represented here, specifically the PTO, the front wheel drive train, the splitter and the creeper gear used to increase the gear number.

Engine vibration is transmitted to these transmission components in an as-yet unknown way. It is unchanged, damped or magnified. If it causes noises, usually reducing vibration will either diminish or eliminate the noises. It is possible to introduce a torsion damper between the engine and the transmission in order to influence vibration behavior. Let us examine this influence, based on the standard distinction between idle and drive mode.

### **Vibration Behavior in Idle Mode**

The presence of several shiftable transmission sections in a tractor transmission means that – unlike in a passenger car – there are several neutral positions. The example we are dealing with here produces 5. When the first transmission section is in neutral position, only the front 4 gear pairs revolve. However, when the driver shifts into any one of gears 1 – 4 while the second transmission section is in neutral, a series of additional components will turn at significantly different speeds, depending on the chosen gear. Consequently, the different neutral positions yield significantly different values for the inertia, which is decisive for torsional vibration. Figure 5 on the right represents this situation. The sample tractor design used here yields inertias from 0.016 to 0.061 kgm<sup>2</sup>, which gives us a ratio of about 1:4.

The left side of the illustration shows the model for a two-mass vibration system. Measurements taken on about 10 different tractors provide empirical values indicating that this model is adequate for accurately describing idle mode vibrations. The variable inertia of the transmission is symbolized by different sized rectangles drawn with broken lines.

Figure 6 illustrates the effect that these considerations have on torsion damper design. The illustration is based on the assumption that the engine ignition frequency excites the resonance speed at 300 rpm. With a design like that represented in the sectional drawing on the right, the engine clearly operates above natural frequency during normal idle mode speeds

of 600 to 700 rpm. Vibration is reduced by about half. The illustration shows the maximum permissible spring rate plotted as a function of the transmission inertia.

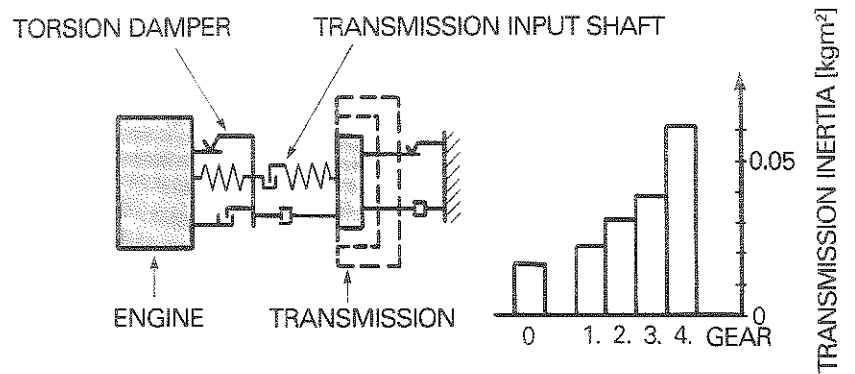


Figure 5: Model for vibration simulation in idle mode

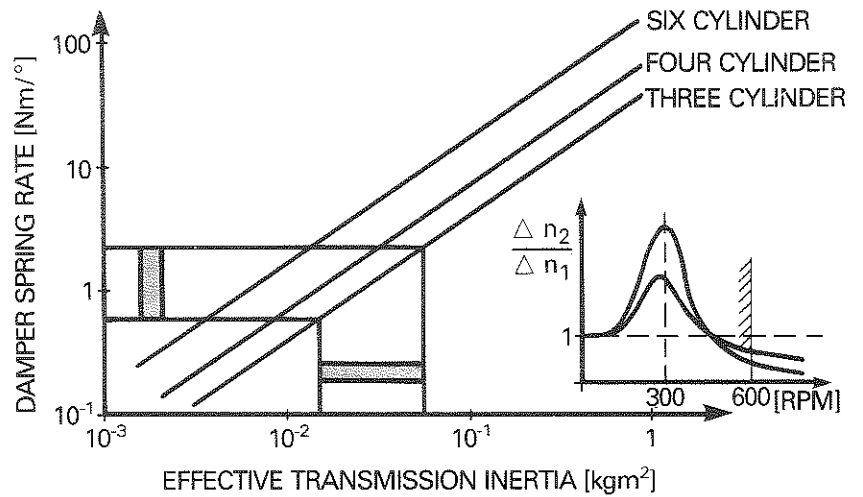


Figure 6: Spring rates for 300 rpm resonance speed

Depending on the shifting configuration, for a three cylinder engine the inertias used in our example would require spring rates of about 0.6 to 2 Nm/°.

Should vibration isolation be required in all cases, we would of course only be able to use the lowest value,  $0.6 \text{ Nm/}^\circ$ .

Inertias for tractor transmissions in idle mode generally lie in a range from just under  $0.01$  to about  $0.1 \text{ kgm}^2$ . Hence, this criterion would require spring rates of about  $1$  to  $2 \text{ Nm/}^\circ$  for smaller tractors with three and four cylinder engines. For larger tractors with six cylinders,  $2 - 5 \text{ Nm/}^\circ$  are possible.

The idle stage characteristics for the production torsion dampers shown in Figure 7 reveal that this requirement is not always met.

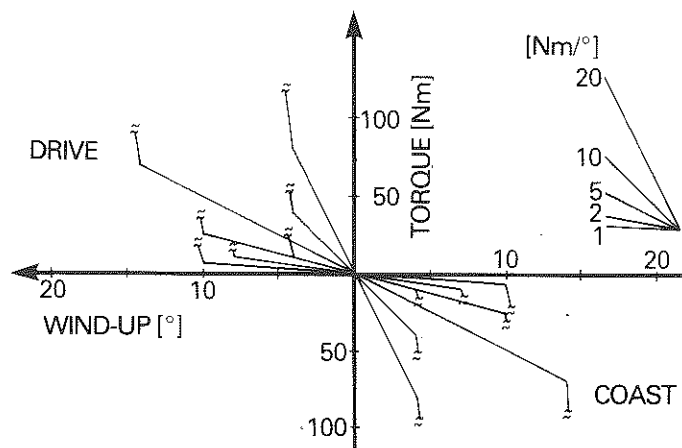


**Figure 7:** Idle mode characteristics for typical tractor torsion dampers

Some of the spring rates are much higher, although they are successfully used to eliminate idle mode noises. This somewhat surprising situation can be explained as follows:

- As a rule, in absolute neutral position, which also represents the lowest inertia, tractor transmissions exhibit acceptable noise performance. Noise problems increase in higher gears, obviously parallel to the increasing rotational speed of the revolving gears. Consequently, it is often sufficient to design the torsion damper for the two highest gears, which at the same time represent the greatest inertia. In smaller transmissions, spring rates of about  $1 - 2 \text{ Nm/}^\circ$  are appropriate for this purpose. Some of the torsion dampers shown in the illustration actually have these slopes. Of course, this design poses the risk that the

transmission will operate in the critical range in lower gears and that the lack of damping in the transmission or in the torsion damper will lead to resonance and consequently to unacceptable noises.

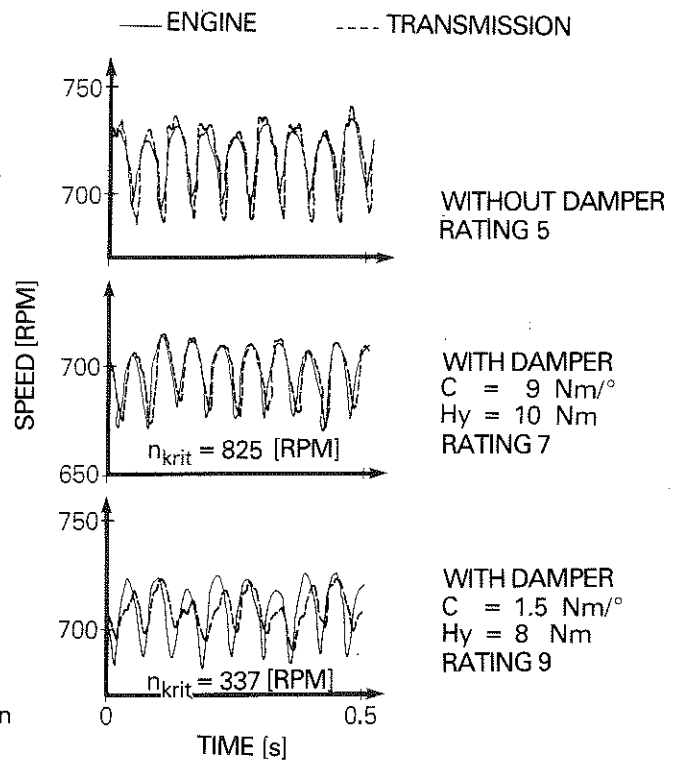
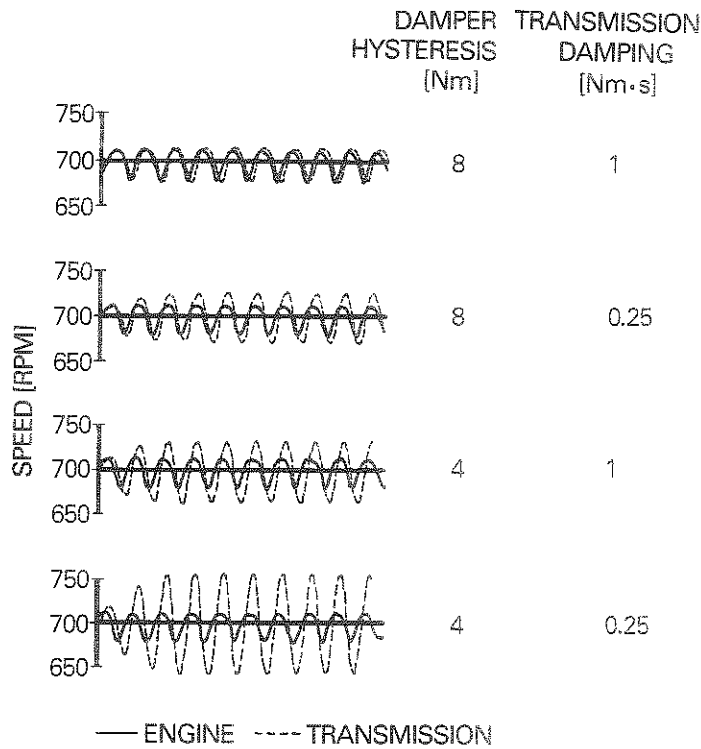


**Figure 8:**  
Vibration measurements in  
idle mode, 2nd gear

- Some of the torsion dampers shown in the illustration have spring rates of 5, 10 and even 20 Nm/°, which does not lead us to anticipate any vibration isolation above natural frequency. Figure 8 illustrates an attempt to arrive at a physical explanation for this condition based on vibration measurements. We conducted measurements using a three cylinder engine in idle mode at 700 rpm, with the transmission in 2nd gear with an inertia of 0.03 kgm<sup>2</sup>. Engine speed is shown as a solid line and transmission speed as a broken line. The top graph shows a measurement using a rigid clutch disk. Because of the unavoidable gear lash between the shaft and the hub, transmission vibration is clearly amplified over the engine vibration, resulting in a subjective rating of 5, which is considered objectionable. The graph in the center shows a measurement using a damper with a slope of 9 Nm/°, which was cited

above as unreasonably high; this is evident from the resonance speed of 825 rpm, which lies close to the idle speed. The damper does little to reduce engine vibration, but the situation is clearly better than operating without any damper at all. The subjective noise rating of 7 is classified as acceptable. Finally, the bottom graph shows a measurement using a spring rate of  $1.5 \text{ Nm/}^\circ$  designed to operate above natural frequency. Transmission vibration has been reduced by about half. The subjective noise rating is 9, which indicates that no noise is audible.

This also explains how an idle stage with an apparently excessive spring rate produces an acceptable noise rating. In such cases, a high spring rate can offer certain advantages. It shortens the required wind-up angle to control drag torque and has a favorable effect on driving operation for low engine loads as well.



CONSTANT PARAMETERS  
 $J_2 = 0,03 \text{ kgm}^2$ ,  $C = 9 \text{ Nm/}^\circ$   
 THREE CYLINDER ENGINE

**Figure 9:**  
 Computer vibration  
 simulation in idle mode

However, since operation close to resonance speed is impossible without adequate damping, this design is always associated with a certain risk. Computer vibration simulation allows us to estimate this risk by varying damper parameters as shown in Figure 9.

The top graph simulates the apparently excessive spring rate of  $9 \text{ Nm/}^\circ$ , which is initially satisfactory with respect to noise. The second graph from the top does not change the torsion damper hysteresis, but does reduce transmission damping to a value that is representative for the passenger car range. The vibration curve is already less favorable than it was previously in Figure 8 for measurement without a torsion damper. Finally, the two bottom graphs show that any reduction in the damper hysteresis produces further deterioration.

Before closing this chapter on idle mode tuning conditions, let us take one more look at engine excitation, since the angular amplitudes for engine excitation are critical for determining the length of the damper torsion curve. Figure 10 shows angular amplitude in idle mode at 700 rpms plotted as a function of the specific inertia.

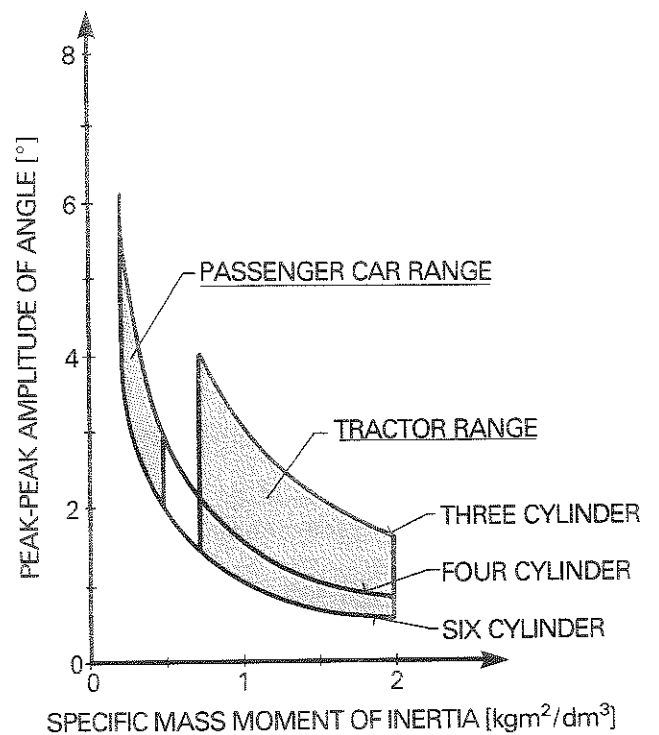


**Figure 10:**  
Angular engine amplitude in idle mode at 700 rpm

With three-cylinder engines, we achieve vibration angles up to  $4^\circ$ . Low spring rates of  $1 - 2 \text{ Nm}/^\circ$  and transmission drag torques of up to  $5 \text{ Nm}$  can lead to idle stage torsion angles of  $10^\circ$ . In contrast, the vibration angle for four and six cylinder engines shown on the right side of the range is only about  $1^\circ$ . If it is possible to have a spring rate of  $5 - 10 \text{ Nm}/^\circ$  at the same time, then an idle stage torsion angle of  $2^\circ$  will be sufficient.

### **Vibration Performance in Drive Mode**

In order to interpret vibration performance for tractor drive mode, it seemed obvious to start out using the 3-inertia model familiar from passenger car tuning. Because of the relatively low torsional spring rates in the half-shafts, for the most part, this model allows the transmission to vibrate on its own with the differential, as if it were disconnected from the wheels and the vehicle mass.

However, vibration measurements taken in tractors during driving operation in the highest gears exhibit inexplicable behavior, as described in the following two examples:

- Figure 11 shows measurements taken on a relatively small three-cylinder tractor, with the same transmission used at the beginning of our discussion while driving under full load between about 750 and 800 rpm. According to the simple 3-inertia model, one would expect to find amplified transmission vibration in response to the engine vibrations because the system is operating below natural frequency. In actuality, we see a clear reduction. This example shows how important it is to conduct vibration measurements.
- Figure 12 shows measurements taken on a relatively large tractor with a completely different transmission and a six cylinder engine driving below 600 rpm. The simple model would have anticipated a slight vibration reduction based on the favorable initial values, but it would not have predicted the nearly perfect isolation.

A vibration model with 4 torsional inertias provides an explanation for this phenomenon, as demonstrated in Figure 13.

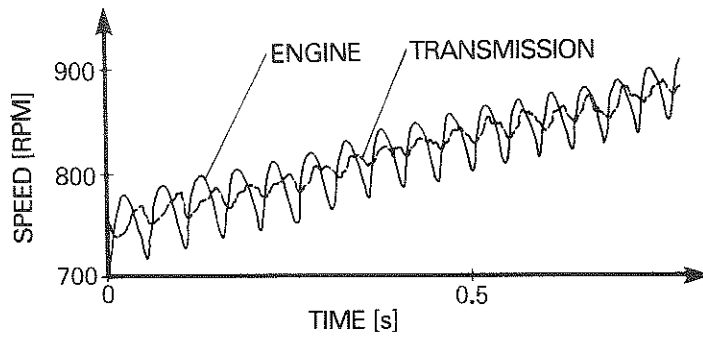


**Figure 11:** Vibration measurement while driving in the 30 km/h gear, full load; low-power tractor with three cylinder engine

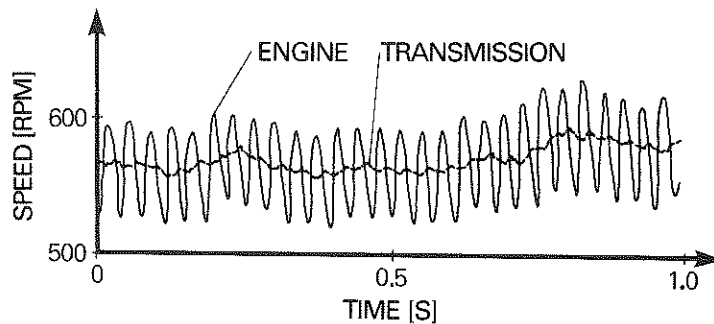
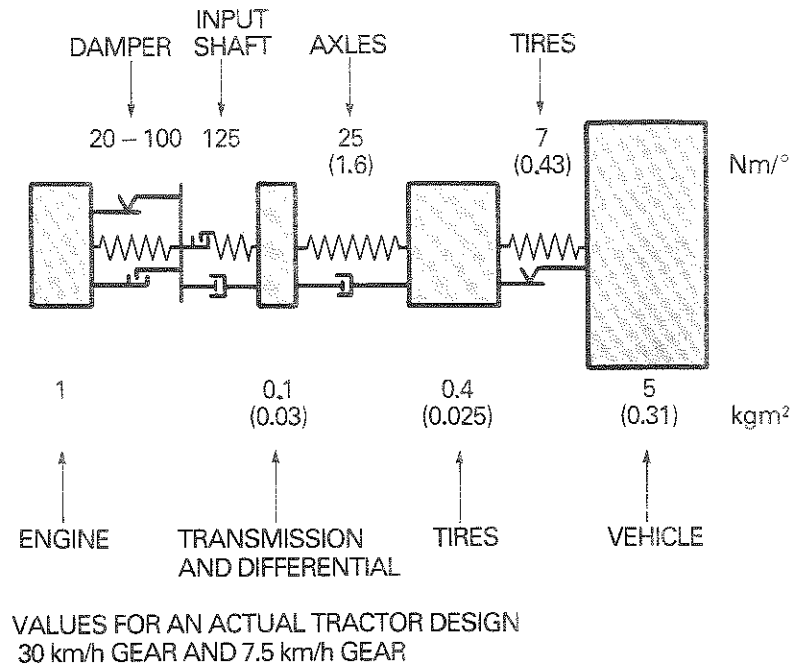


**Figure 12:** Vibration measurement while driving in the 30 km/h gear, full load; high-power tractor with six cylinder engine

As usual, the transmission is combined in one inertia. However, the drive wheels are treated as an additional mass. The concrete values for our sample transmission are entered as effective mass moments of inertia and spring rates. The numbers without parentheses apply for the 30 km/h gear, while the values in parentheses are valid for a 7.5 km/h gear. The decisive factor is that unlike the situation with passenger cars, the drive wheels can no longer just be assumed to be part of the vehicle mass in the high gears. This is attributable to the low spring rate of the tires in relationship to the drive axles. Consequently, the system will generate a vibration mode in which the transmission and the drive wheels vibrate together in opposition to the vehicle and the engine. Taken together, this



produces a considerable mass that shifts the resonance into a favorable position and can lead to good vibration isolation at speeds above this critical condition. In contrast, the high reduction ratios associated with the low gears reduce the effective inertia of the wheels considerably so that it no longer significantly influences vibration performance.



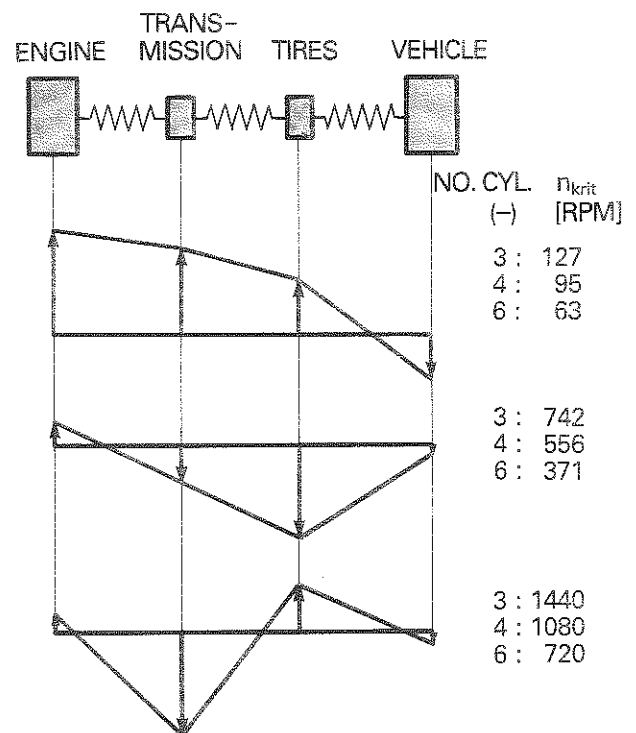
**Figure 13:** Vibration model for driving mode

Figure 14 shows the possible resonances and the natural vibration modes that occur for these 4 masses. These calculations used the numerical values indicated for the 30 km/h gear and a frequently used tractor damper spring rate of 100 Nm/°.

- The top section of the illustration shows a vibration mode during which the complete drive train including the engine vibrates in opposition to the vehicle mass. In passenger cars, this condition would usually result in unpleasant surging, but this is rarely evident in tractors.
- The center diagram shows the previously mentioned condition where the transmission and the drive wheels are vibrating together. Given the numerical values on which this drawing is based, the wheels vibrate considerably more strongly than the transmission. The transmission

does not represent a concentrated, rigid body. Instead, it extends over a great length and represents a flexible component. Hence the representation shown here indicates that vibration amplitudes within the transmission can vary, which means that care must be taken when measuring them.

- The same applies in general for the third possible natural mode shown in the bottom graph, during which the transmission and the drive wheels vibrate in opposition to each other.



**Figure 14:**  
Four-inertia model – natural modes and resonance speeds for spring rate of 100 Nm/°, 30 km/h gear

The graph sections also show the resonance speeds for three, four and six cylinder engines. For instance, these figures may explain the fact that the spring rate of 100 Nm/° cited for tractors with three cylinder engines leads to noise when driving in the lower speed range, but does not cause this problem with four and six cylinder engines.

Finally however, these drawings only represent relative vibration modes. Figure 15 shows the absolute values, which occur for each given spring rate in conjunction with different damping values. This illustration shows the analysis of measurements taken on our model tractor. On these four graph sections, engine speed fluctuations are plotted as a solid line and transmission speed fluctuations are plotted as broken lines and dot-dash lines, all as a function of the engine speed on the abscissa.

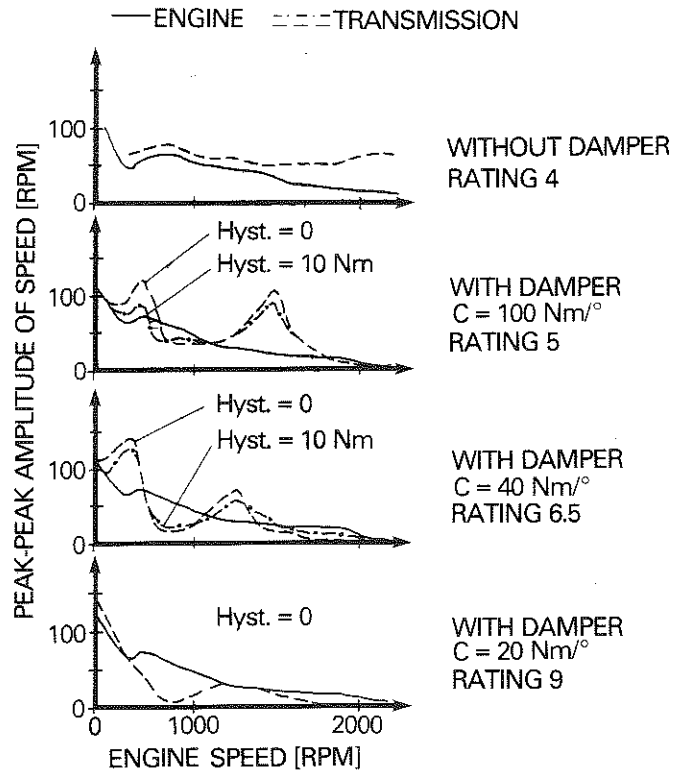


**Figure 15:**  
Analysis of vibration measurements taken during drive mode in 30 km/h gear, full load, three cylinder engine

Viewed from the top down, the first graph shows a measurement taken without a torsion damper, followed by measurements with torsion dampers using 100, 40, and 20  $\text{Nm/}^\circ$  spring rates. The measurements taken at 40 and 20  $\text{Nm/}^\circ$  exhibit a deep isolation valley between the resonance points, which explains the "perfect" vibration patterns shown at the beginning. On the other hand, the resonance points are clearly defined. At these points, vibration performance is worse than without a damper!

Only the 20 Nm/° spring rate provides improvement over the entire speed range. The soft coupling between the transmission and the engine results in a situation where the transmission damping by itself is capable of suppressing peaks at the resonance speeds!

This means that designers will be able to concentrate on idle mode requirements when they select the torsion damper hysteresis.

Subjective noise ratings are indicated to the right of each of the graphs. The ratings indicate that this case is not particularly critical. However, experience has shown that a spring rate of about 25 Nm/° will generally eliminate noise in problem cases involving three-cylinder engines. Consequently, the conditions represented by the illustration are more or less generally valid.

We can use computer simulation to generate characteristic fields for the analysis of vibration behavior with respect to the essential damping and spring rate parameters in the 30 km/h gear. Figure 16 shows the results of this kind of analytical modeling. Again, the vibration amplitudes for engine and transmission speeds are represented as a function of engine speed.

Moving from the top to the bottom, the damper spring rate was reduced from 100 to 40 and finally to 20 Nm/°. Moving from left to right, the hysteresis was increased from 0 to 10 and then to 25 Nm. The far right column with a hysteresis of ∞ represents a clutch disc without a torsion damper.

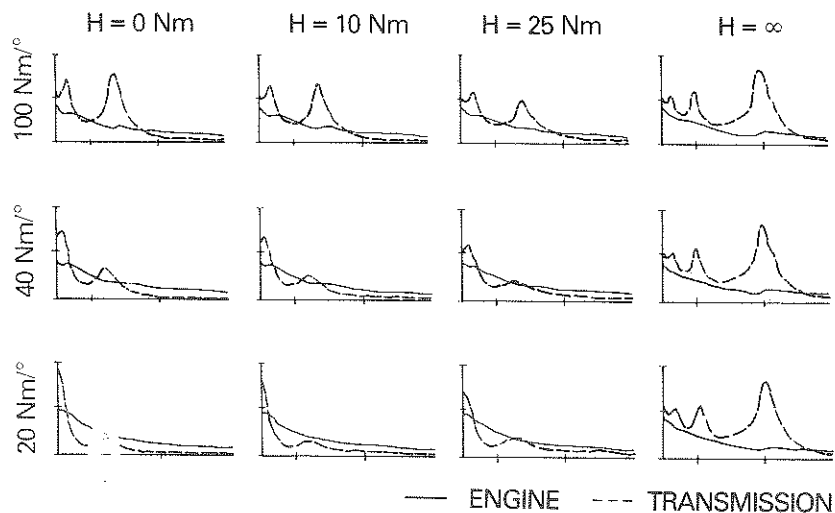


**Figure 16:** Computer vibration simulation for drive mode in the 30 km/h gear

Above all, the illustration confirms that at low spring rates, very low torsion damper hysteresis values can be used to prevent vibration peaks when unavoidably passing through resonance points.

So much for the higher gears with final speeds of 20 to 40 km/h, which cause the greatest noise problems in tractors. In the lower gears, on the other hand, tractor transmissions fairly rarely cause noises because some of the gear pairs turn at greatly reduced speed. This also means that the effective inertia of the transmission will be considerably lower. Furthermore, as a result of the high reduction ratios, the transmission is de-coupled from the drive wheels with respect to vibration behavior.

Figure 17 shows the analysis of vibration measurements taken in drive mode in a typical 7.5 km/h gear using a three cylinder engine. Again, these graphs show engine speed variation entered as a solid line with reference to the engine speed on the abscissa and the transmission speed variation entered as either a broken or a dot-dash line.

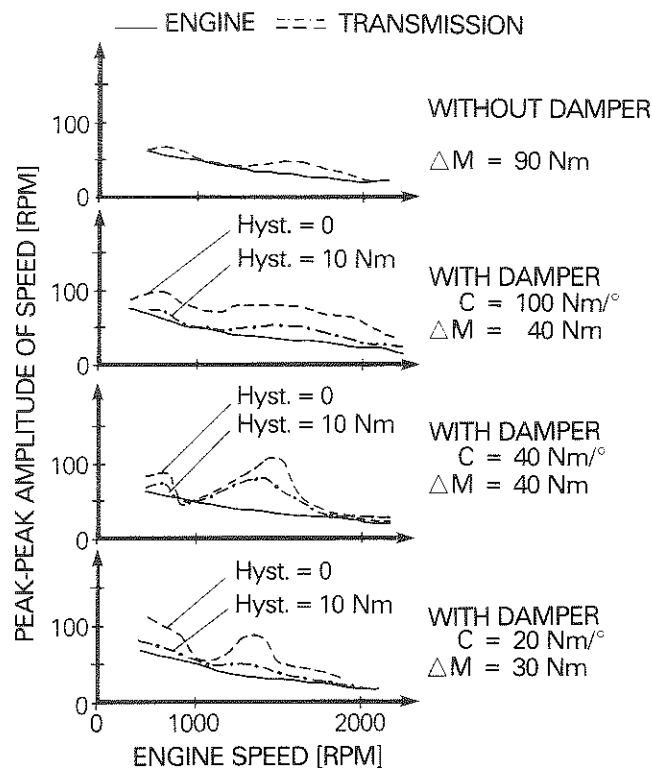


**Figure 17:** Analysis of vibration measurements taken during drive mode in the 7.5 km/h gear, full load, three cylinder engine

Viewed from the top down, the illustration first shows a measurement taken without a torsion damper, then measurements for torsion dampers using 100, 40 and 20 Nm/° spring rates. There was no perceivable noise in any of these cases. The vibration curve without a torsion damper exhibits advantages in comparison to operation with dampers. However, the figures listed to the right of the graph sections, which indicate torque fluctuations  $\Delta M$  at the transmission input, support the use of a damper. These values are measured in a range from 1200 to 2000 rpm. Without a damper, this amounts to 90 Nm, which in this case is approximately 40 % of the averaged torque of 200 Nm. Use of a damper can cut this value down to half or even a third this level. This factor certainly has an influence on the service life of the transmission, since the transmission has to operate in this mode for several thousand hours.

From the standpoint of vibration engineering, satisfactory performance realized without a damper is attributable in this case to the more or less serendipitous convergence of various parameters. As a result, the main resonance lies outside the operating speed range of max. 2500 rpm. The top computer-generated graph shown in Figure 18 illustrates this.

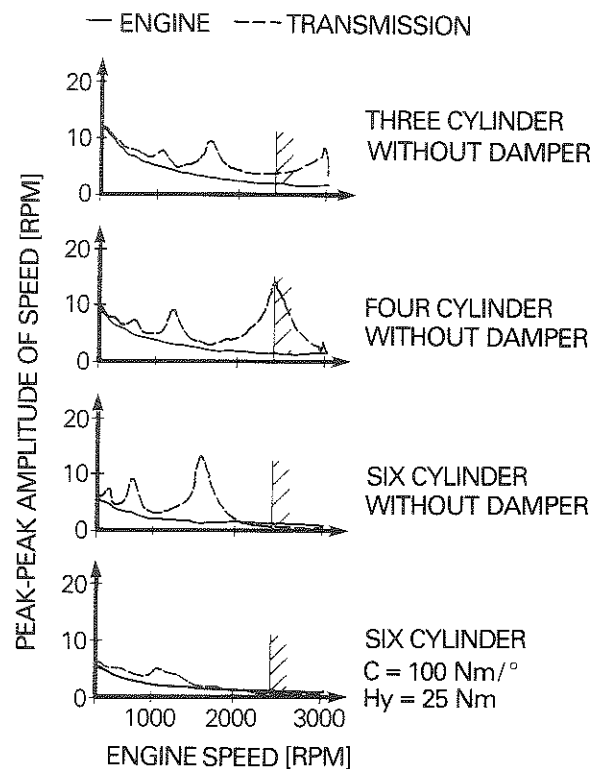


**Figure 18:**  
Computer vibration simulation for drive mode in the 7.5 km/h gear

As an exception, the three cylinder engine has a positive effect in this case.

Computer calculation allows us to estimate the risk involved when using four and six cylinder engines. These engines shift the main resonance closer to or even entirely into the operating speed range. Even a relatively simple torsion damper with a  $100 \text{ Nm/}^\circ$  spring rate such as the one shown in the bottom graph would reduce these amplitudes considerably.

To conclude this chapter on torsional vibrations during drive mode, it is necessary to take an additional look at engine excitation. Figure 19 shows engine excitation as the vibration amplitude of the engine angle for full load at 800 rpm. The value of 800 rpm was chosen because no noise is tolerated at this speed for tractors. As shown, thanks to positive marginal conditions, the problem can be solved. Certainly, engine vibration angles of up to  $5^\circ$ , which we see at the left end of the tractor range, require correspondingly long torsion characteristics.

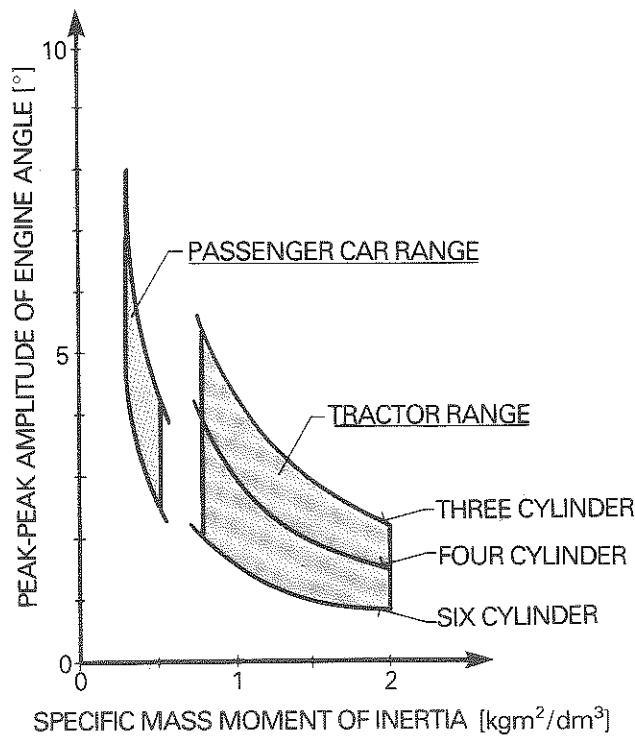


**Figure 19:**  
Engine angle amplitude under full load at 800 rpm

## Special Conditions in Power Shift Transmissions

Figure 20 shows a compilation of the most important characteristics curves used in the clutch discs LuK is supplying to the tractor market. Most of these discs do not feature separate predampers, and some of them have relatively long total torsional travel up to  $35^\circ$ .

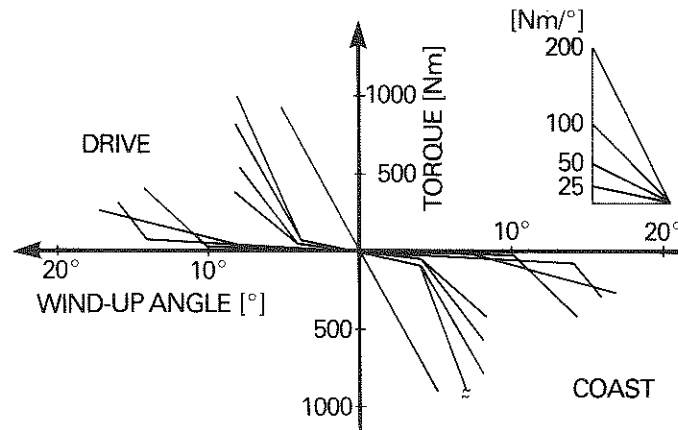


**Figure 20:** Torsion damper characteristics for typical tractor clutch discs

The illustration also shows the spring capacity that can be achieved using the space between the hub and the facings in the conventional clutch disc range from 225 to 350 mm  $\varnothing$ .

The shaded areas in Figure 21 indicate the position of the characteristic curves for these clutch discs. Damper characteristics designed for newer transmissions are also plotted on the graph.

These curves exhibit different dimensions. The common factor for the transmissions in question is that the main clutch itself is installed inside the transmission and the connection with the engine is achieved using a torsion damper. Obviously, this type of design places special demands on the torsion damper.



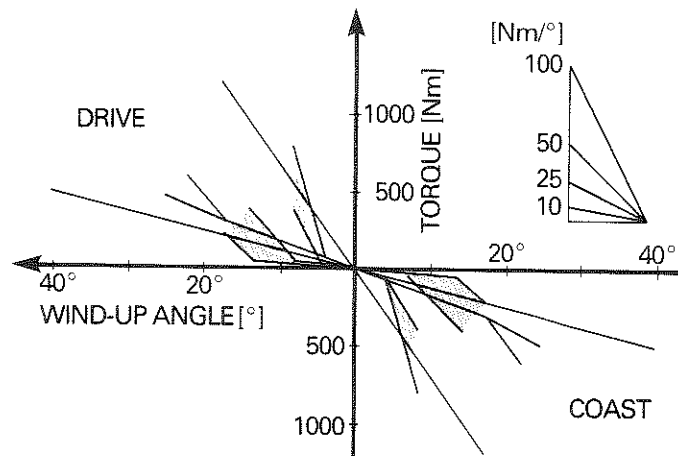


**Figure 21:** Torsion damper characteristics for newer tractor transmissions

### Hydraulic Pump Drives

Let us start with idle mode. Because the damper represents the only connection with the engine, it is also subjected to load from the various hydraulic pumps located in the transmission. If we also account for drag torques for one or more wet friction clutches, we end up with a required torque capacity of 150 to 200 Nm for the torsion damper idle stage. The transmission might require a torsion damper rate of 2 to 5 Nm/° in this case in order to eliminate noise. This would result in unrealistically long torsional travel of 40 to 100° for idle mode. This suggests the serious possibility of introducing a second, independent shaft from the engine to the transmission for the purpose of driving accessories as is the case with conventional transmissions.

### Alignment Error between the Engine and the Transmission

The transmission input shaft for this kind of transmission is not usually centered with respect to the flywheel, but its first bearing point on the transmission side will be relatively close to the flywheel. The misalignment between the engine and the transmission is unavoidable – in extreme cases we have to deal with a chain of up to 10 tolerances. Consequently, this misalignment will result in more pronounced friction variation within

the damper compared to conventional transmissions. This situation can lead to excitations of the 1st order. Figure 22 shows this condition using sample measurements taken from a six cylinder engine. Transmission vibration has been significantly reduced, but during each third engine ignition cycle, that is, once per revolution, vibration, shown as a broken line, becomes more pronounced.

As a result, under these circumstances, we may have to use a damper design featuring low-friction centering, or even elastic suspension of the damper on the flywheel, in order to avoid these excitations.

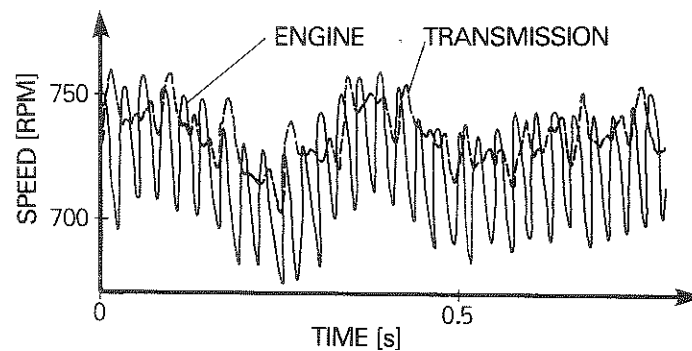


**Figure 22:** Vibration measurement in idle mode for a six cylinder engine; example of excitation of the 1st order

#### **Effects of Positioning the Start-up Clutch inside the Transmission**

Given a certain order of magnitude, slip will prevent the transmission of vibrations to downstream links in the kinematic power flow chain. In conventional transmissions, the main clutch is situated on the engine flywheel, that is at the beginning of the transmission train. During the start-up phase, the engine is de-coupled from the transmission so far as vibration behavior is concerned. However, if the start-up clutch is located in the middle of the transmission, then the upstream transmission components vibrate with the engine during the start-up phase, while the effective inertia can be reduced considerably because the downstream components are disengaged from the engine during this phase. This results in transmission noise during the start-up phase. Figure 23 shows a typical vibration measurement during this kind of start-up.

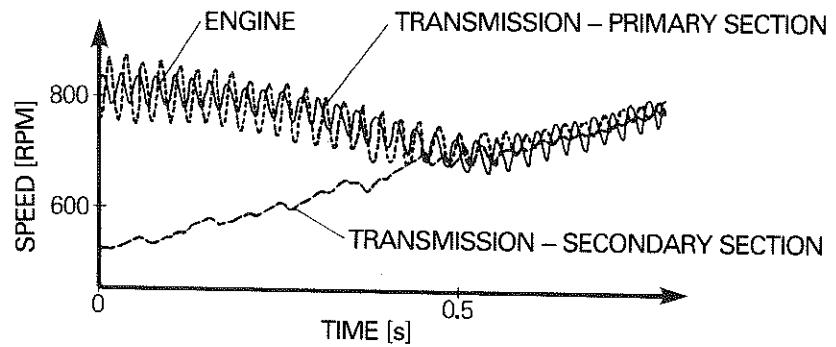


**Figure 23:** Vibration measurement during start-up with the master clutch situated in the middle of the transmission

This measurement also shows that in stable condition after completion of the start-up process, the front and rear ends of the transmission vibrate with significantly different amplitudes. The discussion of natural modes already made reference to this eventuality. Consequently, it is very important to exercise care when taking measurements.

Given the relatively low inertia for the transmission components upstream of the clutch, a spring rate in the magnitude of  $10 - 20 \text{ Nm}/^\circ$  may be required for operation above natural frequency. With this spring rate, it is necessary to achieve approximately the rated engine torque, which again can lead to damper wind-up angles of  $20$  to  $50^\circ$ .

### Starting the Engine with a High Transmission Inertia

Starting the engine with a high transmission inertia is a home-grown problem, to use a popular phrase. We didn't have this problem until we started installing dampers in the transmission. At transmission inertias of, for instance,  $0.2$  to  $0.6 \text{ kgm}^2$ , starting the engine can involve passing through the resonance with torque peaks of several  $1000 \text{ Nm}$  or can even make starting impossible. It is questionable whether this specific problem can be resolved at all using a damper.

## **Power Shift**

Power shift causes internal strain in the transmission, which leads to considerable angular motion among the individual transmission components and can manifest itself in extreme noises. An interesting problem. Contrary to previous assumptions, the damper can exercise either a positive or a negative influence, although it is actually in the wrong position to do so.

At this point, our current measuring technology and our options for documenting vibration conditions are probably stretched to the limit. Curves for speeds or accelerations associated with drastically differing noise intensities look almost the same.

This topic must be analyzed more thoroughly in order to find an explanation.

## **Summary, Forecast**

In the case of conventional tractor transmissions – meaning essentially manually shifted machines with the main clutch situated on the engine flywheel – efforts to eliminate noises using torsion dampers installed in the clutch disc have been successful in almost all cases. However, we cannot overlook the fact that in contrast to passenger cars, we can profit considerably from relative low engine irregularity and high internal transmission damping. Changes in these two parameters will determine the future development of the torsion dampers that will be installed in clutch discs.

New designs that integrate the main clutch into the transmission will require significantly higher torsion damper capacity. It is even possible that we may need to use the arc spring technology developed for the dual mass flywheel in order to implement these solutions. At any rate, the high wind-up angles prevent the use of conventional dry dampers.

In addition to solving individual problems, LuK is also faced with the task of producing standard components in this area, which are urgently needed because of the fairly low quantities we experience in the tractor market.

In spite of their complexity, it is possible to use computer models to simulate the vibration behavior of tractor transmissions. It is impossible to use these calculations to predict noise behavior. However, they do provide decisive information on the physical analysis of vibrations and thus can lead to speedier solutions. Furthermore, they offer an appropriate means of estimating critical boundary values for functional parameters during later field application.

# Development of the Super-Long-Travel Dual Mass Flywheel

Dipl.-Ing. Michael Schnurr

Whenever familiar technology reaches its limits, new approaches and basic improvements are necessary in order to overcome the barriers that arise. In the middle of the 80s, after decades of development on the classic torsion damper, we reached a limit that prevented us from making further improvements in automotive noise comfort. This situation required that we look for new ways to meet rising expectations.

At LuK we took up this challenge. Extensive development work was required, but we found a solution.

## The Dual Mass Flywheel – DMFW

The dual mass flywheel has set a new standard for fighting torsional vibrations.

As is the case with all trail-blazing developments, the DMFW is conceptually simple (Figure 1).

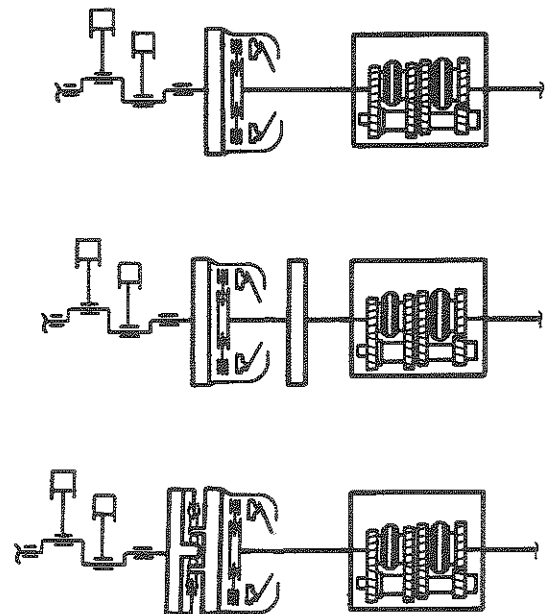
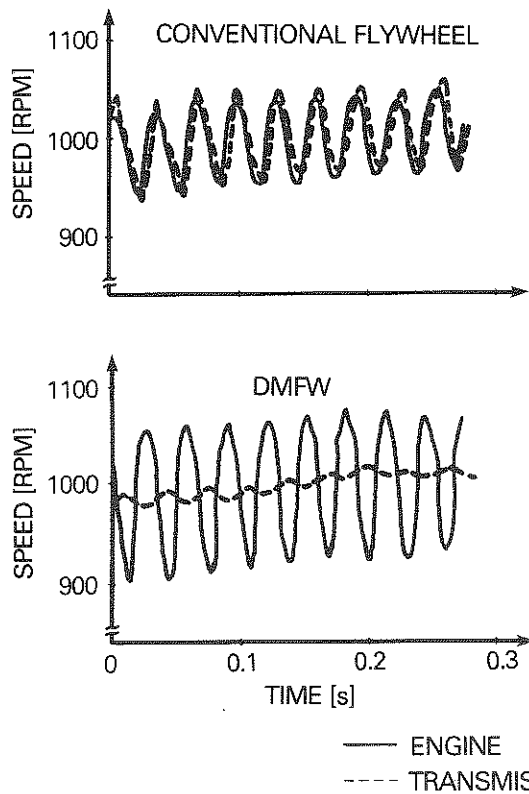


Figure 1:  
Basic solution

In conventional designs, the resonance point lies between 700 and 2000 rpm. We have added a supplemental inertia on the transmission input shaft in order to shift this resonance point into the low-speed range. This change produces a vibration isolation range beginning with idle speed.

Shifting the clutch to a position behind the divided flywheel ensures that the transmission can still be synchronized.

Torsional vibration measurements (Figure 2) for the clutch disc and the DMFW show two totally different conditions [1]. In the speed range around 1000 rpm, the DMFW already provides perfect isolation, reducing vibration amplitudes on the transmission side. At this point, the damped clutch disc is as yet unable to filter out vibrations.



**Figure 2:**  
Comparison: conventional flywheel – DMFW

When we install the DMFW, engine irregularity usually increases, as can be seen in the measurements. This is because the effective mass moment of inertia on the engine side is generally lower. However, this is usually

permissible with respect to gear rattle because the isolation effect of the DMFW provides adequate reserves.

The first generation DMFW was developed for six cylinder vehicles [2,3]. It solved noise problems in these vehicles by achieving the necessary degree of isolation described above.

However, four cylinder vehicles exhibit a higher degree of irregularity, accompanied by higher resonance speeds. Consequently, this DMFW could not be used for these applications. We had to consider other solutions. First of all, we have to draw upon a vibration model in order to make some basic observations.

### **Vibration Model**

As has already been noted in other presentations, complete description of a drive train would require a complicated vibration model [4]. However, if we limit ourselves to the resonance performance of the DMFW, a three-inertia vibration system like that shown in Figure 3 is adequate for explaining the effects of various corrective measures.

The elements of the model are identified as follows:

- $J_1$  = Engine inertia, including the primary flywheel inertia and its damper components
- $J_2$  = Secondary flywheel inertia with clutch, clutch disc and transmission component
- $J_3$  = Vehicle inertia
- $C_{TD}$  = Torsion damper spring rate
- $C_A$  = Drive train spring rate

The three-inertia vibration system has two resonance frequencies with their accompanying natural modes.

During surging, the vehicle  $J_3$  vibrates in opposition to the engine  $J_1$ . The torsion damper and drive train spring elements operate serially between these two inertias. The secondary DMFW inertia lies in the vicinity of a vibration node, which means it has virtually no influence on the system. The related natural frequency of 2 – 5 Hz is so low that any excitation due to the ignition frequency is ruled out. However, this vibration mode can appear after a rapid torque change, such as a tip-in. It takes the form of objectionable surging.



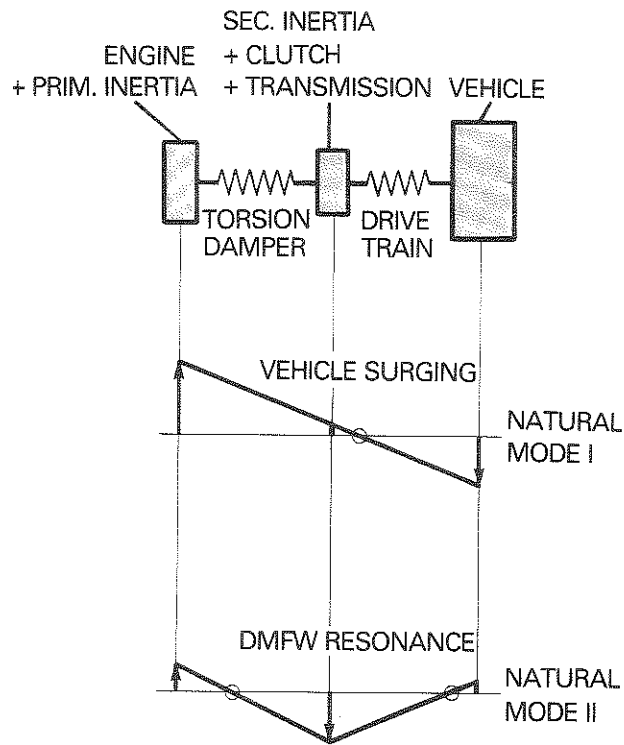


**Figure 3:**  
Vibration model and natural modes

In the case of the second natural mode, a resonance occurs between the primary and the secondary DMFW inertias. At high amplitudes, the two DMFW inertias, which are connected together via springs, vibrate in opposition to one another. The vehicle itself is hardly involved at all. Consequently, the following discussion refers to this second natural frequency as "DMFW resonance." This phenomenon represents an important physical characteristic of the DMFW system, which must be given careful attention when making design calculations.

Both natural modes must also be taken into consideration when designing traditional clutch discs. However, the frequencies and resonance speeds involved are different.

## Resonance Speed Field

As noted during the first presentation for this symposium, engine excitation is not harmonic. Therefore, in addition to the ignition frequency, we have to deal with additional excitation frequencies. The whole-number multiples of the ignition frequency are especially important, since they produce higher order excitations. It follows that there are many conceivable speeds at which the model shown in Figure 3 can pass through resonance. However, these higher order excitations have no real effect, both because of their low energy content and because of the damping capacity inherent in the DMFW.

For this reason, the following discussion will only deal with the primary excitation. Depending on the number of ignition cycles per revolution, this is the 2nd order for a four cylinder engine, the 2.5th order for a five cylinder engine and the 3rd order for a six cylinder engine.

Figure 4 shows the calculated resonance speeds for these kinds of engines plotted as a function of the spring rate realized by the DMFW. In creating this graph, we chose to use system parameters that are typical for a compact vehicle. Resonance speeds are defined as those speeds at which the primary excitation – the ignition frequency – excites the two possible resonances in the drive train. The fact that resonance speeds decrease as the number of cylinders increases is attributable to higher ignition frequency at the same engine speeds.

Transmission ratios change the vibration model. Spring rates and inertias located after the gear set must be adapted using the square of the speed ratio. Consequently, each gear produces a different resonance curve. Therefore, the lower boundary of the various shaded areas represents 1st gear and the upper boundary, 5th gear.

Even in 5th gear, the first natural mode, surging, is positioned below 250 rpm, and exhibits virtually no remaining dependence on the torsion damper spring rate above 10 Nm/°. DMFW resonance, defined as the second natural mode, clearly reflects the influence of the number of cylinders and of the spring rate. However, it is not enough just to know the resonance speed in order to completely describe DMFW performance. We also have to take a look at the vibration amplitudes that occur.

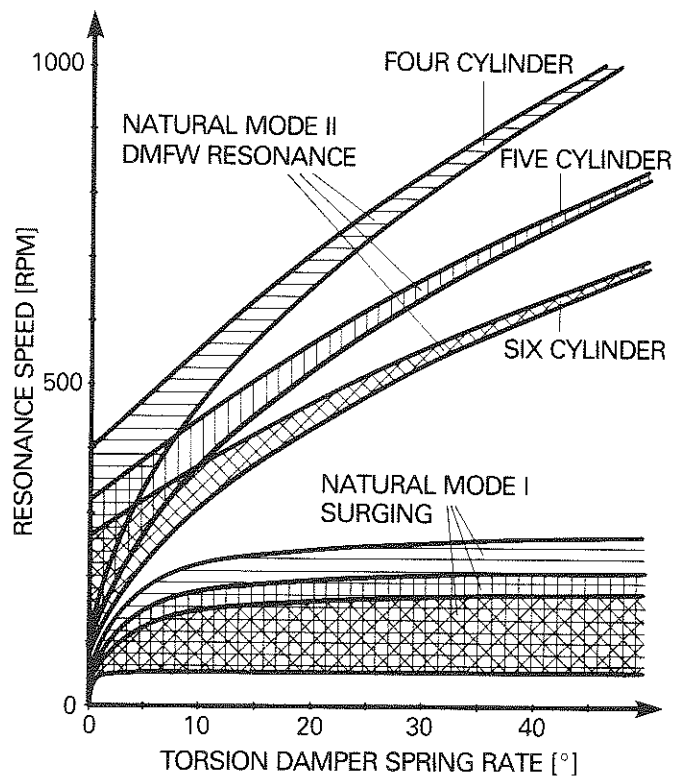


**Figure 4:**  
Resonance speed ranges

### Amplitude Curve

The vibration model shown in Figure 3 allows us to calculate the amplitudes at the transmission input shaft that are critical for transmission rattle.

Diverging from a conventional design, Figure 5 shows increased secondary inertias. This demonstrates one option used with 1st generation DMFWs. All other parameters for the model of a four cylinder application remain constant. Increasing the inertia shifts the resonance point to lower speeds. However, the vibration amplitudes increase considerably.

Although it is possible to reduce the peak amplitude, this kind of reduction requires design features such as friction or damping elements that impair the function of the DMFW in the vibration isolation range.

High peaks in transmission amplitude are typical for vibration systems that employ a large secondary inertia to shift the resonance speed. During

start-up and shut-off, the vibration system can pass through resonance. This problem can require additional complicated damping mechanisms.

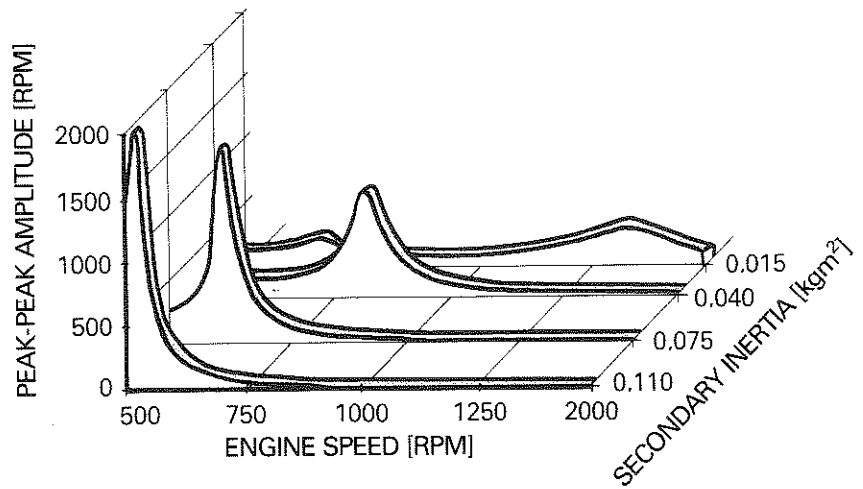


Figure 5: Variation in the secondary inertia

A higher secondary inertia on the transmission side, coupled with a lower spring rate, can significantly shift the resonance speed in a favorable direction. Figure 6 shows resonance curves for a DMFW whose secondary inertia – 0.110 kgm<sup>2</sup> – corresponds to the first curve in Figure 5. In this case, the torsion damper spring rate has been varied.

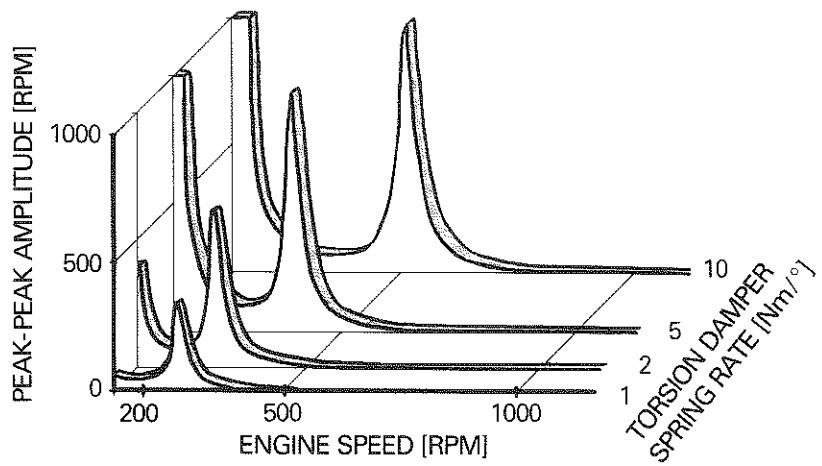
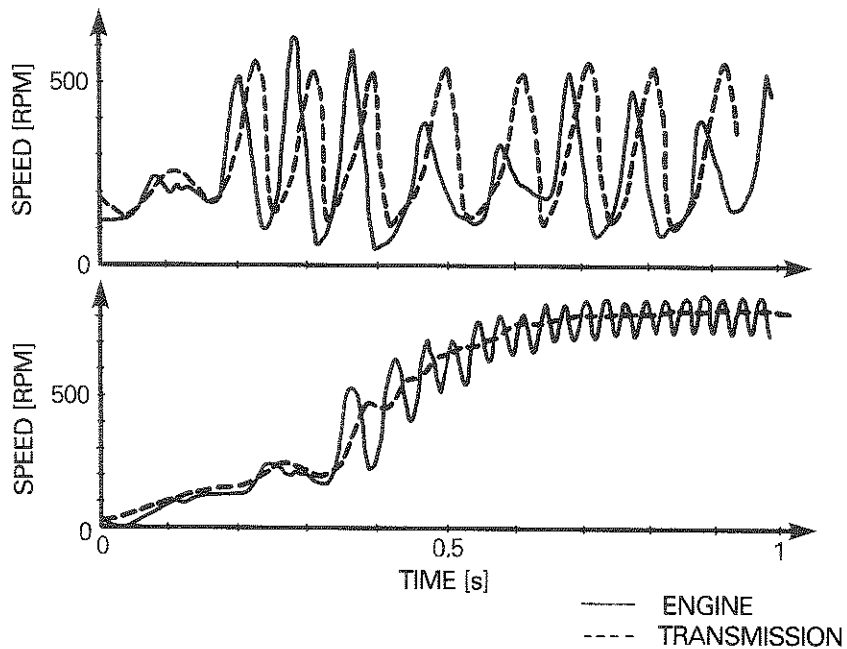


Figure 6: Variation in the spring rate  $C_{TD}$

Note in particular in this case that using softer springs not only shifts the resonance range to lower speeds, but also reduces vibration amplitudes considerably without introducing any additional corrective features, that is, without adding supplemental damping devices.

### Start-up Measurements

The graph in Figure 7 shows the measured curve for engine and transmission input speeds during engine start-up. These curves illustrate the undesirable consequences that can result when the system passes through resonance in conjunction with a high spring rate. This is an example where the system gets stuck in the resonance range. This can occur primarily in diesel vehicles after a very brief activation of the starter motor.



**Figure 7:** Measured start-up curve (diesel)

Because the diesel fuel injection pump is already injecting fuel at the maximum rate during this phase, it is even impossible to accelerate up to idle speed by stepping on the gas. In this kind of extreme circumstance,

very severe dynamic stresses can occur, which vastly exceed the maximum engine torque and can destroy the dual mass flywheel in a very short time.

The graph shown in the bottom of the illustration demonstrates how we can completely eliminate this tendency to "get stuck" in the resonance mode. This is accomplished by significantly decreasing the spring rate, which in turn reduces the associated resonance speed to about 200 rpm. In this case, we achieve good vibration isolation above starter speed. This eliminates the overloading of the DMFW during resonance operation. This advantage is associated with additional improvements in noise comfort when the system does pass through resonance, such as during engine start-up and stop.

In the case of gasoline engines, there is no danger of start-up resonance. However, a low spring rate does produce clear-cut improvements during the start-up phase (Figure 8). Lower spring rates enable us to achieve lower transmission amplitudes during start-up, which yields improved noise performance.

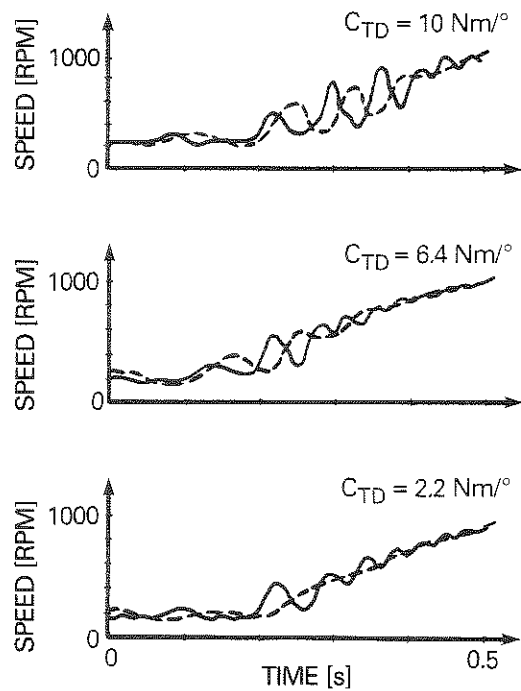


**Figure 8:**  
Measured start-up curve  
(gasoline engine)

— ENGINE  
- - - TRANSMISSION

## Damper Capacity

Up to this point, the discussion has clearly indicated the decisive significance of a low spring rate for ensuring reliable DMFW operation. Vibration isolation can be extended to significantly lower speeds, and the start-up resonance, which was much-feared in the early years of DMFW development, can be avoided without employing additional, expensive corrective measures.

Hence the spring rate or damper capacity has become the deciding factor for achieving optimum DMFW performance today. The elastic energy  $Q$  stored in the springs of a torsion damper is described by the area under the wind-up characteristic, which can be calculated for a linear spring rate using the equation

$$Q = \frac{1}{2} \cdot M \cdot \varphi \quad (1)$$

where  $M$  = torque capacity [Nm]

and  $\varphi$  = maximum wind-up angle [°]

The maximum amount of energy that can be stored in the damper – in short the damper capacity – constitutes the primary design variable. Figure 9 provides a graphic illustration of the historical development of damper capacity in dual mass flywheels.

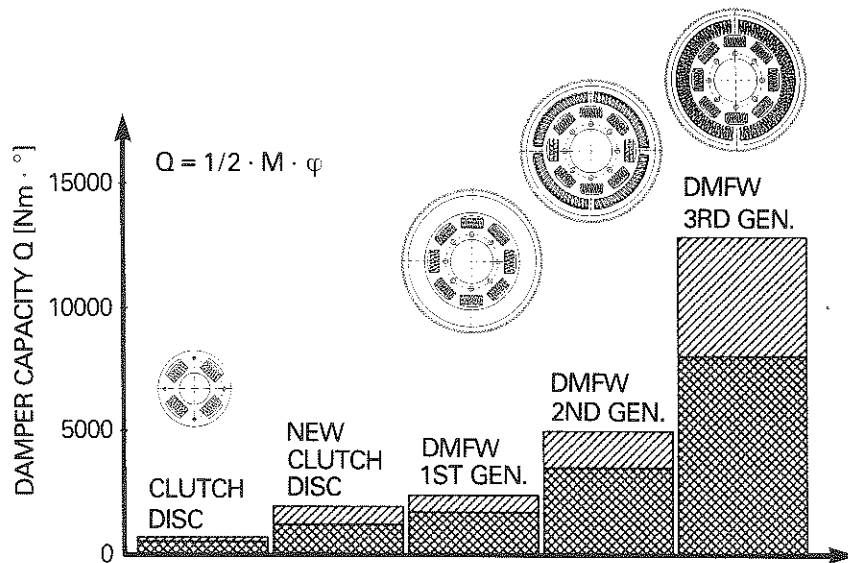


Figure 9: Torsion damper capacity

As the basis for our comparison, we chose a conventional torsion damper in a standard design that is still widely used. This damper is shown on the left of the chart in Figure 9, followed by a modern LuK long-travel clutch disc.

The first generation DMFW contained spring configurations like those used in conventional torsion dampers, with the coil springs arranged far to the inside. This design provided only a minimal space for coil springs, accompanied by modest damper capacity.

Without increasing the installation space required by the dual mass flywheel, we have been able to achieve a five-fold increase in damper capacity by:

- shifting the springs to the outside
- using a serial instead of parallel spring arrangement wherever possible
- using large-diameter coil springs.

### **Implemented Spring Rates**

Equation (1) shown above indicates that damper capacity is proportional to the product of the max. torque and the max. wind-up angle. Hence, the lowest achievable spring rate depends on the available installation space as well as the maximum engine torque. Figure 10 shows the spring rates achieved for different DMFWs in different vehicles, plotted as a function of engine torque.

The differences between the three DMFW generations are very clear. The first generation of DMFWs was based on mass as the primary design consideration. These were special solutions that could not be employed for a wide range of applications because of their high spring rates. With the newly developed DMFWs of the third generation, we can solve the noise problems in virtually all vehicles.

In spite of variations in installation space and DMFW-diameter, spring rates lie very close to the line of best fit drawn on the graph. This graph also allows us to make a rough estimation of the slopes that we can expect to use in future vehicles.

Figure 10 shows the achievable spring rate as a function of engine torque. However, it is impossible to read the resonance speed from this graph. As noted above, this value depends on the number of cylinders and hence on the order of the primary excitation.



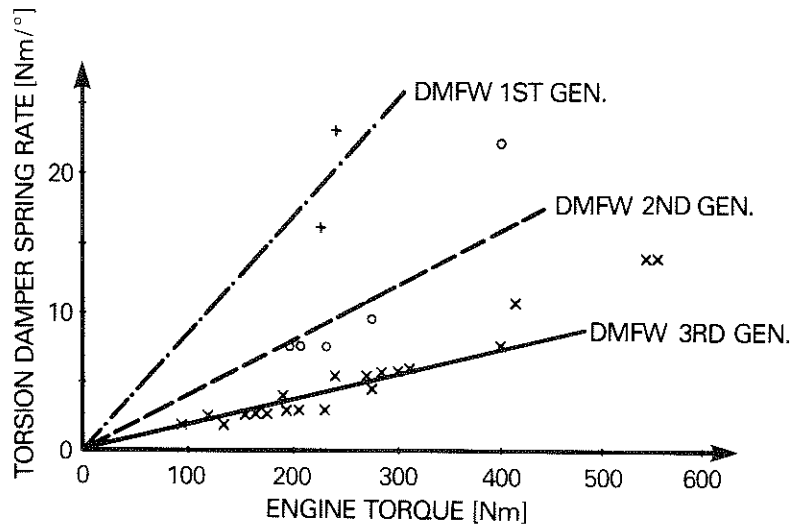


**Figure 10:** Spring-rate – engine torque

Figure 11 shows the resonance speeds actually obtained, plotted as a function of the maximum engine torque and the number of cylinders.

The vertical bars represent the critical speed ranges in the various gears for a given vehicle. The top of each bar corresponds to fifth gear and the bottom to first gear. This speed value can also be used for idle mode, provided that there is no separate torsion damper stage.

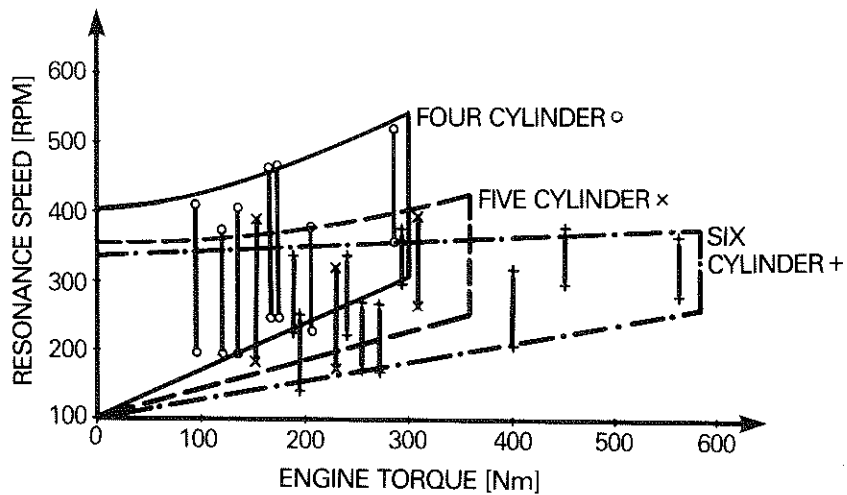


**Figure 11:** Resonance speed ranges for four, five and six cylinder engines

## Distribution of Mass

In order to obtain the lowest possible resonance speed for a given total DMFW mass, theoretical considerations [5, 6] indicate a mass distribution of:

$$\lambda = J_1/J_2 \leq 1$$

Where  $J_1$  is the sum of the torsional inertias associated with the primary flywheel ( $\approx 60\%$ ), the crankshaft plus the rotating components of the crank drive ( $\approx 35\%$ ) and the damper components, and where  $J_2$  includes the torsional inertias for the secondary flywheel ( $\approx 50\%$ ), the clutch ( $\approx 40\%$ ), the clutch disc, damper components, and the transmission.

However, there are frequently a number of reasons why we have to deviate from this ideal value ( $J_1 \leq J_2$ ). For instance, we must provide an acceptable thermal capacity for the clutch system on the secondary side of the DMFW. In addition, engine irregularity is determined by the inertia of the primary side of the DMFW. Maximum permissible engine irregularity is determined by the accessory drives attached to it. Figure 12 shows values that are currently realistic.

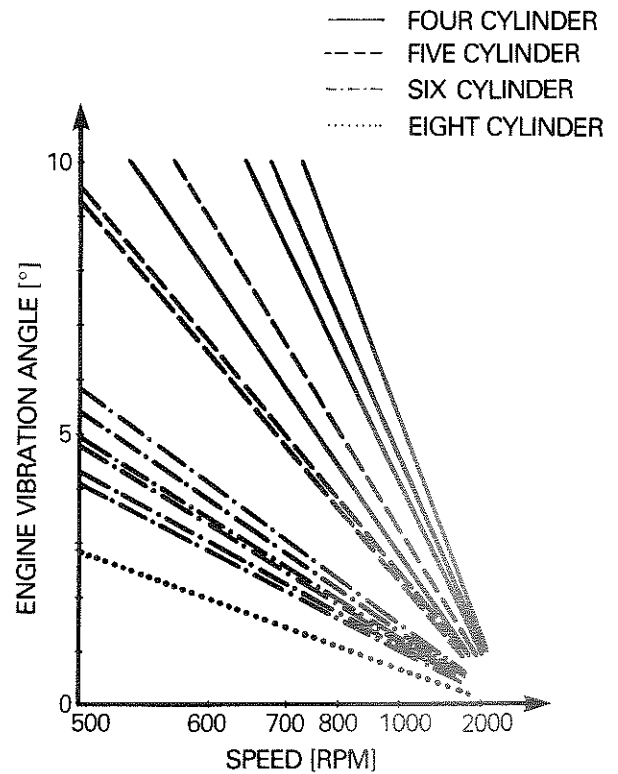


**Figure 12:**  
Comparison of engine  
vibration angles

The engine vibration angle – measured at full load – is plotted as a function of engine speed for a wide variety of vehicles.

The speed scale is plotted quadratically in order to approximate straight lines. As anticipated, engine irregularity is higher for lower cylinder numbers.

It is impossible to make general statements about max. permissible values because these values are determined individually in each vehicle based on marginal conditions. In isolated cases, it is necessary to employ an additional ring-shaped inertia on the primary side in order to reduce irregularity. Even in such special cases, LuK has proven solutions available.

### **DMFW with Torque Limiter**

Figure 13 shows the simplest modern DMFW design.

The primary flywheel is made of formed sheet metal parts. The main functional component of the DMFW consists of two arc springs, each featuring a second inside spring. These spring assemblies are arranged in two 170° semi-circles. The spring guide races are situated far to the outside of the flywheel in order to provide the most favorable effective diameter. A second important functional component, the torque limiter, is located further in toward the center of the flywheel. This device features a carefully designed slip coupling, which absorbs any torque peaks that occur. The maximum torque that can be transmitted by this component determines the stress limit for all other components.

The inside of the primary side of the DMFW is filled with grease. A membrane that requires very little axial installation space provides an effective seal to prevent this grease from contaminating surrounding components.

If the primary and secondary sides of the DMFW are rotated in opposition to one another, the lubricated arc-shaped coil springs glide in the spring guide races.

Because the springs are arced, the actuating forces on the two springs are not oriented in the same direction. As a result, the arc springs load the spring guide races with a radial force component. Centrifugal force

increases this radial force of the arc springs. This generates friction between the spring coils and the spring races, which has a critical influence on the characteristics of the DMFW.

In order to study this important effect and to account for it with respect to the DMFW design, LuK designed a new kind of test stand for dynamic measurement of DMFW and conventional torsion damper characteristics at different speeds. The test stand can achieve wind-up angles of up to  $\pm 50^\circ$  with frequencies of 0 – 30 Hz and speeds up to 6,000 rpm.

This test stand has provided the impetus for DMFW development.

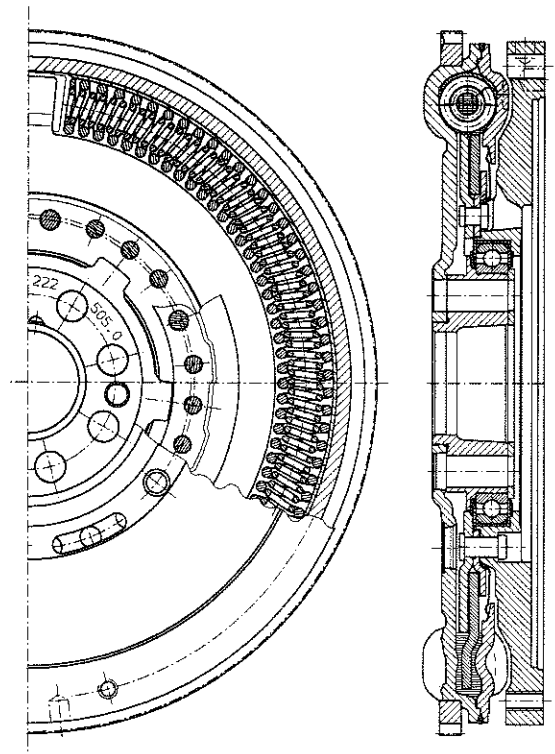


**Figure 13:**  
DMFW with torque limiter

The measurements in Figure 14 show effects that are only obtainable with the dynamic torsion test stand.

We measured so-called partial loops. The test was run with an angle of  $\pm 1^\circ$ , working around an operating point of 150 Nm in drive mode at a frequency of 1 Hz. The superimposed speed was varied in stages from 0 to 2,000 to 6,000 rpm. The results indicate a massive change in the characteristic for the partial loops. The frictional hysteresis increases with the speed. At the same time, the characteristic becomes stiffer because part of the arc spring coils are blocked by static friction.

The stiffer spring rate increases the resonance speeds, and the increased frictional hysteresis increases damping. Both factors diminish the isolation effect of the DMFW. In most vehicles, this does not cause any problems because engine irregularity decreases at higher speeds, so trade-offs can be made with respect to the filtering function.

However, in individual cases, boom and rattle noises are still audible at higher speeds, thus requiring improved vibration isolation. LuK offers the DMFW with a decoupled inner damper as a solution for these vehicles.

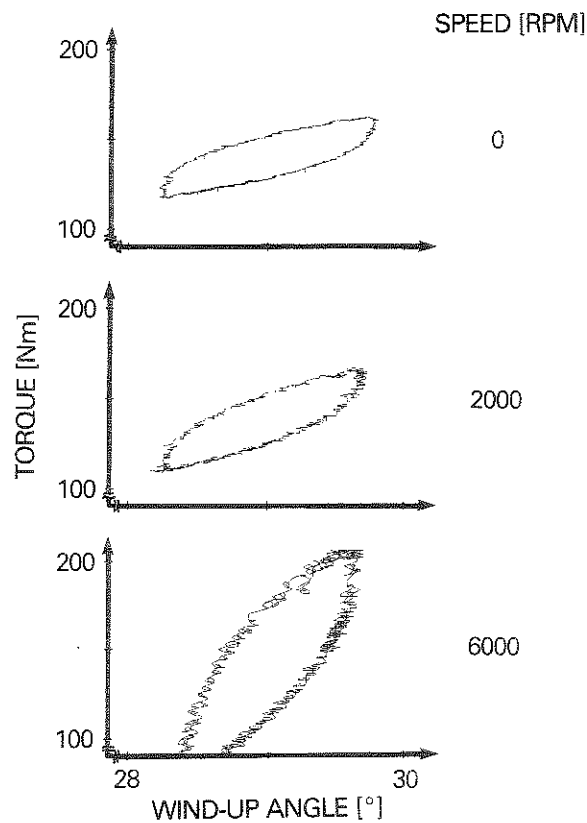


**Figure 14:**  
DMFW with torque limiter  
partial loop in the drive  
range

## DMFW with De-coupled Inner Damper

Once we had recognized the problem posed by centrifugal forces in certain vehicles, we attempted to decrease friction at high speeds. These efforts resulted in a DMFW like the one shown in Figure 15. This design uses two serial dampers, which, to a certain extent, serve two different functions.

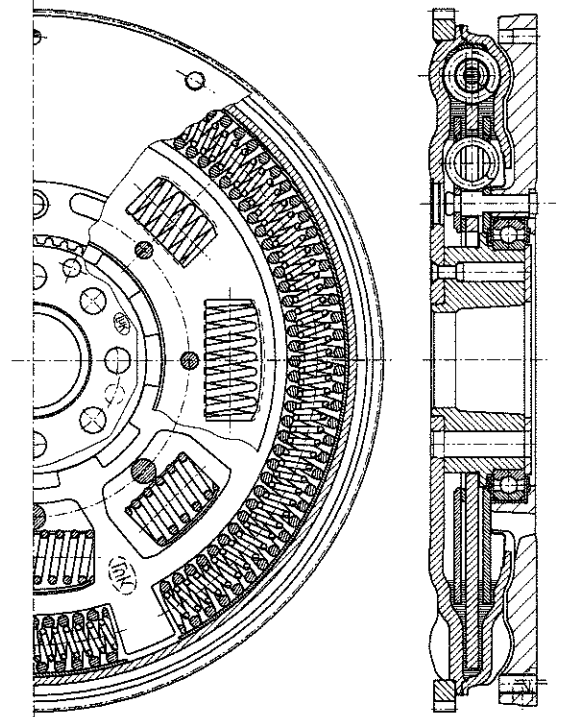


**Figure 15:**  
DMFW with de-coupled  
inner damper

The outside damper design corresponds essentially to the large arc springs described in Figure 13, with their favorable effective diameter and their low spring rate. The spring rate and hysteresis of the arc spring damper are speed-dependent, as shown above. A second serial damper with short straight coil springs in conventional spring windows is installed on the inside of the dual mass flywheel in place of a torque limiter. Because only the end coils of the springs make contact and the actuating forces at the spring ends are oriented in the same direction, the internal friction of this damper is virtually independent of load and speed. Hence

we can speak of it as being decoupled. Consequently, as shown in Figure 16, the frictional hysteresis and the effective spring rate no longer increase with rising speed. The good vibration isolation of the DMFW is maintained up to the highest speeds. As a result, this design is called a DMFW with de-coupled inner damper.

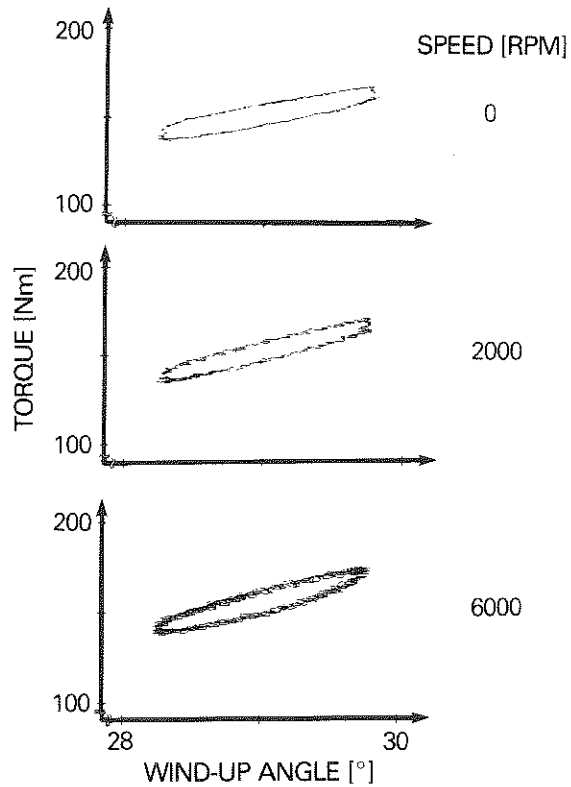


**Figure 16:**  
DMFW with de-coupled inner damper; partial loop in the drive range

The static spring rate for the inner damper is naturally higher than that for the outer arc spring damper because of the lower achievable damper capacity. When combined with the secondary dual mass flywheel inertia attached to the transmission, this somewhat stiffer characteristic curve is quite sufficient to cope with higher speeds (see Figure 5). The very soft serial arc spring damper becomes effective at higher vibration amplitudes, for instance as a result of increased engine irregularity at lower speeds or also because of tip-in/back-out.

The models shown in Figure 17 summarize both basic systems used in current DMFW designs. The speed-dependent arc spring damper is combined with either a torque limiter or an inner damper and arranged between the two DMFW inertias.

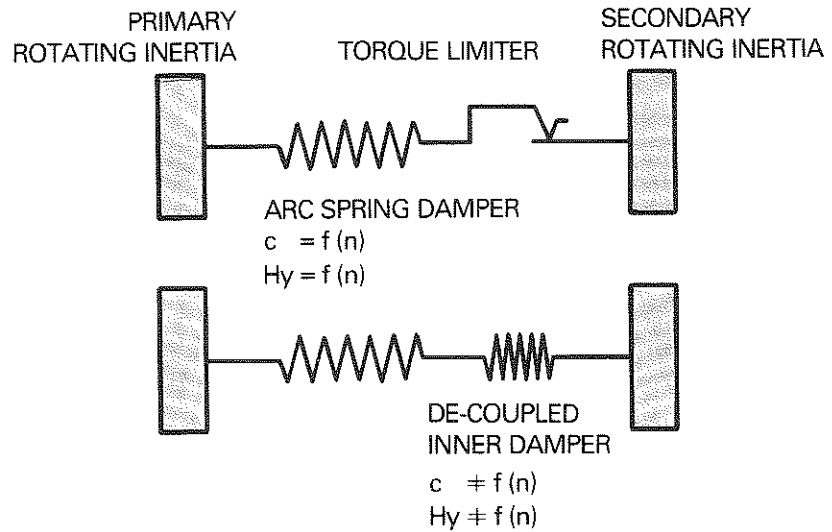


**Figure 17:** DMFW vibration model

One further closing comment on DMFW design must be noted here. The foregoing discussion of DMFW design options has presented the two subsystems – the torque limiter and the decoupled inner damper – as alternatives. It is important to note that the inner damper cannot fulfill the role of the torque limiter, which is to say, it cannot reduce excessive torques. It can be necessary to combine the two systems.

Actually, in many cases it is also possible to do without the torque limiter. The serial arrangement of the inner damper achieves additional reduction in the DMFW spring rate, accompanied by low resonance speeds and vibration amplitudes, as shown in Figure 6. The incidence of resonance operation, for instance when a vehicle stalls in gear at a traffic signal or during start-up, is diminished or even fully eliminated. In these cases, excessive torques are prevented entirely, rendering the torque limiter unnecessary.

LuK's experience, plus a few tests on our engine tests stands and in special vehicles, provide the necessary information for determining whether a torque limiter is required. These tests can be limited to the resonance range, that is to start-stop operation and driving at extremely low engine speeds.



## Tip-in / Back-out Performance

Up until now, this discussion has dealt with the 2nd natural mode of the vibration model shown in Figure 3, which is responsible for resonance conditions in the DMFW. The following section of this presentation will deal with the influence of the new DMFW generation on surging and tip-in/back-out performance. These operating conditions are described by the 1st natural form of the basic model.

As shown in Figure 3, the central inertia, that is the secondary flywheel mass, is located very close to a vibration node and is therefore hardly involved in the vibration. The total effective spring system situated between the engine and the vehicle can be viewed as a serial arrangement consisting of the torsion damper and the drive train. This observation reveals that the only way to affect tip-in/back-out performance is to decrease the torsion damper spring rate until it is in the order of magnitude of the drive train spring rate.

It is impossible to achieve the required spring rate using a conventional torsion damper. By introducing the super-long-travel DMFW, we have been able to obtain values below the drive train spring rate.

This applies particularly for 3rd, 4th and 5th gears because the spring rate of the drive train is proportional to the square of the drive line ratio and thereby significantly higher in higher gears. Hence it is that much simpler to remain below this value and thus to improve surging.

We have to consider tip-in and back-out in the lower gears to be the critical operating conditions. We have plotted measurements and calculated values for second gear in order to illustrate these influences.

Let us look again at Figure 4. The lower section of the graph shows the resonance ranges for "surging vibrations" in the first natural mode as a function of the torsion damper spring rate. The resonance speed depends greatly on the gear selected. This factor is reflected in the very broad fields for the different cylinder numbers. It is impossible to achieve any significant influence on the surging resonance speed until we get below a  $10 \text{ Nm/}^\circ$  rate in the torsion damper. This point comes at the beginning of the upper limiting curve for the 5th gear.

Until now, only the influence of the spring rate on the resonance speed has been viewed with respect to surging natural mode. If we use a correspondingly low spring rate, it is possible to shift this speed, which means we can change the frequency at which surging becomes

perceptible in the vehicle during tip-ins and back-outs. However, this factor alone will not produce any improvement in tip-in/back-out performance. In fact, theoretically speaking, the lower spring rates can even result in deteriorated tip-in/back-out performance. Consequently, in addition to the spring rate, the damping performance of the super-long-travel DMFW is very important.

The computer simulation shown in Figure 18 is designed to clarify the relationships involved here. These calculations were based on a typical compact vehicle in which vehicle surging – as described by the engine and transmission speeds – is calculated based on a sudden tip-in/back-out. At point 1, the driver steps down full on the gas, and at point 2 he lets up on it suddenly. The graphs show variations in the hysteresis, which acts as a damping factor in the DMFW.

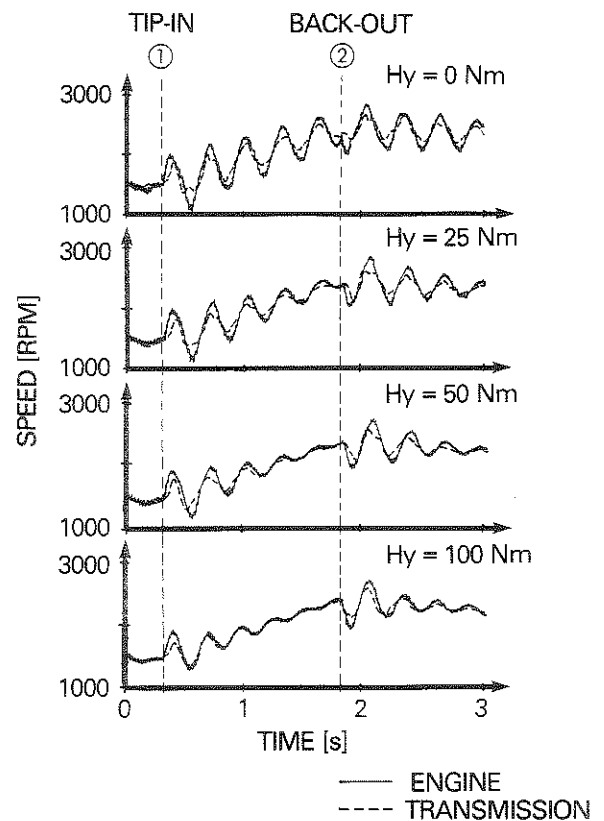


**Figure 18:**  
Tip-in/back-out calculations  
with hysteresis variation for  
 $C_{TD} = 2 \text{ Nm}/^\circ$

The top section of the graph shows the situation for a DMFW that displays virtually no friction. Damping in the drive train is limited. The vibration excited by the tip-in and the later back-out only decays slowly.

We do not achieve good damping performance until we superimpose an appropriate frictional hysteresis on the very long torsion characteristic. Consequently, we can't allow the damping factor to approach zero for the kind of wide wind-up angles that occur in the DMFW during tip-in and back-out. This consideration runs counter to the requirement for the best possible isolation of high-frequency engine excitation in the range above the natural frequency.

However, the following measurements shown in Figure 19 indicate that LuK's super-long-travel DMFW exactly meets these requirements, even though they appear at-first-glance to be contradictory. Partial loop measurements using small wind-up angles such as those that occur during constant load condition show a low frictional hysteresis. This indicates low damping accompanied by correspondingly good isolation. However, when we measure the DMFW characteristic over the entire wide wind-up angle, we discover a high hysteresis. This very high DMFW friction is effective over a very wide wind-up angle and is capable of effectively damping objectionable surging vibrations during tip-in/back-out.

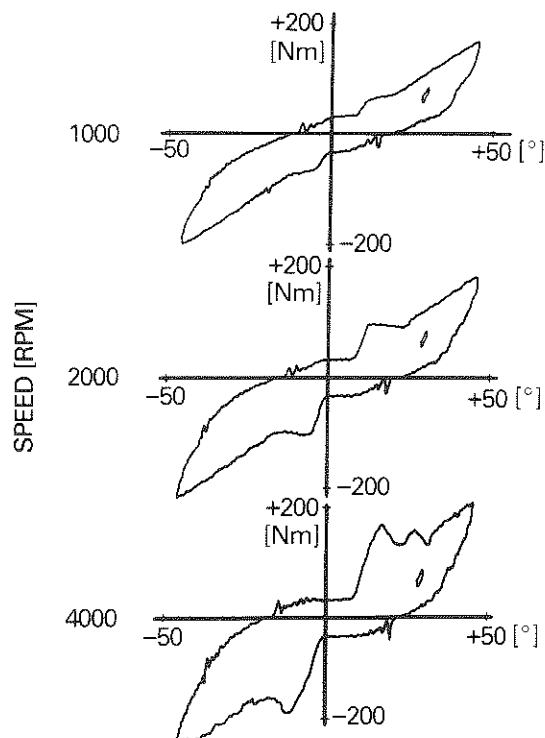


**Figure 19:**  
Dynamic measurements  
tip-in/back-out and  
partial loop

This damping performance is generated primarily by the fact that the arc springs are radially supported against the spring guide races. Furthermore, we can also introduce an additional controlled frictional hysteresis by adding a friction control plate in order to tailor the DMFW characteristic to the requirements of the vehicle in question. Due to these design features, the friction generated in this system is not significantly dependent on centrifugal force.

The interaction of a DMFW with a very low spring rate and an appropriately designed frictional hysteresis for damping purposes improves vehicle performance during tip-in and back out. The tip-in/back-out calculations shown in Figure 20 again clearly illustrate the influence of the torsion damper spring rate in this context.

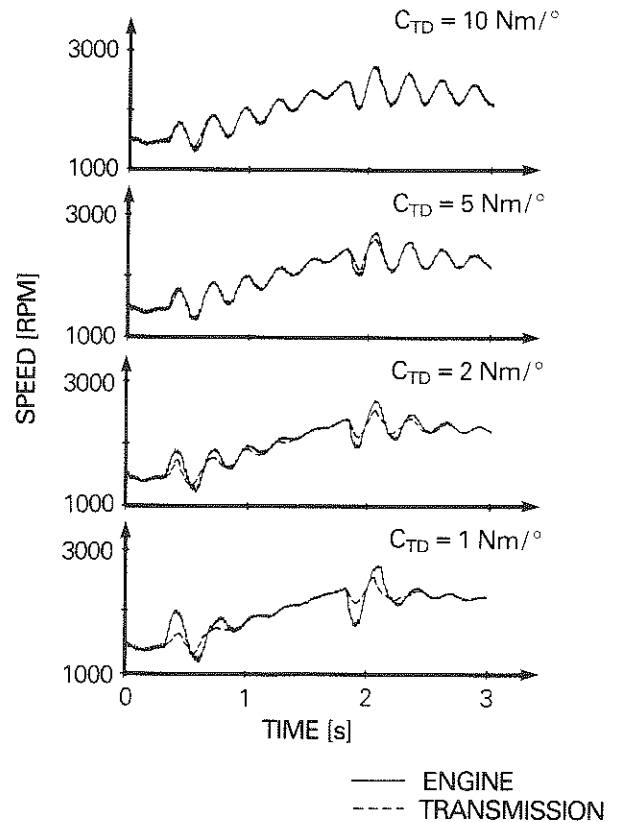


**Figure 20:**  
Tip-in/back-out calculations  
with spring rate variation  
for  $H_y = 75 \text{ Nm}$

Damping accelerates as the torsion damper spring rate decreases, although the first peak engine amplitude increases as a result of good decoupling.

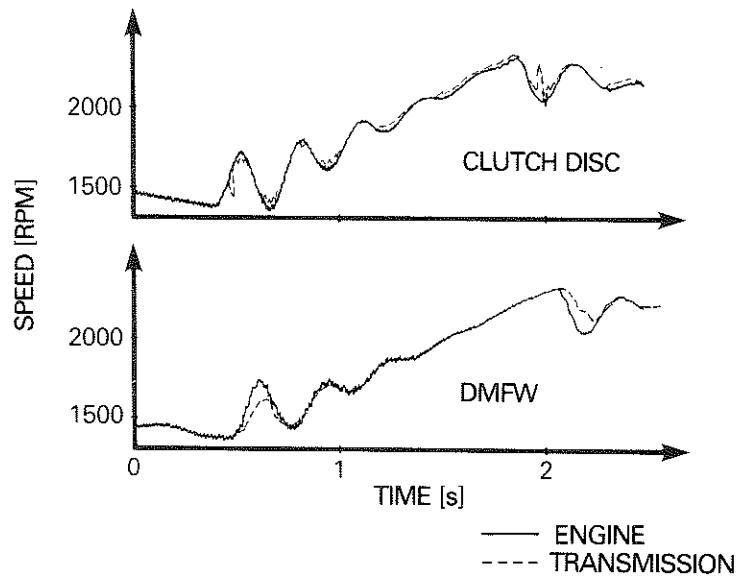


**Figure 21:** Tip-in/back-out measurements 2nd gear with clutch disc and DMFW

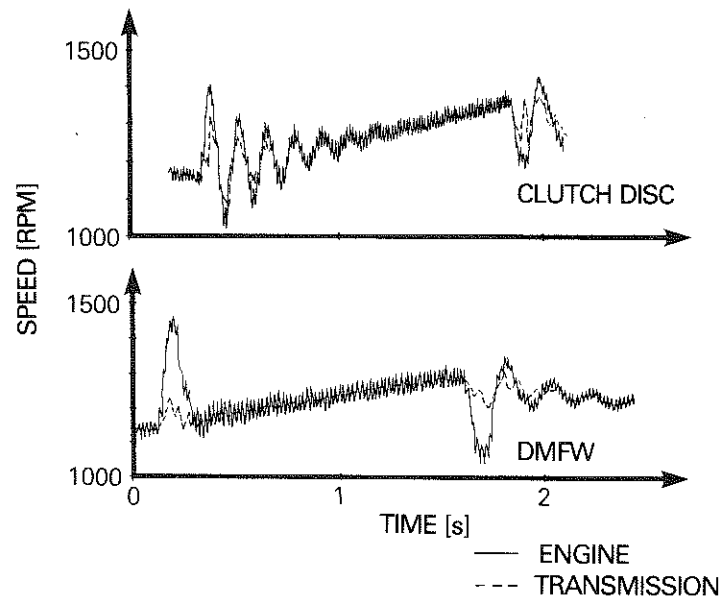


**Figure 22:** Tip-in/back-out measurements 4th gear with clutch disc and DMFW

In the case shown (Figure 21), the 2nd gear torsion damper spring rate  $C_{TD}$  and the drive train spring rate  $C_A$  are of the same magnitude, at  $2.5 \text{ Nm}/^\circ$  each. Surging amplitudes decay rapidly with the DMFW.

In 4th gear (Figure 22) with a drive train spring rate of  $7 \text{ Nm}/^\circ$ , we register no subsequent bounces, while several bounces were still evident when we conducted the same measurement for the clutch disc.

## Summary

Thanks to on-going, consistent development of the DMFW, LuK can now offer a dual mass flywheel solution to improve noise comfort and driving performance for almost all vehicle models and for a wide variety of engines, including four cylinder engines.

LuK's newest DMFW designs demonstrate that resonances can be shifted far out of the driving range and that transmission rattle and boom can be effectively eliminated. We have been able to prove this trend on many vehicles, using measurements, theoretical calculations, and subjective evaluations. We are even able to achieve positive results combatting vehicle surging.

Increased production and unbroken interest confirm that the dual mass flywheel is an ideal solution for increasing noise comfort and improving the future marketability of modern vehicles. LuK is in a position to commit its entire DMFW know-how to an individual customer's needs with respect to development, production and quality assurance in order to ensure a mutually profitable future through improved technology.

## Bibliography

- [1] Reik, W.  
Schwingungsverhalten eines Pkw-Antriebsstranges mit Zweimassenschwungrad [Vibration Performance of a Passenger Car Drive Train with Dual Mass Flywheel], VDI Berichte 697, p. 173/21
- [2] Sebulke, A.  
The Two-Mass Flywheel – A Torsional Vibration Damper for the Power Train of Passenger Cars – State of the Art and Further Technical Development, SAE Technical Paper Series (870394), 1987, p. 1/10
- [3] Lorenz, K., Wanzung, F.  
Zwei-Massen-Schwungrad – Erfahrungen in Fahrzeug und am Prüfstand [Dual-Mass Flywheel – In-vehicle and Test Stand Experience], VDI Berichte 697, p. 195/22
- [4] Schöpf, H.-J., Jürgens, G. and Fischer, R.  
Optimierung der Komforteigenschaften des Triebstranges von Mercedes-Benz-Fahrzeugen mit Schaltgetriebe [Optimization of Comfort Characteristics in the Drive Train of Mercedes Benz Vehicles with Manual Transmissions], Automobiltechnische Zeitschrift 91 (1989), p. 568 – 575
- [5] Schulte, L.-F.  
Funktion und Konstruktion eines Zweimassenschwungrades [Function and Design of a Dual Mass Flywheel], Automobil Industrie 2, 1987, p. 199/26
- [6] Reik, W.  
Das Zweimassenschwungrad [The Dual Mass Flywheel], 1st Aachener Symposium for Vehicle and Engine Engineering 1987, p. 615–35

# Torque Control Isolation (TCI) The Smart Clutch

Dr.-Ing. Albert Albers

In recent years the main emphasis in the development of clutches and clutch discs has shifted more and more in the direction of the torsion damper [1, 2], as has been indicated by the previous presentations. This work is centered on drive train dynamics, with the goal of improving driving comfort with respect to:

- transmission noises (rattle)
- body boom
- tip-in/back-out performance (surging)

Developments in modern automotive engineering have contributed to the importance of this design trend as a result of

- reduced idle speeds to improve fuel efficiency
- more rapid combustion and higher engine torque output
- transmission designs that allow driving at low engine speeds with respect to the gear selected
- reduced weight designs
- traffic situations (traffic jams, stop & go traffic).

Conventional torsion dampers (as shown at the top of Figure 1) affect drive train dynamics only with respect to spring rate and hysteresis. The dual mass flywheel shifts the distribution of inertial masses in the drive train and allows further spring rate reductions. Application of these systems alters the parameters of the torsional vibration chain, but does not allow for any on-going adjustment in overall performance.

Another approach to affecting drive train dynamics returns us to the clutch itself. In a conventional system, the clutch represents a shiftable shaft connection that has no effect on performance during normal driving operation. Consequently, the clutch does not appear explicitly in either the model for the torsion damper or the model with the dual mass flywheel.

However, if we introduce the clutch with its transmitting parameters as an element in the vibration model, we completely alter the system. The clutch clamp load represents a constantly changing system variable that not only



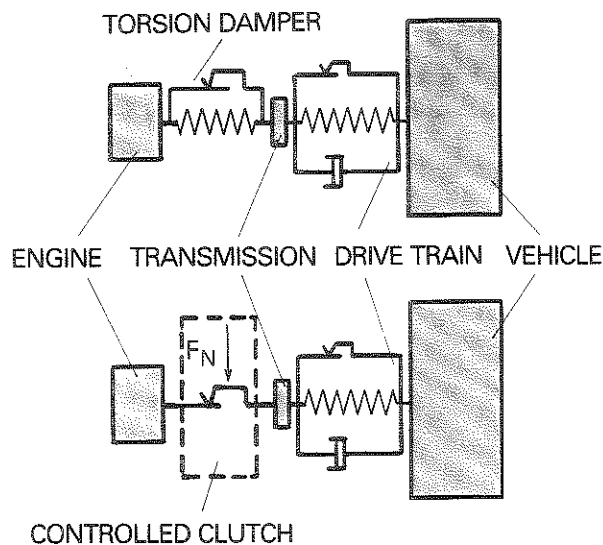
actively affects dynamic behavior, but which can actually be used to manage it [3, 4, 5, 11, 19].

In developing torque control isolation (TCI), LuK has created a total system in which an electronically controlled clutch has been designed to have an impact on overall dynamic drive train performance.

With TCI, LuK has succeeded in significantly improving two major areas:

- Original clutch actuation for start-up and shifting gears is automated, thus considerably increasing vehicle operating comfort. At the same time, the design improves driving safety because gear shifting procedures have been simplified considerably.
- Active control of dynamic drive train performance during vehicle operation, coupled with vibration isolation of torsional engine irregularities, considerably enhances driving comfort.

#### VIBRATION MODEL – CONVENTIONAL SYSTEM



#### VIBRATION MODEL – TORQUE CONTROL ISOLATION SYSTEM

**Figure 1:**  
Vibration models for vehicles with Torque Control Isolation

## Drive Train Configuration in Vehicles with TCI A Model of the Vibration System

The bottom section of Figure 1 shows the simplest vibration model for the vehicle drive train with TCI in comparison to the conventional model. Between the engine and the transmission inertias, we have now introduced a component that allows torque transmission via lock-up between the friction surfaces. The torque transmitted can be controlled by the clamp load. In this model, the entire drive train represents a controlled system. In order to develop an appropriate control strategy for this system – the entire drive train – it is necessary to determine and describe the controlled system mathematically, along with any possible disturbance variables. We will discuss a number of important basic relationships.

### Force Transmission via Friction Surfaces The Physical Principle

The most important component in this controlled system is the clutch with its friction surfaces. The friction phenomenon between two bodies manifests itself in two different forms:

- resistance to the maintenance of an existing relative movement between two bodies: dynamic friction
- resistance to the initiation of a relative movement of one body relative to another: static friction.

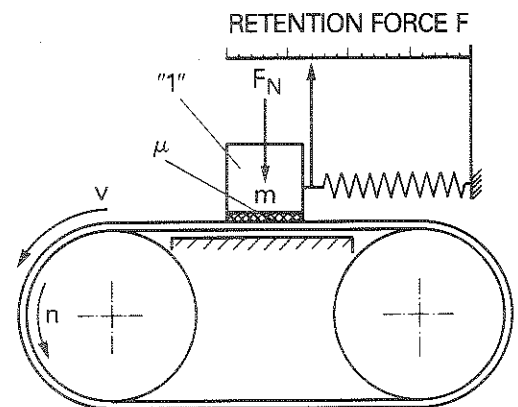


Figure 2:  
Coulomb friction

$$F_R = \mu \cdot F_N$$

Figure 2 shows a simple model representing the relationships described here. Body 1 having the mass  $m$  rests with the weight  $F_N$  on a belt. The rollers can set the belt into motion. A spring holds Body 1 in place.

If the belt starts to move, Body 1 starts to move along with it, and the static friction force  $F_{RH}$  transmitted due to friction contact deflects the spring. According to Coulomb [6], the friction force is proportionate to the normal force exerted on the contact surface, that is:

$$F_{RH} \leq F_{R,o} = \mu_o \cdot F_N.$$

As soon as the retention force  $F$  reaches the maximum transferrable static friction force  $F_{R,o}$ , Body 1 cannot deflect the spring any further. Since the belt continues to move, a relative motion occurs between the belt and Body 1. The dynamic friction

$$F_R = \mu \cdot F_N$$

acts by the proportionate factor  $\mu$ , which is the dynamic coefficient of friction.

If we assume that the static coefficient of friction  $\mu_o$  and the dynamic coefficient of friction  $\mu$  are equal and constant, then there is no difference between the forces  $F_{RH}$  and  $F_R$ . Given this assumption, Body 1 remains in the equilibrium position for the spring.

Increasing or decreasing the speed of the belt does not change the position of Body 1 because dynamic friction remains constant. A periodic motion, for example such as that produced by the irregularity of an internal combustion engine as described in Presentation 1, can be introduced at the belt drive without moving Body 1 from the equilibrium position it has assumed. Dynamic friction shields Body 1 from the irregular motion of the belt, that is, it constitutes a filter.

Of course, the friction coefficient  $\mu$  is by no means a natural constant [6, 7, 8]. Among other factors,  $\mu$  is a function of material mating characteristics, surface condition, unit pressure and also of the slip speed.

Slip speed variation assumes considerable importance for clutch control. Figure 3 shows basic possible curves for the dynamic coefficient of friction as a function of slip speed, differentiated according to:

- the constant friction characteristic, which corresponds to ideal Coulomb friction

- an increasing friction characteristic
- a decreasing friction characteristic.

As shown in Figure 3, if a periodically changing slip speed is introduced to the band drive for the model shown in Figure 2, it is apparent that Body 1 will remain in the equilibrium position only if the friction coefficient remains constant.

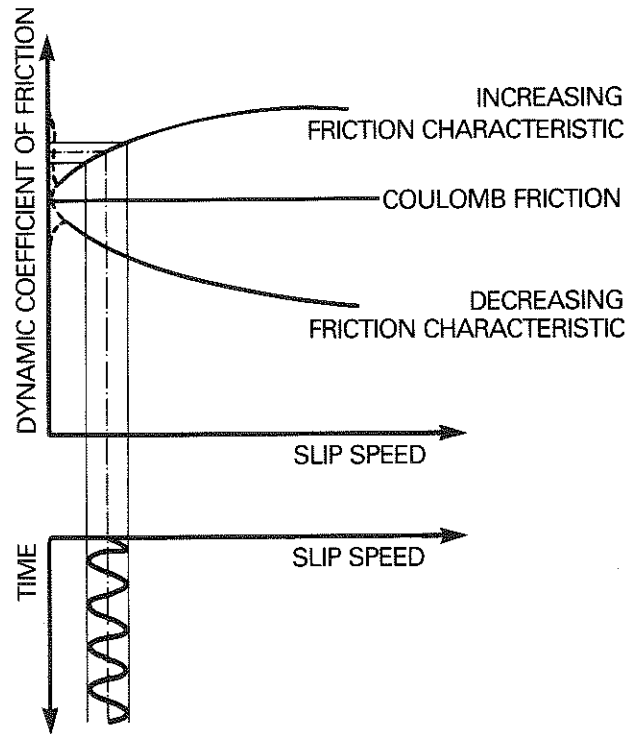


**Figure 3:**  
Basic friction coefficient curves

Given a changing slip speed, the other two friction characteristics lead to different dynamic coefficients of friction and thus to changing transmitted friction forces. This also leads to different retention forces  $F$ . Consequently, Body 1 will move in accordance with the spring characteristic in order to achieve equilibrium positions. Hence the theoretical filter effect is not 100% effective. In fact, the decreasing friction characteristic can even lead to the excitation of natural vibrations in the vibration system consisting of "Body 1 + spring" [7, 8, 9].

The following presentation on "Chatter" will treat this topic in more detail. Frictional vibrations have a decisive impact on the development of a control system because they determine the stability limits of the control loop. Furthermore, the increasing friction characteristics combined with the response times and delay components present in every system can produce phase-excited instabilities in the controlled system. These factors must also be considered in designing the control strategy.

A simple model represents some of the most important characteristics of the controlled system for such a drive train with a friction clutch. If we represent the simplified linear system as the rotational vehicle drive train system, then the "belt" becomes the friction surfaces of the clutch and the flywheel. "Body 1" with the "retention spring" becomes the rest of the drive train, consisting of the clutch disc with its facings, the transmission and the vehicle, as well as the spring characteristics of the drive train (spring rate) (Figure 4).

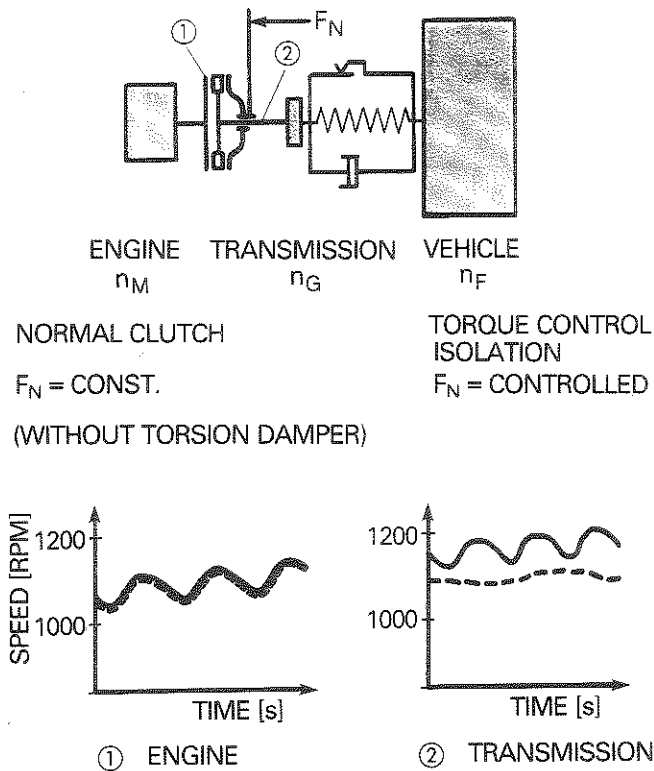


**Figure 4:**  
The friction clutch as a vibration filter

The bottom section of Figure 4 shows two speed measurements. Measuring point 1 is located on the engine flywheel and measuring point 2 is located at the transmission input shaft. In a system with a "normal" clutch, the clamp load  $F_N$  is designed so that even the highest engine torque is transmitted due to static friction. In the measurement, it becomes clear that the periodic irregularity of the engine is completely transmitted to the transmission input and thus, for instance, excites gear rattle. When we use the LuK TCI as shown in the measurement on the right, the filter effect achieved becomes evident. The clutch is controlled so that the engine torque is transmitted with a defined relative movement, that is, sliding with a certain slip. In spite of the fact that the excitation remains identical on the engine side, virtually no irregularity occurs at the transmission input (measuring point 2) – the "slipping clutch" filter is doing its job. The difference between the average engine speed and the transmission input speed corresponds to the controlled slip.

### **LuK's Torque Control Isolation (TCI) In-Vehicle Realization**

In order to turn the clutch into a "smart" clutch and to achieve the demonstrated filter effect in the vehicle, LuK has developed an electronic clutch control system as shown in the block diagram in Figure 5. The system consists of 4 major components:

- mechanical single-disc clutch as an actuator
- hydraulic power control of the actuator
- electronic microcomputer control
- sensor system.

The interaction of all four components must be carefully optimized in order to solve the problems associated with both

- automatic clutch operation and
- driving with torque control isolation.

A setpoint is selected in order to determine the torque to be transmitted by the responding actuator – the clutch. The 40 – 60 bar hydraulic system actuates the clutch via a servo cylinder controlled by a proportional valve. Figure 6 shows the most important components.

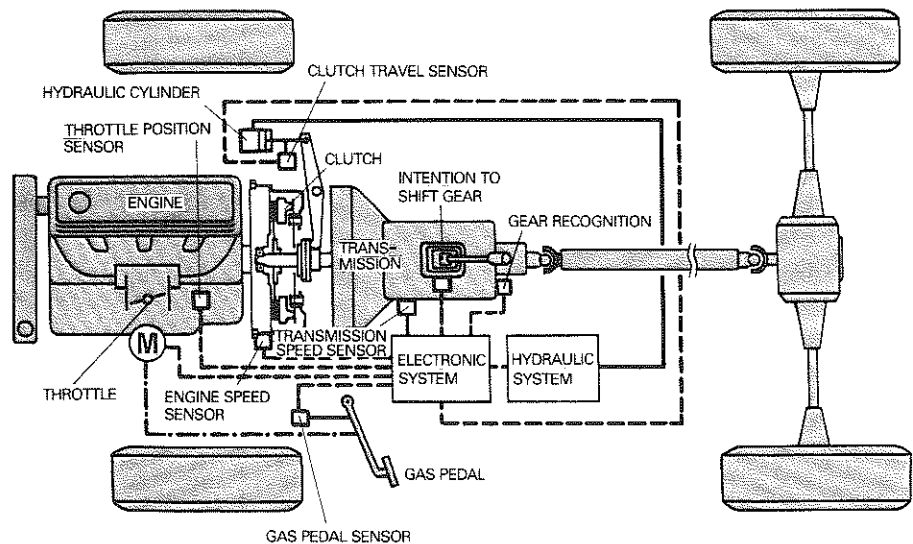
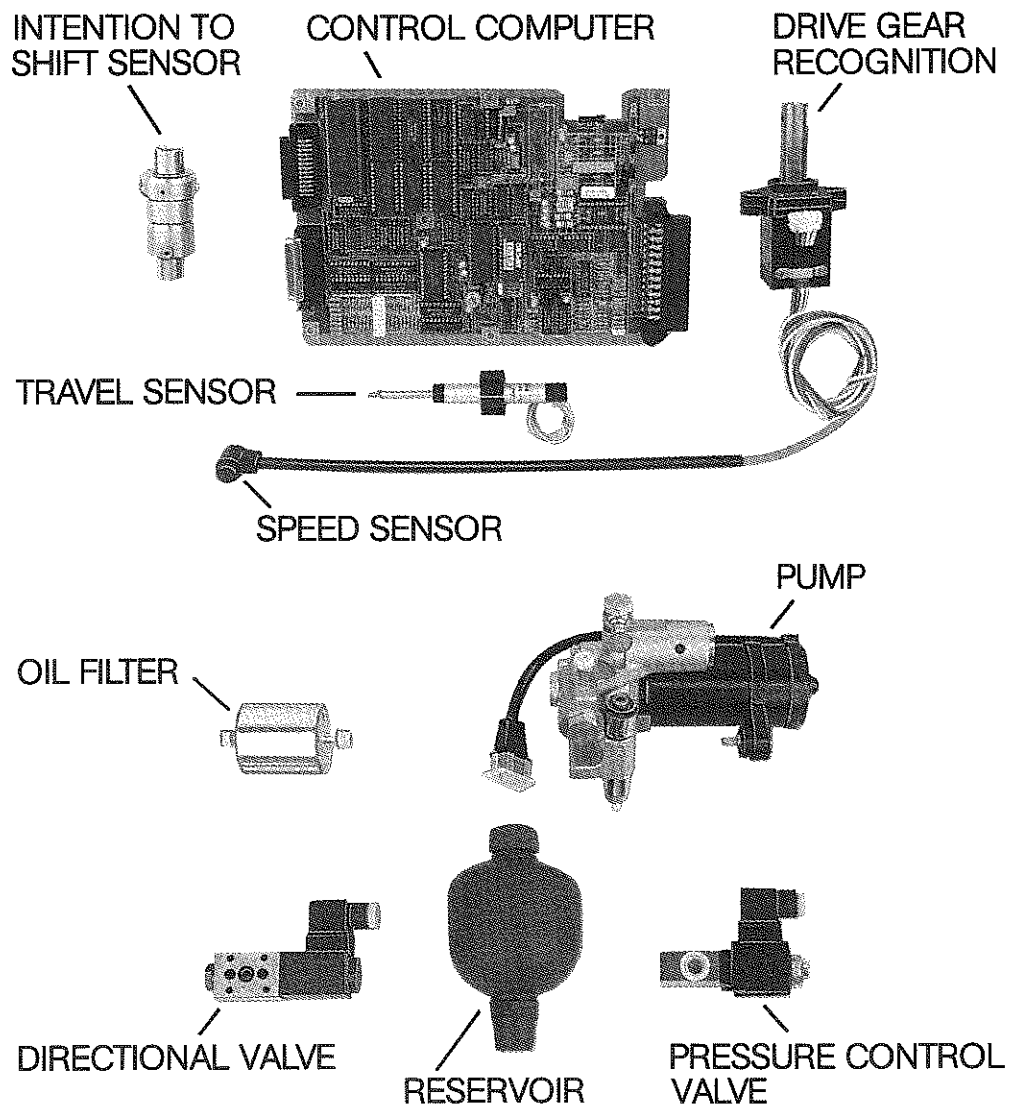


**Figure 5:** Electronic Torque Control Isolation TCI

A separate electric pump unit or – if available – the central vehicle hydraulic system provides the power supply (Figure 6). The electronic control system triggers the proportional valve [10]. The heart of the electronic control system is a microcomputer driven by a program containing the control algorithms and control strategy. The sensor system provides information to the microcomputer for determining system condition. The system includes sensors to register:

- clutch travel
- gear recognition
- recognition of the intention to shift gears
- engine speed
- transmission input speed
- gas pedal position
- throttle position.

LuK uses sensors that operate according to proven physical principles and that have been adapted to meet rugged vehicle performance requirements.



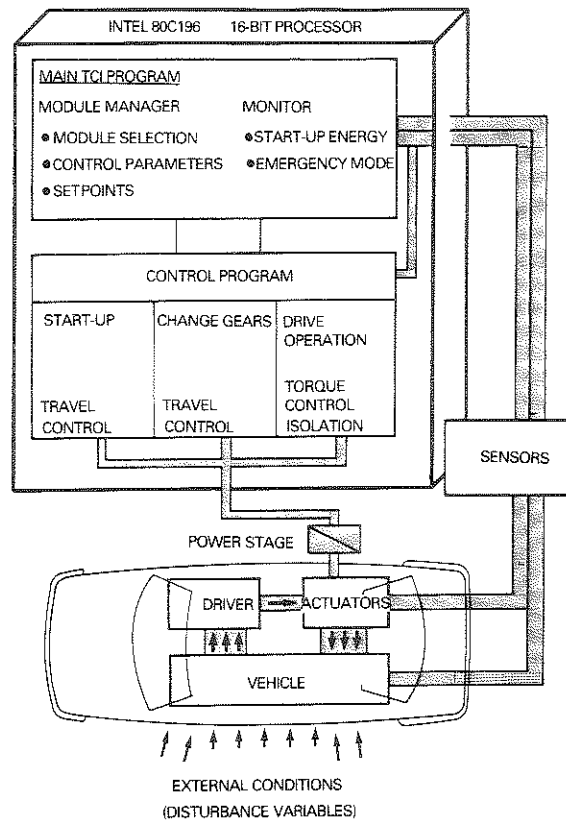
**Figure 6:** TCI-components



Figure 7 shows the design structure and the signal flow in the TCI system. The driver's senses constantly provide him with information on vehicle operating status. He bases his reactions on this information and responds to the vehicle via actuators – such as the steering wheel, shift lever, light switches, gas pedal and clutch pedal.

The vehicle then reacts to the driver's setpoint instructions. This internal control loop in the conventional vehicle is affected by various external conditions, which constitute disturbance variables – weather, road conditions, traffic situations, etc. The TCI system is superimposed on this conventional control loop.

Part of the information on the status of the actuators (clutch travel, gas pedal, throttle, shift lever) as well as on the current operating condition of the entire vehicle (engine rpm and transmission speed) is collected by the sensors and converted to be fed to a microcomputer.



**Figure 7:**  
Signal flow and software structure in TCI vehicle

This microcomputer is based on the INTEL 80C196 16-bit processor and uses a special software program to process the information collected from the sensors.

The software has been designed and developed according to strict modular criteria for structural programming in order to ensure maximum flexibility, universality, functional capability, reliability, and efficient data maintenance. Figure 7 illustrates the basic software structure. The TCI software is made up of the main program and the controller program. The module manager for the control program resides in the main program. Depending on the driving status recognized by the sensor system, the module manager activates the currently appropriate controller module. At the same time, the module manager transmits control setpoints and control parameters in order to actively adapt the controller to prevailing external conditions. Based on the actual sensor values, control parameters and setpoints are either calculated or read directly out of multi-dimensional fields. Parallel to this procedure, monitoring, diagnosis and emergency operation functions are also implemented in the appropriate software modules included in the main program.

The controller program consists of three main modules for:

- Stand-still and start-up  
(Idle mode, start engine, turn off engine, start-up vehicle, stop, start up on a grade ...)
- Changing gears  
(Disengage, engage, maximum speed monitoring)
- Drive operation  
(Drive, coast, maneuvering)

The first two main modules implement a travel control feature for the clutch travel and the third main module implements the slip control between the engine speed and the transmission speed [12]. The digital controller determines a setpoint and activates the hydraulic power stage, which consists of the proportional valve with the servo cylinder and responds by adjusting the clutch clamp load. So it is at the clutch that we are able to intervene in the controlled system represented by the vehicle, thus influencing the system.

## The Torque Control Loop Design and Strategy

The three controller modules work together with the main program module manager to solve all the problems that occur in any given operating situation. The system simplifies start-up on a steep grade just as readily as maneuvering or shifting gears. The following discussion provides a brief description of the electronic control system for torque control operation during normal driving (Figure 8).

The block diagram for the control loop shows the controlled system – that is, the vehicle represented as a 3-mass model; the actuator; the slave cylinder and clutch; and the controller, represented by the box surrounded by a broken line. The system features cascade control with proportional, integral and differential components. [12, 13].

System sensors collect data for engine speed  $n_M$  and transmission speed  $n_G$ . Then the slip control loop (bottom of graph) first determines the actual slip  $n_S$  and compares it with the slip setpoint. Then the PI-controller corrects the slip variation  $\Delta n_S$ . In order to prevent the engine rpm from revving too high during tip-ins, the cascade control provides a feedback control for engine speed. In the case of a hard tip-in, this feedback of the engine peak causes the clutch to close more tightly. Additional features designed to improve controller characteristics include a differential element to provide feedback of the actual clutch travel value and a high order form filter.

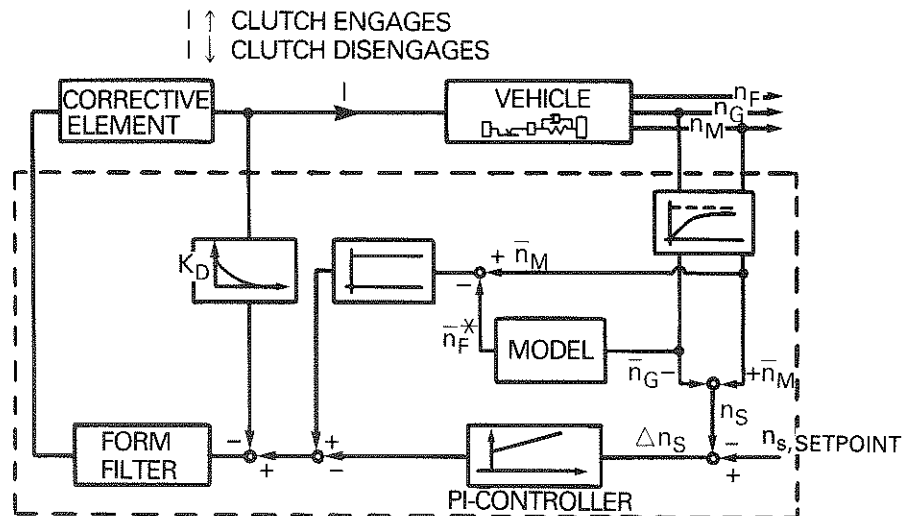
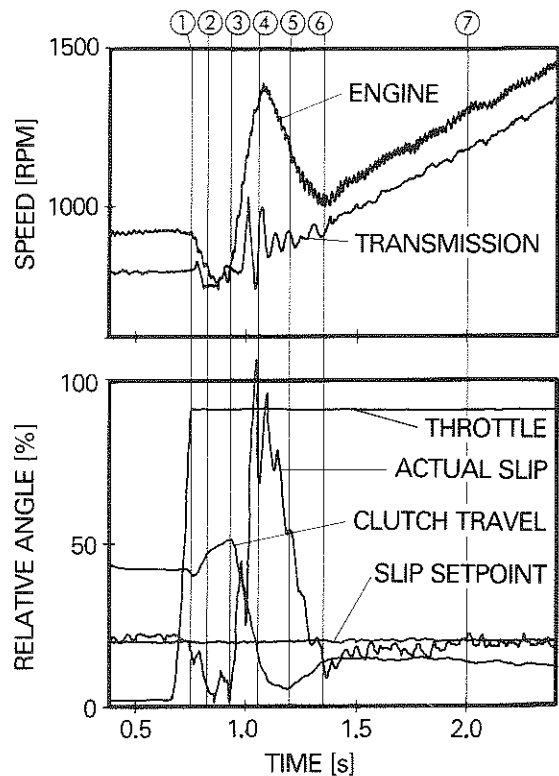


Figure 8: Electronic control loop during TCI operation (simplified)

Figure 9 shows the reaction of a vehicle equipped with TCI to a tip-in.

The top graph shows the engine and transmission speed curves, while the bottom section shows several system signals. The throttle valve is fully opened at Point (1). At first, the engine hesitates (2), but then builds up increasing torque and accelerates (3). From (1) to (3), the actual slip decreases significantly, so the controller opens the clutch. As the engine accelerates, the system recognizes the great increase in the engine speed and the engine speed feedback control quickly closes the clutch (3 – 4). The stronger coupling with the vehicle mass causes the engine to brake again (4 – 6). The clutch opens. At this point, the PI controller corrects the slip deviation (6 – 7).

This example illustrates the way the control system operates. The overall TCI system is highly flexible and features numerous parameters that can be used to adjust the system to prevailing vehicle conditions. Individual tuning is always required. No universal "off-the-shelf" solution can completely realize the full potential of the TCI system.



**Figure 9:**  
Control performance during acceleration

## TCl on the Road Torque Control for Improved Comfort

The following illustrations show measurements taken in a TCl vehicle and are designed to demonstrate the practical advantages offered by the "smart" clutch system. Figure 10 shows a measurement taken in drive mode. The left side of each graph represents a rigid clutch disc, and the right side shows the measurement taken with an active TCl system. The upper section of both graphs shows engine and transmission speed, while noise measurements and subjective ratings are entered in the bottom sections.

During drive mode measurement, speed increases continuously as a function of time. Magnified sections demonstrate rigid performance without TCl (transmission and engine speed are identical). With TCl, the difference between the engine and the transmission speeds reflect the actual slip. Without TCl, a clear maximum noise with a rating of 3 – 4 occurs until about 15 sec., that is, 2,000 rpm. With active TCl, the rating is 9 throughout the entire speed range covered. The increase in the noise signal with increasing engine speed can be explained by vehicle rollover noises at higher speeds and therefore cannot be influenced.

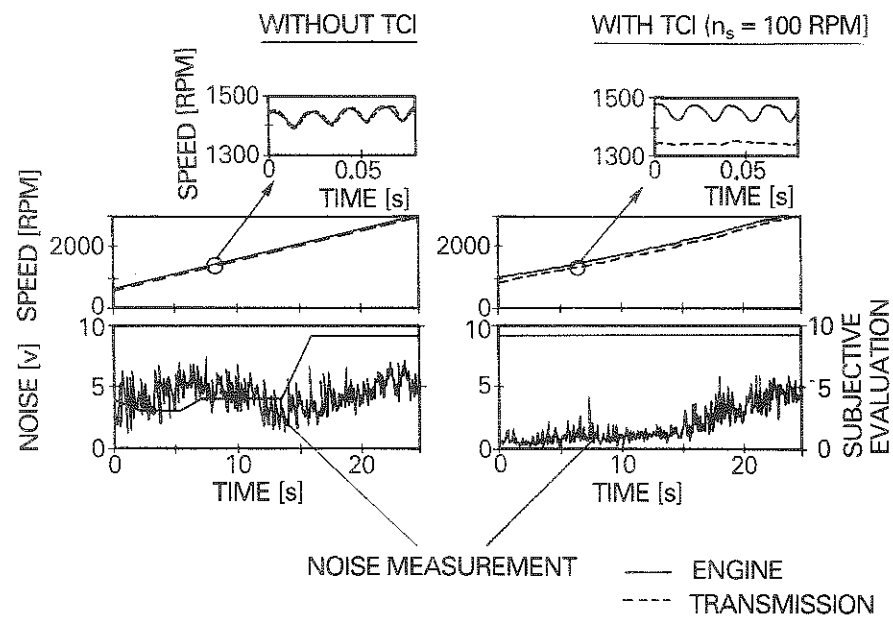


**Figure 10:** Effect of Torque Control Isolation on noise-related comfort factors in drive mode, 4th gear

The measurements shown in Figure 11 for coast mode without TCI show a typical noise peak in the higher speed range (in this case after 15 sec. at about 3,000 rpm). This maximum value is associated with rollover noise, which is reduced proportionate to the decreasing engine speed. It is reflected in the subjective rating, which falls to 4. With the active TCI system, this gear rattle does not occur, which yields a subjective noise rating of 9 over the entire vehicle speed range.

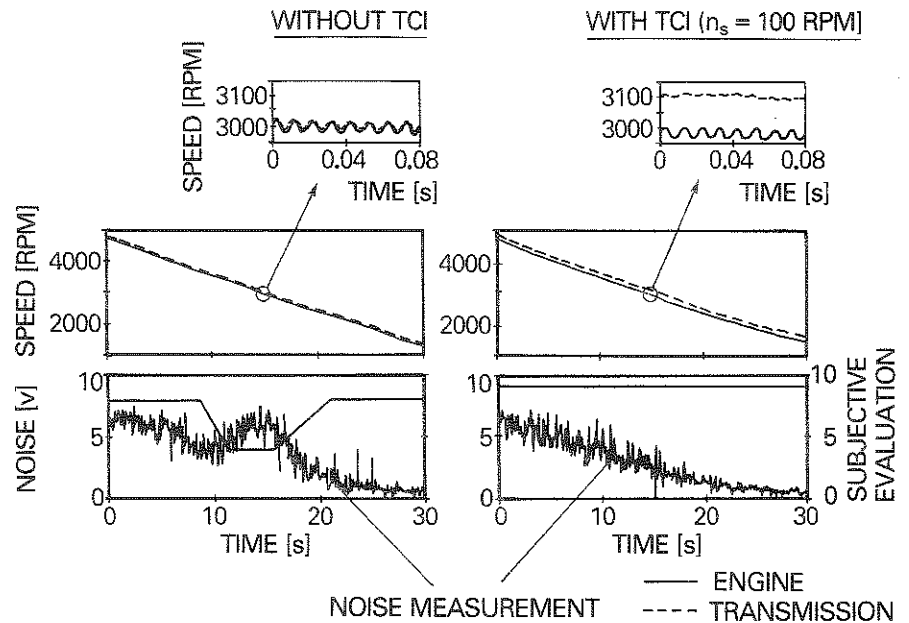


**Figure 11:** Effect of Torque Control Isolation on noise-related comfort factors in coast mode, 3rd gear

The last two figures show the filter effect of the TCI system on high frequency vibrations that can lead to gear rattle and body boom. However, the TCI system provides vibration isolation down to very low frequencies, which enables us to counteract low-frequency phenomena such as surging and tip-in/back-out jerk.

Figure 12 shows an example of measurements taken for tip-in/back out behavior in second gear.

The lower graph shows the fore-aft acceleration measured in the vehicle at driver head height.

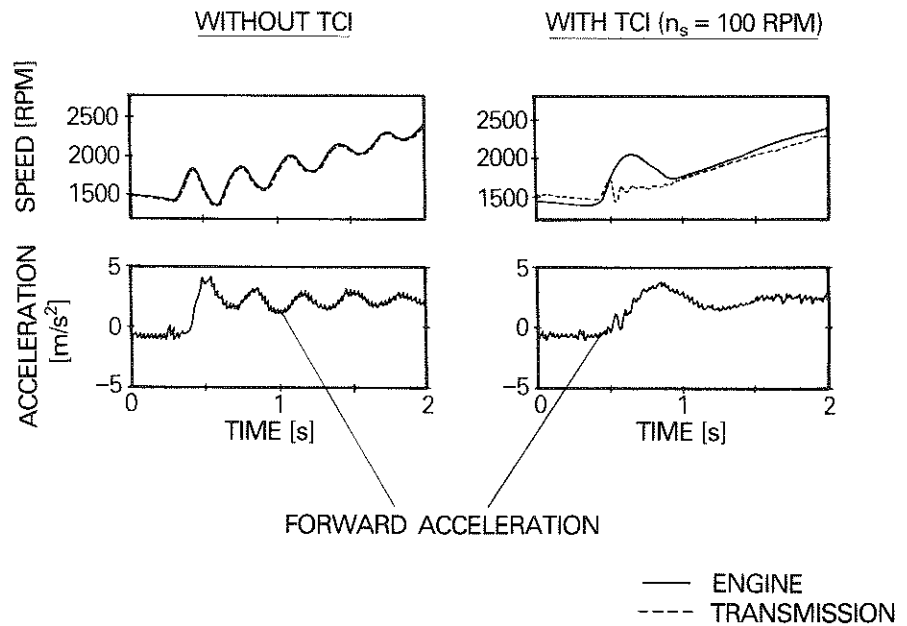


**Figure 12:** Improvement in tip-in/back-out performance in 2nd gear using TCI

Without TCI, the broad-band excitation occurring after rapid acceleration excites the vehicle to natural vibrations in the first natural mode of the system. The driver perceives these vibrations as "surging" in the vehicle. When the TCI system is activated, this surging no longer occurs.

The fore-aft acceleration peak occurs only as a result of the increased available engine torque in the higher speed range and the utilization of kinetic energy during the braking of the engine inertia. Neither the engine speed peak nor the initial low frequency acceleration peak are perceived as negative in an optimally tuned vehicle.

The following measurements illustrate another important positive effect of the TCI system (Figure 13). After short tip-ins in the rolling vehicle (for instance, stop-and-go traffic, creeping), the vehicle exhibited self-induced, escalating surge vibrations in the first natural mode. This leads to extremely unpleasant vehicle reactions (jerky ride). This phenomenon disappears entirely when TCI is activated.

These few examples have demonstrated TCI's ability to increase driving comfort.

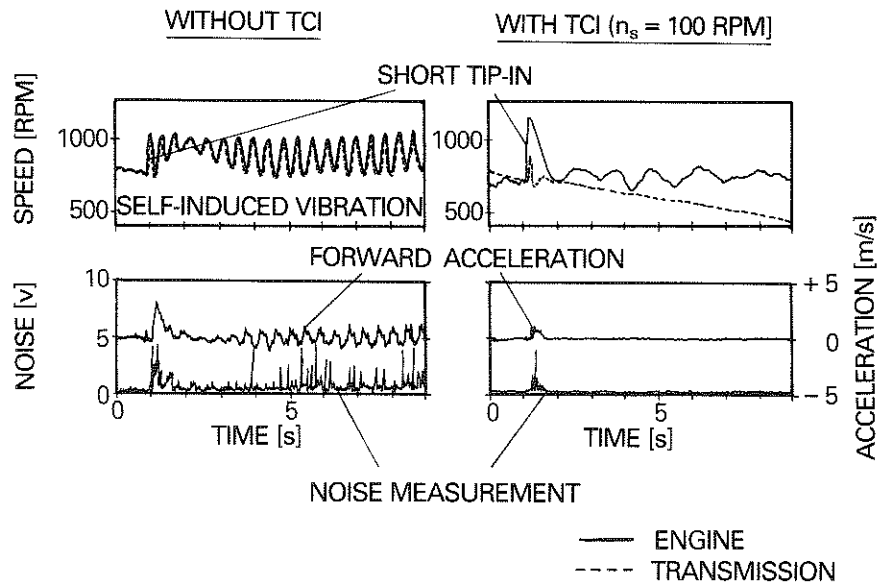


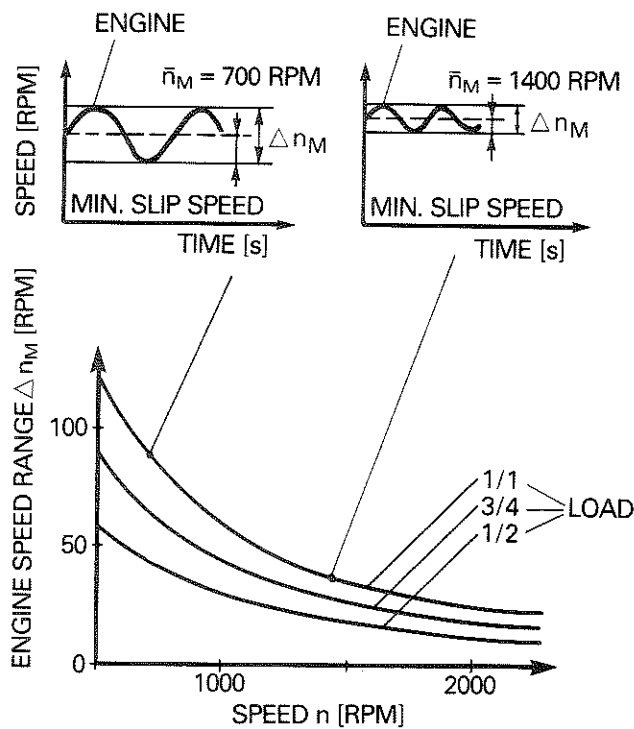
**Figure 13:** Eliminating self-induced drive train vibrations (tip-in, 2nd gear) using TCI

### Combining TCI with Conventional Torsion Dampers Minimizing Required Slip

As with torque converters, the positive effects achieved using torque control isolation have a downside – there is some power loss due to the inherent slip in the system. The design objective must be to keep this slip as low as possible.

In general, the amount of slip must always be greater than the amplitude of the engine irregularity  $\Delta n_{mot}$  (Figure 14). In internal combustion engines, torsional irregularity is strongly dependent on speed and load (Figure 14, top). Consequently, a torque control isolation system must provide a flexible method for specifying the slip setpoint. LuK's TCI concept stores slip setpoint values in multi-dimensional fields as a function of speed, load and the selected gear (other parameters can be accounted for).





FOR OPTIMUM VIBRATION ISOLATION  
 SLIP SPEED  $> 0.5 \times$  ENGINE SPEED RANGE  $\Delta n_M$

**Figure 14:**  
 Required slip setpoint

Figure 15 shows one possible slip setpoint field for one gear.

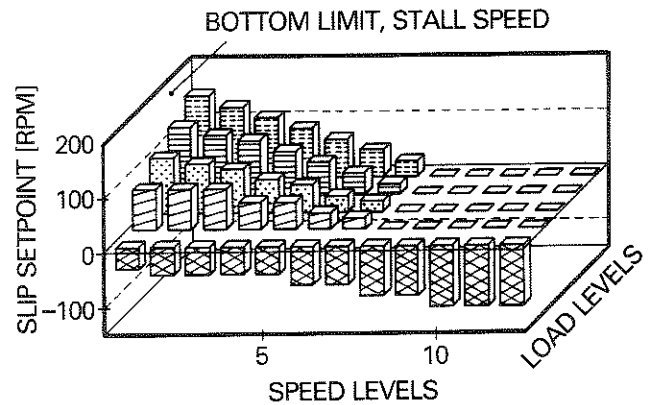
For this purpose, the engine speed range is divided into 12 speed levels and 4 load levels (throttle settings). These ranges can be defined as freely as desired. During vehicle tuning, the slip setpoint is determined using the following criteria:

- vibration isolation
- minimization of energy dissipation.

The effect of different slip setpoints can be studied in Figure 16.

The center column shows the noise measurements recorded as a function of speed. The right column for each row indicates engine and transmission speed curves in the 1,100 rpm range. For the engine speed range under 2,200 rpm, noise performance first increases with increasing slip, but then

remains stable above 50 rpm. For engine speeds over 2,200 rpm, a rigid clutch disc without the TCI system rated a "9". Obviously, as shown in Figure 15, we can reduce the slip setpoint to "0".



LOAD LEVELS (E. G. THROTTLE VALVE ANGLE)  
 ☒ COAST ☒ 0 ☒ 1 ☒ 2 ☒ 3

TUNING FOR EACH GEAR

CRITERIA FOR OPTIMIZATION

- VIBRATION ISOLATION
- MINIMIZATION OF DISSIPATED ENERGY

**Figure 15:**  
 Specification of slip setpoint  
 for TCI

If necessary, the TCI system can also be combined with a conventional torsion damper. Figure 17 shows the main relationships for gear rattle.

The graph shows the ratio of the amplitude of the irregularity between the engine output and the transmission input as a function of engine speed. The spring rate defined in the torsion damper and the torsional inertias of the drive train determine the resonance speed.

At this speed, low damping (that is, Coulomb friction in the torsion damper), causes high peak vibration amplitudes at the transmission input. However, a good isolation effect is achieved in the driving range above natural frequency. It is possible to reduce resonance peaks by increasing torsion damper damping, but this is achieved at the cost of isolation above natural frequency. The TCI system provides satisfactory isolation

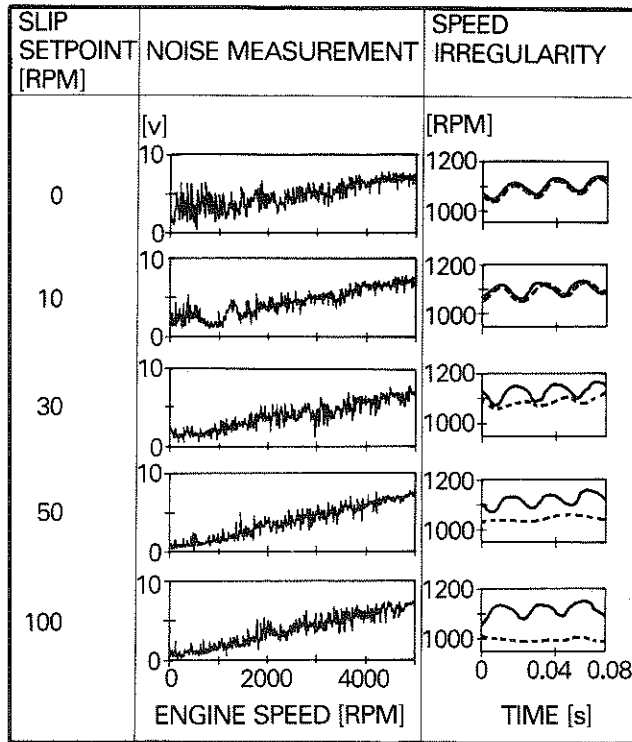
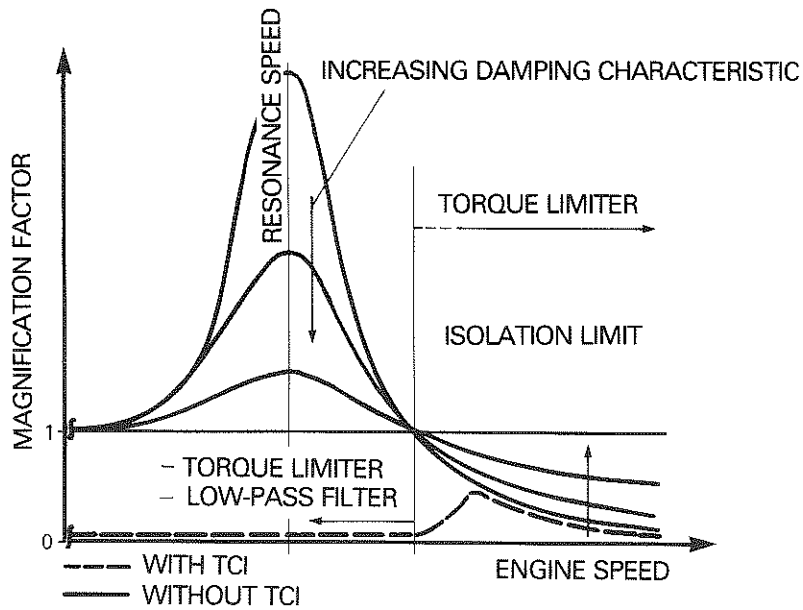


**Figure 16:**  
Effects of the slip setpoint on noise behavior in drive mode (2nd gear)

— ENGINE  
- - - TRANSMISSION

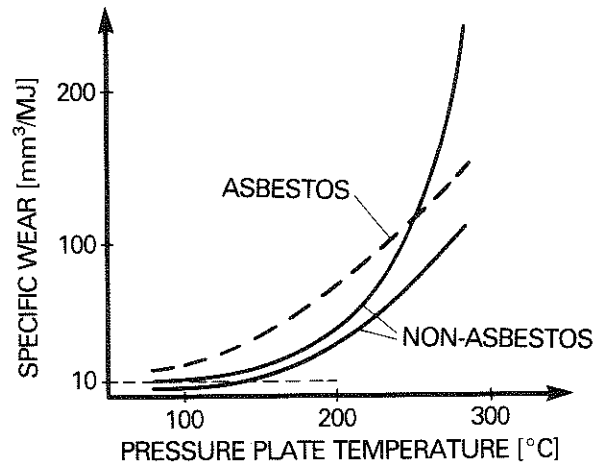
**Figure 17:**  
Performance of a vehicle with torsion damper with or without TCI



throughout those speed ranges where it is possible to drive with adequate slip. If we combine both systems, then it is possible to drive with slip in the lower speed range only, while a conventional torsion damper with low damping affords the necessary degree of isolation without introducing slip. In this way, we are able to reduce the overall amount of slip. Of course, it is necessary to carefully tune both systems to each other.

### Friction Facings Wear Performance and Requirements

The slip actually achieved, that is, the energy converted into heat, is not only important for the efficiency, but also for the wear of the friction facings.



EXAMPLE:

AVERAGE SLIP PERFORMANCE  
(SLIP UP TO 2000 RPM) : 0.50 KW

AVERAGE CLUTCH LOAD FOR  
START-UP AND SHIFTING GEARS : 0.25 KW

SPECIFIC WEAR : 10  $\frac{\text{mm}^3}{\text{MJ}}$

OPERATING TIME IN SPEED RANGE  
WITH SLIP (UP TO 2000 RPM) : 1850 h

**Figure 18:**  
Estimating facing service  
life

Figure 18 shows specific wear as a function of the operating temperature for several facings. The advantage of non-asbestos friction facings with respect to wear in the low and average temperature ranges is clear to see. It becomes evident that continued high temperature operation must be avoided.

Vehicle measurements provide information on the overall thermal situation. Figure 19 shows an example of measured results for Autobahn driving in 5th gear at a speed of 70 mph (corresponds to about 3,000 rpm). Operating temperature increases with increasing slip and can be lowered considerably by ventilating the clutch housing (for instance with openings).

The necessary slip speed decreases with increasing engine speed, as shown in Figure 14. However, at the same time, the engine torque increases. If we also take into consideration the fact that the slip speed setpoint cannot be fully adjusted to engine irregularity because of possible control variations, the required dissipation of slip speed often remains nearly constant, varying only with respect to the load level (throttle valve position).

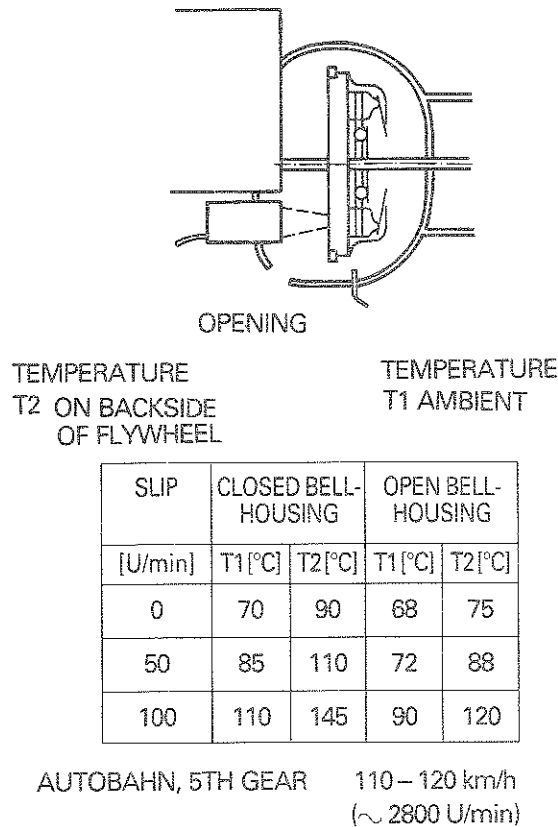


Figure 19:  
Temperature measurement in the vehicle

For the compact cars discussed here,

$$P_{\text{Slip, 1/1}} \approx 0.8 \text{ kW} \quad 1/1 \text{ load}$$

$$P_{\text{Slip, 3/4}} \approx 0.4 \text{ kW} \quad 3/4 \text{ load}$$

$$P_{\text{Slip, 1/2}} \approx 0.3 \text{ kW} \quad 1/2 \text{ load}$$

If we can assume more or less equal incidence of the three load levels during normal driving operation, then we arrive at an average slip performance of:

$$P_{\text{Slip}} = 0.5 \text{ kW}$$

In order to account for average clutch stress due to shifting and start-up procedures, we can assume that total driving time is made up of three more or less equivalent components, city traffic, country roads, and Autobahn driving:

$$P_{\text{Slip+start-up}} \approx 0.25 \text{ kW}$$

Given specific facing wear of  $10 \text{ mm}^3/\text{MJ}$ , a wear reserve of 1 mm and a facing surface of  $25,000 \text{ mm}^2$ , this assumption yields a total operating hour value of

$$T_h = 1,850 \text{ h}$$

in the speed range up to 2,000 rpm.

Given an average total number of vehicle operating hours of 3,000, about 60% could be driven in the speed range under 2,000 rpm [16, 17, 18].

Even if the increased comfort afforded by the TCI system increases the proportionate amount of time spent driving at lower rpms by 10% in comparison to current figures, we would still not reach the service life limits for the friction facings.

Extensive testing of facing characteristics is required to guarantee safe, properly dimensioned friction facing selection for use with a TCI system. The most important factors involved in this testing procedure include:

- the influence of slip speed on the friction coefficient
- wear performance
- long-term stability of the friction coefficient.

LuK performs these tests on specially designed test stands. The following presentation will discuss these tests in more detail.



- start-up without using the clutch pedal
- problem-free start-up on a grade
- no stalling
- shifting gears without manual clutch operation
- shifting without letting up on the gas
- increased driving safety thanks to simplified shifting cycles
- no idle mode rattle
- reduced idle speed
- no drive and coast rattle
- strongly reduced body boom
- torque limiter function
- no bucking bronco effect
- meaningful enhancement of ABS and ASR
- energy savings by virtue of free-wheeling function.

LuK's TCI system promises considerable improvement in both driving comfort and driving safety in order to ensure your share of the motor vehicle market of the future.

#### **Bibliography**

- [1] Schöpf, H.-J., Jürgens, G. and Fischer, R.  
Optimierung der Komforteigenschaften des Triebstranges von Mercedes-Benz-Fahrzeugen mit Schaltgetriebe [Optimization of Comfort Characteristics in the Drive Train of Mercedes-Benz Vehicles with Manual Transmissions], *Automobiltechnische Zeitschrift* 91 (1989), p. 568 – 575
- [2] Jürgens, G. and Fischer, R.  
Vergleich verschiedener Systeme zur Verringerung von Triebstrangschwingungen [Comparison of Various Systems for Reducing Drive Train Vibrations], *VDI-Berichte* Nr. 697 (1988), p. 233
- [3] Lutz, O.  
Kupplungsmanagement – ein Baustein zur Drehschwingungsdämpfung [Clutch Management for Damping Torsional Vibrations], *VDI-Berichte* 697, 1988, p. 219
- [4] Winkelmann, S. and Harmuth, H.  
Schaltbare Reibkupplungen [Shiftable Friction Clutches], Springer, Berlin 1985
- [5] Nagler, F. and Westerdorf, H.  
Regelstrategien für Trockenkupplungen [Control Strategies for Dry Friction Clutches], 2nd Aachener Symposium, *Vehicle and Engine Engineering '89*, p. 588 – 607
- [6] Coulomb, C. A.  
Théorie des machines simples, en ayant égard au frottement de leurs parties et à la raideur des cordages [The Theory of Simple Machines with Regard to Friction between Their Parts and the Stiffness of Ropes], Bachelier, Paris, 1821



- [7] Krause, H. and Poll, G.  
Mechanik der Festkörperreibung [The Mechanics of Friction between Solid Bodies], VDI-Verlag, Düsseldorf, 1980
- [8] Kayaba, T. and Kato, K.  
Theoretical Representation of the Coefficient of Friction for Multiple Contact Points, *Wear*, 52 (1979), P. 117 – 132
- [9] Niemann, G. and Ehrlenspiel, K.  
Anlaufreibung und Stick-slip bei Gleitpaarungen [Start-up Friction and Stick-slip due to Sliding], *VDI-Zeitschrift*, Vol. 105, No. 8, p. 221 – 284, 1963
- [10] Runge, W.  
Simulation des dynamischen Verhaltens elektrohydraulischer Schaltungen [Simulation of the Dynamic Performance of Electro-hydraulic Circuits], Springer, Berlin, Heidelberg, New York (1984)
- [11] Zimmermann, F.; Oetting, H., Heidemeyer, P. and Haack, R.  
An Automatic Dry Friction Clutch for Passenger Cars and Light Duty Trucks, SAE-Paper 860383
- [12] Böcher, J., Hartmann, I. and Zwanzig, Ch.  
Nichtlineare und adaptive Regelsysteme [Non-linear and Adaptive Control Systems], Springer, Berlin, Heidelberg, New York
- [13] Braess, H.-H.  
Steuerung und Regelung im Kraftfahrzeug – Eine systematische Betrachtung [Open and Closed Loop Control in Motor Vehicles – A Systematic Approach], *VDI-Berichte* 612 (1986), p. 539
- [14] Seyboldt, H.  
Ein Verfahren zur Ermittlung der Auslegung einer Kraftfahrzeug-Schaltkupplung [A Procedure for Designing a Vehicle Clutch], *Automobiltechnische Zeitschrift* 83 (1981) 7/8, p. 355 – 358
- [15] Krause, H. and Christ, E.  
Kontaktflächentemperatur bei technisch trockener Reibung und deren Messung [Contact Surface Temperature for Technically Dry Friction and Its Measurement], *VDI-Zeitschrift* 118 (1976), no. 11, p. 517 – 524
- [16] Kraftfahrtechnisches Taschenbuch [Automotive Handbook], Bosch, 20th Edition
- [17] Reicher, H.  
Dimensionierung von Reibkupplungen nach der zulässigen Wärmebelastung [Designing Friction Clutches Based on Permissible Thermal Stress], *Antriebstechnik* 13 (1974), No. 12, p. 673 – 678
- [18] Bausch, E.  
Grenzen der Schaltbarkeit an Reibelementen von Kupplungen und Bremsen [Shiftability Limitations in Friction Elements of Clutches and Brakes], *Antriebstechnik* 18 (1978), No. 7 – 8, p. 367 – 370
- [19] Soong, T-T. and Natke, H.G.  
Von der aktiven Schwingungsbeeinflussung zur aktiven Struktur [From Active Vibration Control to Active Structures], *VDI-Berichte* 697 (1988), p. 1 – 38
- [20] Hofmann, R.  
Unterm Blech regiert der Chip [The Microchip Calls the Shots under the Hood], *VDI-Nachrichten*, No. 40, 6 Oct 1989, p. 42

- [21] Ehlers, E.  
Automobilelektronik – Start gelungen, wie geht es weiter?  
[Automotive Electronics – We're Off to a Good Start, Where Do We Go from Here?],  
VDI-Berichte 612 (1986), p. 547

# Clutch Chatter

Dipl.-Ing. Paul Maucher

One primary goal of automotive development is the elimination of torsional vibration and its associated noises in the motor vehicle drive train. One of the previous presentations cited various types of torsional vibrations and their excitation sources, including frictional vibration in the drive train and its source, "the chattering clutch."

These frictional vibrations, generally called clutch chatter, judder, or shudder, pose a problem that remains unsolved even today, although it has been around ever since the automobile was invented. Designers are still trying to eliminate or improve by the dubious and time-consuming "trial and error" method. The chatter problem has even been exacerbated by the shift from asbestos to non-asbestos facings and therefore urgently requires thorough, systematic investigation.

Consequently, the following discussion deals with torsional vibrations generated in the vehicle drive train by clutch chatter, its causes, and the basic principles governing this behavior. These studies are limited to dry friction clutches. However, the general insights established here apply in principle to wet friction clutches as well.

## Sources of Chatter Vibrations

Figure 1 shows a typical start-up. During clutch engagement, that is, during the slip phase, the transmission shaft is accelerated from an at-rest condition up to the engine speed. For start-up without chatter, the acceleration of the transmission shaft is very uniform, as shown by the broken line in the illustration. On the other hand, when chatter is involved during start-up, vibrations occur in the form of periodic torsional vibrations, which generally continue as a rule until the transmission has come up to engine speed. Chatter manifests itself as objectionable, oscillating vehicle acceleration in the form of surging and annoying vehicle noise.

The literature [1 – 3] contains only a few publications on the subject of frictional vibrations, and positions tend to be contradictory.

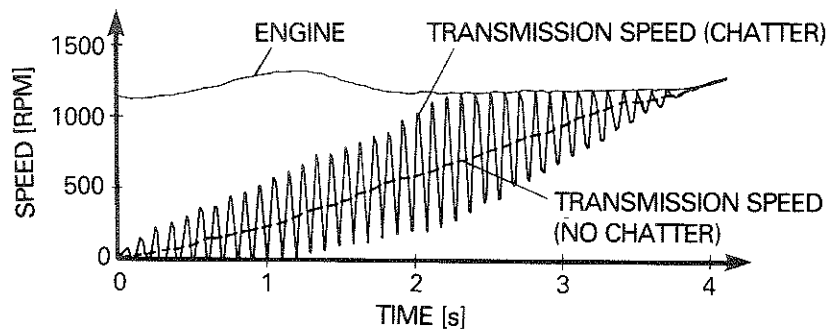


**Figure 1:** Start-up curves with and without chatter vibrations

Current thinking attributes chatter to a decreasing friction coefficient of the clutch facings, coupled with increasing slip speed. The following discussion characterizes this curve with a decreasing friction coefficient and negative gradients of the friction coefficient.

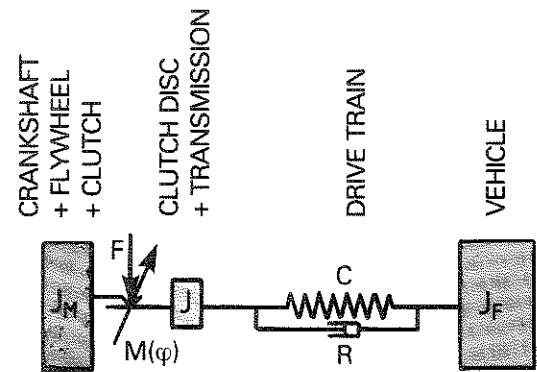
In addition to the previously cited decreasing friction coefficient, additional sources for chatter vibrations in motor vehicle drive trains include:

- the torsional irregularity of the engine
- clamp load fluctuations due to lack of parallelism between the clutch and the clutch disc
- inadequate drive train damping.

### **The Frictional Vibration Model for the Motor Vehicle Drive Train**

We have simplified the drive train vibration model in order to provide a graphic representation of the physical relationships involved in clutch chatter and its associated frictional vibrations (Figure 2). The clutch disc and the transmission are represented by the combined inertia  $J$ , which is connected to the vehicle inertia  $J_F$  by a spring and damper system. The inertia  $J_F$  is assumed to be  $\infty$  because it is very great in comparison to  $J$ . The inertia  $J_M$  for the crankshaft together with the flywheel and the clutch is also viewed as a very large and constantly rotating inertia.

## VIBRATION MODEL



$$\text{CLUTCH TORQUE } M(\varphi) = F \cdot 2 \cdot r \cdot \mu(\varphi)$$

**Figure 2:**

Simple vibration model of the drive train

RELATED DIFFERENTIAL EQUATION

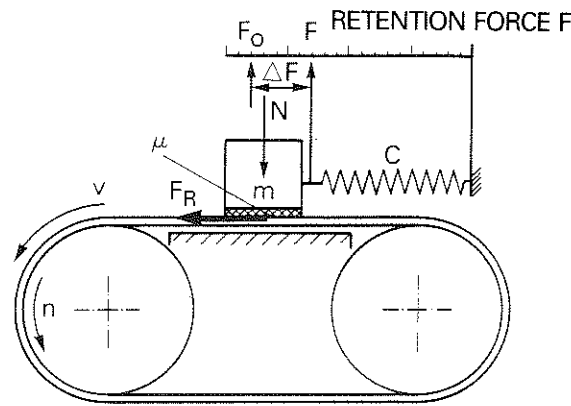
$$J \cdot \ddot{\varphi} + R \cdot \dot{\varphi} + C \cdot \varphi = M(\varphi) = F \cdot 2 \cdot r \cdot \mu(\varphi)$$

During start-up, the clutch disc creates a frictional connection with the engine via the clutch, being only partially closed. The frictional torque  $M$  of the clutch is established by the clamp load  $F$ .

### **Load Transmission due to Friction The Effect of the Decreasing Friction Coefficient on the Vibration System**

The friction facing, reflected by the curve of its friction coefficient, is the essential element involved in torque transmission. Fluctuations in the friction coefficient play no role in stationary force transmission, in contrast to engagement during vehicle start-up.

The model in Figure 3, which was already used in the previous presentation, is designed to explain the effect of the friction coefficient curve in a vibrating system.



MAXIMUM FRICTION FORCE  $F_{R0} = N \cdot \mu_0$

MINIMUM FRICTION FORCE  $F_R = N \cdot \mu$

$$\Delta F = F_0 - F = N (\mu_0 - \mu)$$

**Figure 3:**  
Effect of the decreasing friction coefficient in the vibration system

A body is pressed with normal force  $N$  against a moving belt driven by two rollers. The body is retained by an elastic spring.

We can make the following assumption with respect to the friction coefficient: the friction coefficient is at its greatest as static friction and decreases as the slip speed increases.

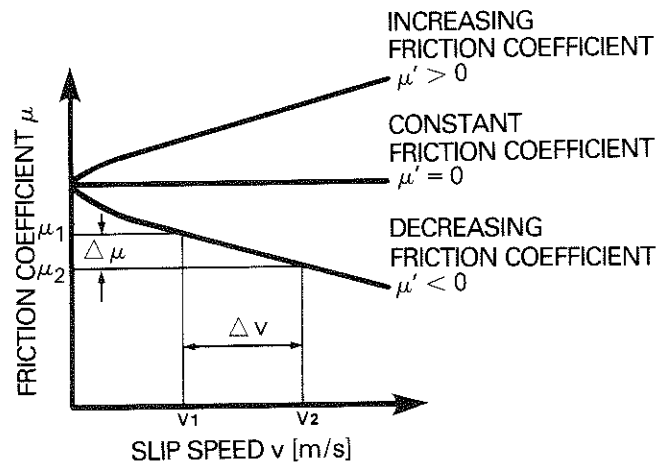
If the belt is driven at a constant speed, the body initially moves along with the belt, whereby the static friction force  $F_{R0}$  generated between the body and the belt deflects the spring. As soon as the retention force  $F_0$  reaches the maximum friction force  $F_{R0} = N \cdot \mu_0$ , the body stops moving. The belt continues to move, which results in relative movement between the body and the belt. The friction coefficient changes from the static to the lower dynamic friction coefficient. The friction force generated between the body and the belt is reduced by the fact that the body migrates back toward its original position. Its slip speed relative to the belt increases until a new equilibrium is established. The body stops moving, which again decreases the slip speed between the body and the belt. The friction coefficient, and hence the friction force, increases again, so that the body is once more carried along by the belt. The same process repeats itself, producing a periodic back-and-forth motion in the spring-anchored body. This motion is caused by the falling friction coefficient, which is itself attributable to the increasing slip speed. This is the explanation for self-induced frictional vibration.

## The Gradient of the Friction Coefficient

Testing and evaluation of facing materials with respect to chatter properties requires that we define a generally applicable identifying variable for the slip-speed-dependent friction coefficient curve (Figure 4). This slip-speed-dependent friction coefficient curve is defined as the gradient of the friction coefficient

$$\mu' = \frac{\Delta \mu}{\Delta v} = \frac{\mu_2 - \mu_1}{v_2 - v_1} \text{ [s/m]}.$$

and is used in the following calculations and discussions.



DEFINED AS THE GRADIENT OF THE FRICTION COEFFICIENT

**Figure 4:**

Gradient of the friction coefficient  $\mu'$

$$\mu' = \frac{\Delta \mu}{\Delta v} = \frac{\mu_2 - \mu_1}{v_2 - v_1} \text{ [s/m]}$$

If the friction coefficient increases with increasing slip speed, then  $\mu' > 0$  and the gradient of the friction coefficient is positive. If the friction coefficient decreases as the slip speed increases, then  $\mu' < 0$  and is negative. If the friction coefficient is constant with respect to the slip speed, then  $\mu' = 0$ , as described in Coulomb's law.

## Calculating Frictional Vibrations

The frictional vibration behavior of the simplified drive train as represented in Figure 2 is influenced by the following factors:

- the gradient of the friction coefficient  $\mu'$
- the damping value R
- the inertia J
- the drive train spring rate C
- the clamp load F for the slipping clutch.

The torsional vibrations for this vibration model are described by the differential equation

$$J \cdot \ddot{\varphi} + R \cdot \dot{\varphi} + C \cdot \varphi = M(\varphi)$$

where the clutch torque,  $M(\varphi) = F \cdot 2 \cdot r \cdot \mu(\varphi)$ , varies with the slip speed and acts as a vibration source.

All these calculations are based on a  $\varnothing$  200 clutch with a friction radius of  $r = 84.5$  mm.

Figure 5 shows simulation calculations for an engine speed of 1000 rpm, an output speed of 750 rpm and a clamp load of 1500 N.

The damping value and the gradient of the friction coefficient were varied in the form of a matrix. From the top to the bottom, the gradient of the friction coefficient decreases from 0 to  $-15 \cdot 10^{-3}$  s/m. From left to right, the damping value increases from 0.005 to 0.3 Nms. Each individual graph in the matrix shows the speed vibration of the clutch disc as a function of time. There are virtually no or very minimal vibrations for  $\mu' = 0$ , regardless of damping. These vibrations increase as the gradient of the friction coefficient decreases, but decrease with increased damping. They disappear beyond a certain damping value, which is greater the lower the gradient of the friction coefficient.

Let us assume that  $\mu'$  is constant with respect to the slip speed, that is, that the friction coefficient decreases linearly with respect to the slip speed. We can then use the differential equation to derive the limiting condition for the incidence of frictional vibrations

$$R = -2 \cdot F \cdot r^2 \cdot \mu'$$

If the damping value  $R > -2 \cdot F \cdot r^2 \cdot \mu'$ , the system is vibration-free.



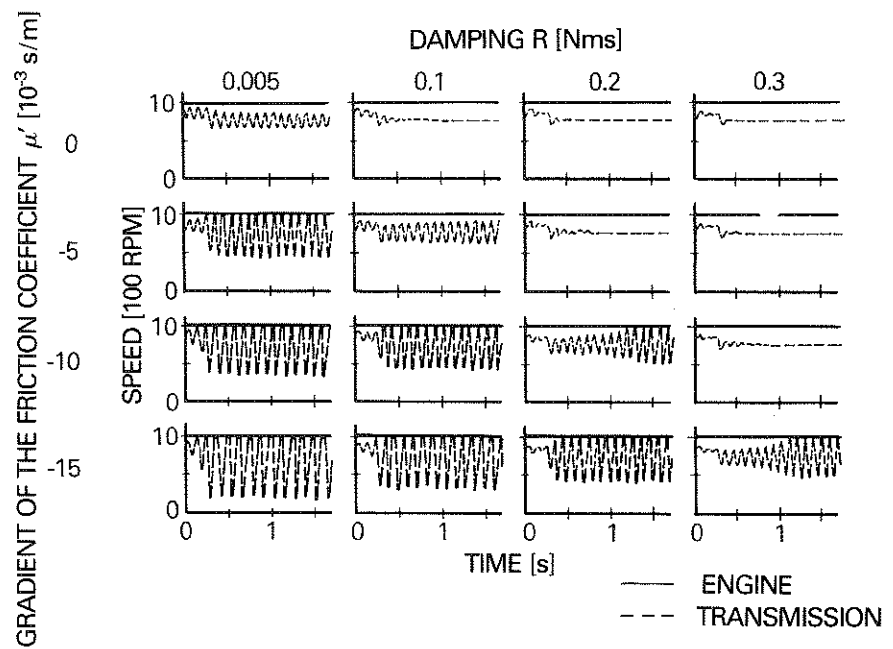


**Figure 5:** Torsional vibrations as a function of damping and of the gradient of the friction coefficient

On the other hand, if  $R < -2 \cdot F \cdot r^2 \cdot \mu'$ , frictional vibration occurs. The greater the currently prevalent clamp load  $F$ , the greater the damping value required to prevent frictional vibrations. The graph in Figure 6 shows this limiting condition plotted as a function of the damping value and the gradient of the friction coefficient. The lines plotted on the graph represent different values for  $R = -2 \cdot F \cdot r^2 \cdot \mu'$ , where the clamp load  $F = 1000$  N is represented as a broken line,  $F = 1500$  N is a solid line, and  $F = 2000$  N is a dash-dot line. Each of these lines represents the frictional vibration limit for its respective clamp load values. Frictional vibrations occur below the line, and the system is vibration-free above it. The frictional vibration area for clamp load  $F = 1500$  N is shaded.

Figure 6 shows that the frictional vibration area is determined by the three variables: the damping value, the gradient of the friction coefficient and the clamp load.

In general, the following holds true:

For positive gradients of the friction coefficient, that is, when  $\mu' > 0$ , frictional vibrations never occur. For negative gradients of the friction coefficient, that is, when  $\mu' < 0$ , frictional vibrations occur in a sector that increases as the clamp load increases.

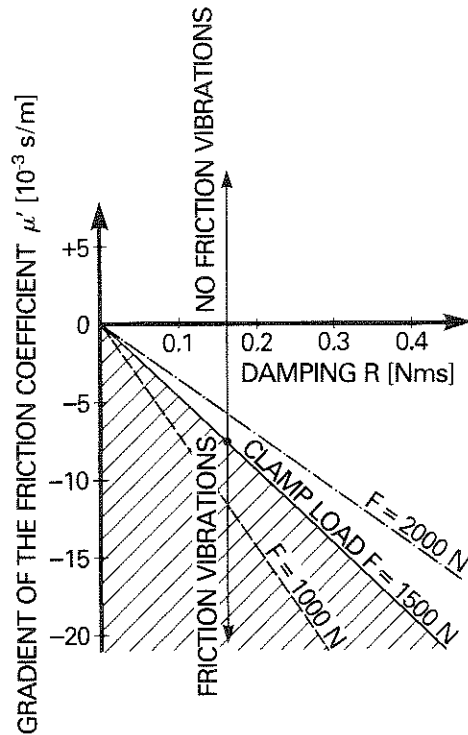


**Figure 6:**  
Friction vibration range as a function of damping, clamp load, and the gradient of the friction coefficient

Figure 7 shows the influence of the torsional spring rate and the mass moment of inertia in the vibration system when the gradient of the friction coefficient and the damping value are assumed to be constant.

The peak-to-peak amplitude of speed decreases only slightly both with an increasing torsional spring rate, as shown in the upper graph, but also with an increasing inertia, as shown in the bottom graph. Consequently, we can hardly expect to achieve noticeable improvement in chatter performance by changing the torsional spring rate and the mass moment of inertia.

Up till now, vibration calculations have treated the clamp load as a constant, thus ruling it out as a possible source of excitation.

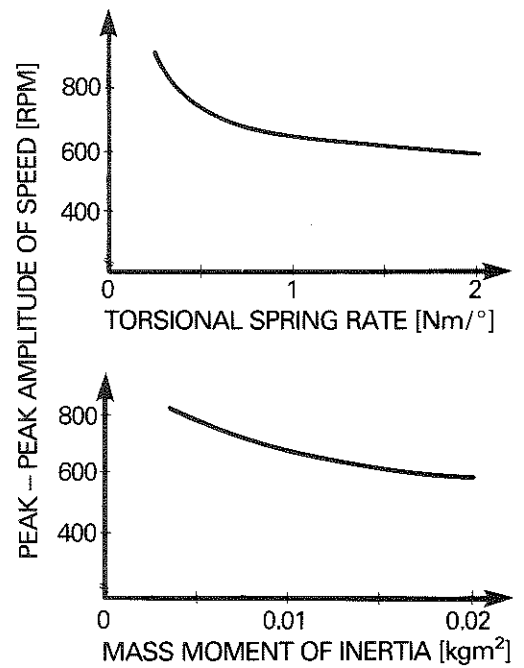


**Figure 7:**  
Speed amplitude as a function of torsional spring rate and the mass moment of inertia

$$\mu' = -10 \cdot 10^{-3} \text{ s/m}; R = 0.1 \text{ Nms}$$

The following example shows that even when the curve for the friction coefficient is constant ( $\mu' = 0$ ), frictional vibrations are possible. For instance, if a non-parallel clutch disc is paired with a non-parallel clutch pressure plate, the resulting clamp load pulses at a frequency that corresponds to the speed differential between the engine and the transmission.

Figure 8 shows the influence on the peak-to-peak amplitude of speed with respect to the difference between the engine and transmission speeds. This graph was calculated based on a clamp load of 1500 N, subject to periodic change of  $\pm 5\%$ .

At the differential speed, which corresponds to the resonance speed of the drive train, speed vibrations occur. Their magnitude depends on the damping value, and they diminish rapidly on either side of the resonance speed.

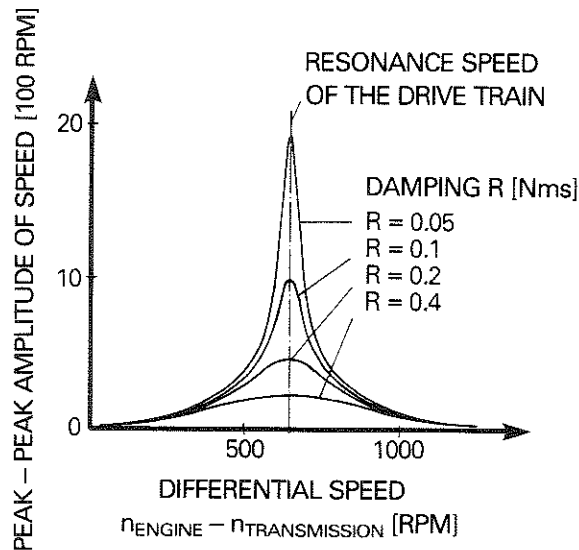


**Figure 8:**  
Torsional vibrations excited by clamp load fluctuations

Frictional vibrations that are caused in this way occur at precisely defined speed differentials between the engine and the transmission. Consequently, it is easy to pinpoint this cause by measuring vibrations in the vehicle.

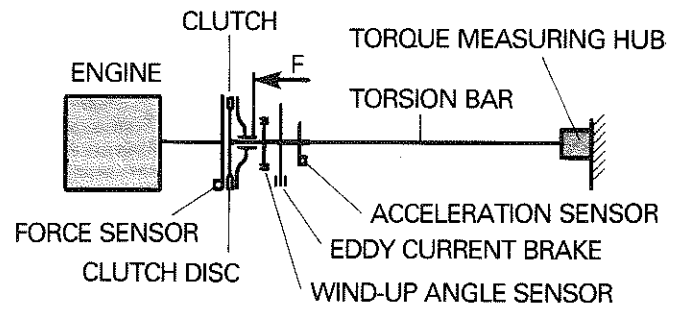
### **Chatter Test Stand for Determining the Gradient of the Friction Coefficient**

Test stands that are currently in use for the purpose of facing development are not appropriate for representing the high, speed-related fluctuations that occur at frequencies of approximately 10 Hz in conjunction with chatter. Furthermore, only forced vibrations are possible, as opposed to self-induced vibrations. Therefore, these test stands are inappropriate for determining the gradient of the friction coefficient.

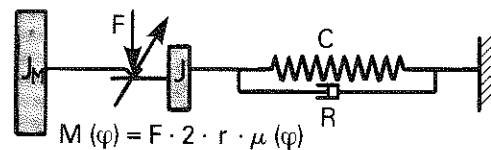
In order to study friction vibrations and specifically to determine the gradient of the friction coefficient, LuK has developed a new test stand.

Figure 9 shows a block diagram of this test stand, the vibration model, and the related differential equation.

## FRICTIONAL VIBRATION TEST STAND



### VIBRATION MODEL



**Figure 9:**  
Frictional vibration test stand and vibration model

$$J \cdot \ddot{\varphi} + R \cdot \dot{\varphi} + C \cdot \varphi = M(\varphi) = F \cdot 2 \cdot r \cdot \mu(\varphi)$$

The clutch is driven by a controlled-speed electric motor. On the output side, the clutch disc is attached to one end of a long torsion bar, which simulates the torsionally elastic drive train. Sensors are attached to the torsion bar to measure torsional movement in terms of the torsion angle and acceleration. An eddy-current brake allows the introduction of a speed-proportional damping value. The other end of the torsion bar is rigidly clamped in a torque measuring hub. The adjustable clutch clamp load is determined using load sensors.

The torsional spring rate  $C$  of the torsion bar corresponds roughly to that of the drive train for a compact passenger car. The inertia  $J$  includes the clutch disc and the transmission.

Figure 10 shows typical test results with a chattering facing for a drive speed of 500 rpm. The clutch disc vibrates with an amplitude of 500 rpm and always achieves the engine speed in short static friction phases.

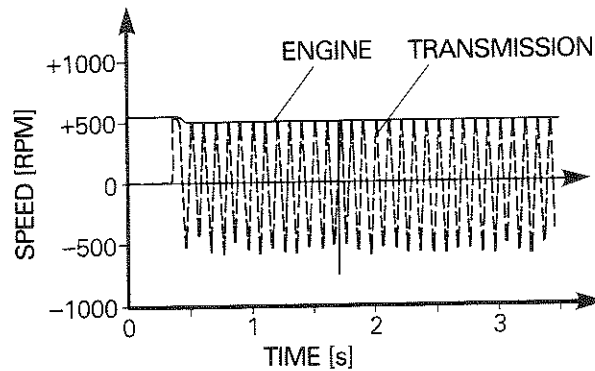


**Figure 10:**  
Speed curve during chatter

The top graph in Figure 11 shows a schematic section of this measurement. Below this graph, we see a synchronous curve for the differential speed. Using the measured curves for the torsion angle and clutch disc acceleration, it is possible to calculate the clutch torque at each point in time by means of the differential equation and to determine the curve of the friction coefficient with respect to time, as plotted in the bottom graph. The friction coefficient pulses periodically with the frequency of the frictional vibrations and is always at its maximum in conjunction with the minimum slip speed and vice versa.

Figure 12 shows the friction coefficient as a function of the slip speed for one period. The curve is almost identical for both increasing and decreasing slip speed. In this example, the friction coefficient decreases in inverse proportion to the slip speed.

The friction coefficient curve yields a gradient of:

$$\mu' = \frac{\Delta \mu}{\Delta v} = \frac{\mu_2 - \mu_1}{v_2 - v_1} = \frac{0.37 - 0.43}{8 \text{ m/s} - 0 \text{ m/s}} = -7.5 \cdot 10^{-3} \text{ [s/m]}$$

During testing, as has already been clearly noted from Figure 10, recognizable amplitude fluctuations occur between the individual vibrations. They are probably attributable to minimal fluctuations in  $\mu'$ . In this test, the variation for  $\mu'$  lay between  $-8.5 \cdot 10^{-3} \text{ s/m}$  and  $-7 \cdot 10^{-3} \text{ s/m}$ . The gradient for the friction coefficient  $\mu'$  must therefore be determined based on the average value of several vibrations.

We used this procedure to calculate the gradient of the friction coefficient for standard production facings. The clamp load was constant at 1500 N, and we varied the temperature and the speed.

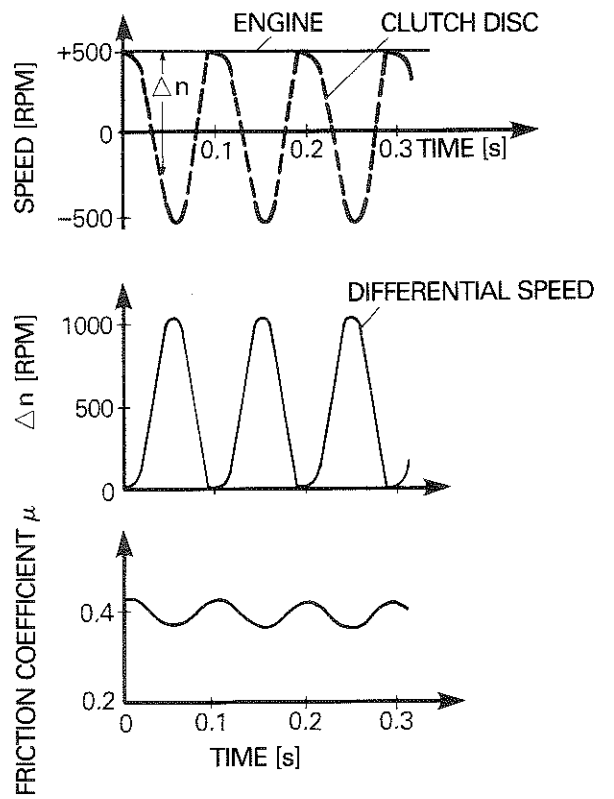
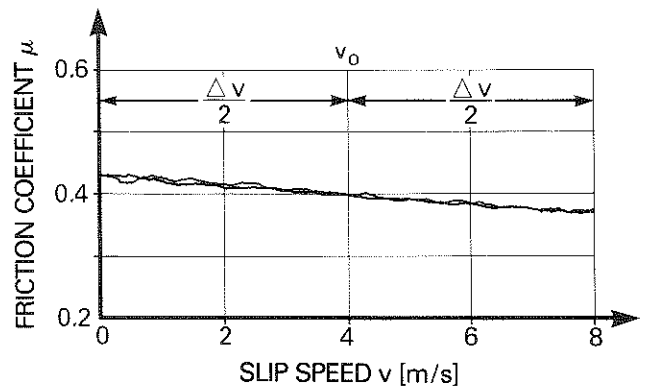


**Figure 11:**  
Speed, differential speed  
and friction coefficient in the  
friction vibration  
test



GRADIENT OF THE FRICTION COEFFICIENT

$$\mu' = \frac{\Delta \mu}{\Delta v} = \frac{\mu_2 - \mu_1}{v_2 - v_1} = \frac{0.37 - 0.43}{8 \text{ m/s} - 0 \text{ m/s}} = -7.5 \cdot 10^{-3} \text{ [s/m]}$$

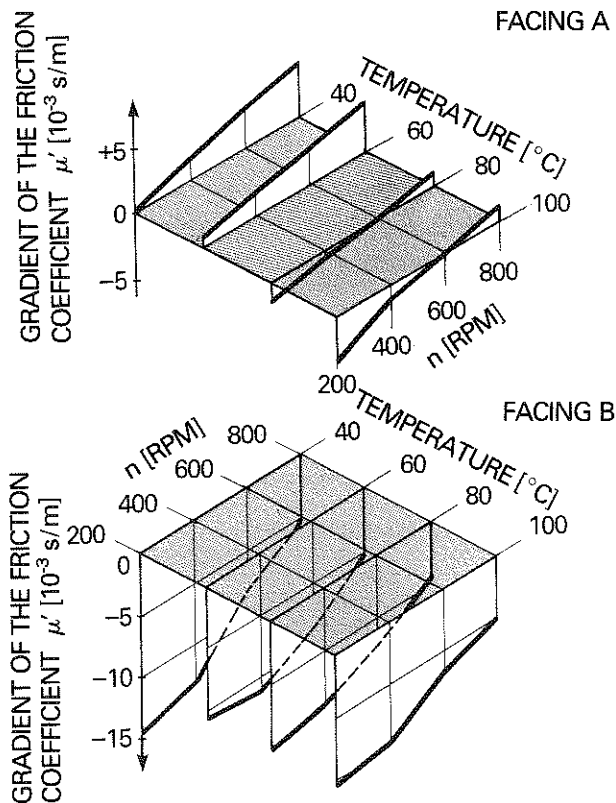
**Figure 12:** Friction coefficient curve and the gradient of the friction coefficient

Figure 13 shows the results for two facings. Facing A is a chatter-resistant material that has been used successfully to solve numerous problem cases, while Facing B is only applicable for vehicles that are not prone to chatter. Each graph shows the gradient of the friction coefficient  $\mu'$  for a temperature of 40°C, 60°C, 80°C and 100°C as a function of the speed, which varies from 200 rpm to 800 rpm.

Comparison of the two graphs shows the very high difference in the gradient of the friction coefficients for both facings with very low  $\mu'$  values for Facing B in comparison to Facing A.

As can be seen in the top graph, the gradient of the friction coefficient  $\mu'$  for facing A increases with increasing speed and decreases a little when the temperature increases. In the lower temperature range, the  $\mu'$  values are positive. Only higher temperatures, starting at about 80°C, and low differential speeds yield negative, that is, decreasing friction coefficients.

Facing B produces only negative gradients of the friction coefficient, which increase as a function of both speed and temperature.



**Figure 13:**  
Gradient of the friction coefficient  $\mu'$  comparison of facing A with facing B



Previous tests to determine the gradients of the friction coefficient have encompassed a limited speed and temperature range and need to be expanded to include the entire stress spectrum. However, currently existing values for the gradient of the friction coefficient present excellent possibilities for evaluating the chatter performance of friction materials.

If we compare the values determined for  $\mu'$  with Figure 6, we can see that the drive train for Facing A is free of frictional vibrations starting from a damping value of about 0.1 Nms, while frictional vibrations occur with Facing B up to a damping value of about 0.4 Nms. According to our measurements, drive train damping in the passenger car tested lay between about 0.1 and 0.5 Nms. Thus Facing A is chatter-free. This corresponds to our practical experience.

Because most clutch facings are hygroscopic and impregnation with sodium nitrite ( $\text{NaNO}_2$ ) makes this problem worse, we studied the effect of humidity on chatter.

In the case of wet, non-impregnated facings, the gradient for the friction coefficient falls to  $\mu' = \text{about } -20 \cdot 10^{-3} \text{ s/m}$ , but it rises to a normal level again after a few seconds because the facings dry out rapidly due to frictional heat. In the case of facings with sodium nitrite impregnation, the gradient of the friction coefficient decreases to about the same value as without impregnation, but increases then much more slowly. Possibly more moisture is bonded in the form of water of crystallization due to the sodium nitrite. This water is only given off very slowly and in conjunction with considerably higher temperatures. Consequently, we should avoid impregnation with sodium nitrite if at all possible.

## Summary

Based on theoretical studies, the basic principles governing frictional vibrations have been presented with respect to

- the gradient of the friction coefficient
- the damping value
- the clamp load
- the mass moment of inertia and
- the torsional spring rate of the drive train.

The discussion has revealed that frictional vibrations occur essentially in the presence of low drive train damping values and a negative gradient of the friction coefficient. Clamp load has a smaller effect. Other parameters studied have hardly any effect on chatter. Because of the good efficiency required and other comfort aspects, drive train damping cannot be increased significantly.

Consequently, our primary goal should be to develop friction materials with positive gradients of the friction coefficient.

The "chatter test stand" introduced here provides a simple means for determining the gradient of the friction coefficient, which is essential for chatter. Curves for the gradient of friction coefficient can be quickly found and used for optimizing facing materials.

If this option is fully exploited, it is possible to develop facings specifically for positive gradients of the friction coefficient without having to resort to otherwise time-consuming in-vehicle chatter tests.

Hence this development represents a way to overcome in-vehicle clutch chatter.

#### **Bibliography**

- [1] Newcombe, T. P. and Spurr, R. T.  
Clutch Judder, International Automobile Congress of FISITA 1972, 1/16
- [2] Jarvis, R. P. and Oldershaw, R.M.  
Clutch Judder in Automobile Drivelines, Proc Instn Mech Engrs 1973, Vol 187 27/73
- [3] Krause, R.  
Selbsterregte Reibschwingungen bei Kupplungslamellen [Self-induced Frictional Vibrations in Clutch Plates], Dissertation, Karlsruhe 1965

# **Torsional Vibration Isolation in the Drive Train An Evaluative Study**

Dr.-Ing. **Wolfgang Reik**

The previous presentations have described the vibration isolating effect of conventional torsion dampers, dual mass flywheels and slipping clutches. Other vibration isolating systems are also employed in motor vehicles. Prop shaft dampers mounted at the transmission output shift resonance frequencies. Hydrodynamic couplings and torque converters have been used successfully in automatic transmissions for decades. And other systems are in development, such as the viscous coupling.

The following presentation provides an overview of the physical options available for reducing torsional vibrations in the drive train. All known coupling elements used between the engine and the transmission will be discussed. However, this article will not deal with the reduction of engine irregularity by structural modification of the engine design, such as the addition of more cylinders. These kinds of comparative studies are known in the literature [1, 2], but each is based on a specific vehicle.

In contrast, this presentation assumes a simple, generally applicable drive train. There will be no attempt to discuss special, isolated drive train problems. This limitation is necessary in order to communicate an overview of existing and conceivable systems for vibration isolation.

## **Vibration Model**

The proven three-inertia vibration model of the drive train will be used for comparative evaluation of vibration isolation options (Figure 1). The mass moments of inertia and torsional spring rates chosen correspond to those for a compact passenger car operating in 3rd gear.

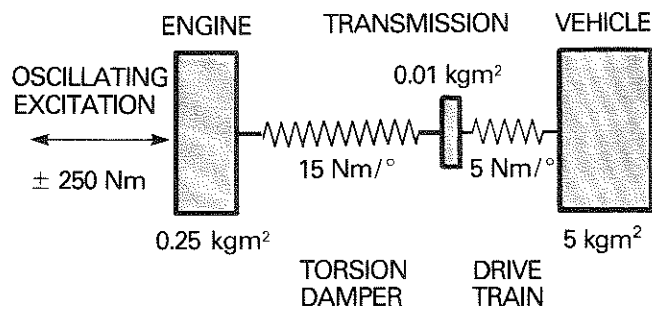


**Figure 1:**  
Vibration model with harmonic excitation

In contrast to the previous studies, vibrations affecting this vibration model will not be derived primarily from actual engine excitation. Engine excitation involves, in addition to the basic excitation, components that are multiples of the basic frequency. In fact, any abrupt change in gas pedal load will even result in broad-band excitation.

Harmonic excitation proves more appropriate for a basic comparison of different variations in the drive train. Therefore, a sinusoidal excitation torque  $M = M_0 \cdot \sin \omega t$  with the amplitude  $M_0 = 250 \text{ Nm}$  is introduced into all the following calculations.

The vibration model reacts to this excitation with vibrations, which will be the subject of discussion. The reaction of the transmission and the vehicle mass are critical for vehicle comfort. Vibration and control engineering designates this as a system response. In the higher frequency range, the acceleration amplitudes in the transmission are closely associated with gear rattle. Typical rattle ranges occur in association with excitation frequencies of 30 to 200 Hz. The oscillating acceleration of the vehicle generally causes few or no noises. However, in some cases the driver perceives this condition as objectionable surging and even clunk.

### Conventional Torsion Dampers

Normally, in a manual transmission automobile, the engine and the transmission are connected using an elastic connection, the clutch disc torsion damper. Engine irregularity is not supposed to pass through to the transmission, at least not in certain speed ranges. As discussed in a number of previous presentations, this effort is not totally successful.

Figure 2 shows this relationship for a sample torsion damper with an ordinary spring rate of  $15 \text{ Nm/}^\circ$ . The angular acceleration of the transmission and the vehicle has been standardized in order to provide a better overview. For this purpose, the amplitude at the transmission has been referenced to the angular acceleration that would result using a rigid connection between the engine and the transmission. Therefore, values below 1 indicate vibration isolation, and those above 1, amplification. The acceleration amplitude of the vehicle was also standardized in similar fashion. It was referenced to the acceleration that would result from a totally rigid drive train. The center graph shows the standardized amplitude of the vehicle acceleration, and the bottom graph, the transmission acceleration as a function of the harmonic excitation frequency. Since both accelerations and frequencies extend over a wide range, a logarithmic scale was used.

The vehicle acceleration shown in Figure 2 would lead us to expect strong surging at about 4 Hz for a conventional torsion damper if an appropriate excitation were present. Significantly higher frequencies are no longer capable of exciting the large, inert vehicle mass to vibration.

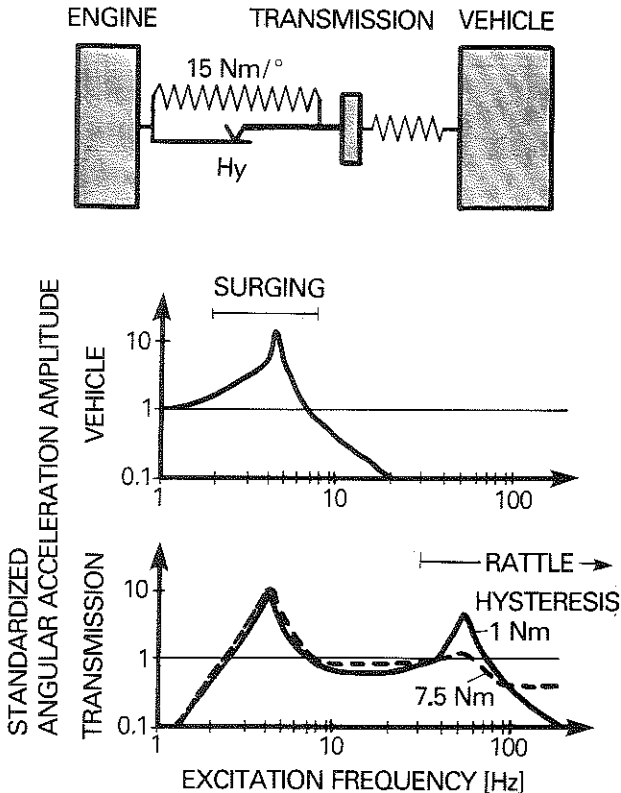


**Figure 2:**  
System response with conventional clutch disc

Of course, the transmission excitation also exhibits relatively high acceleration amplitudes in conjunction with the surging frequency, but no objectionable gear rattle is generated. Surging and clunk are usually the only objectionable response.

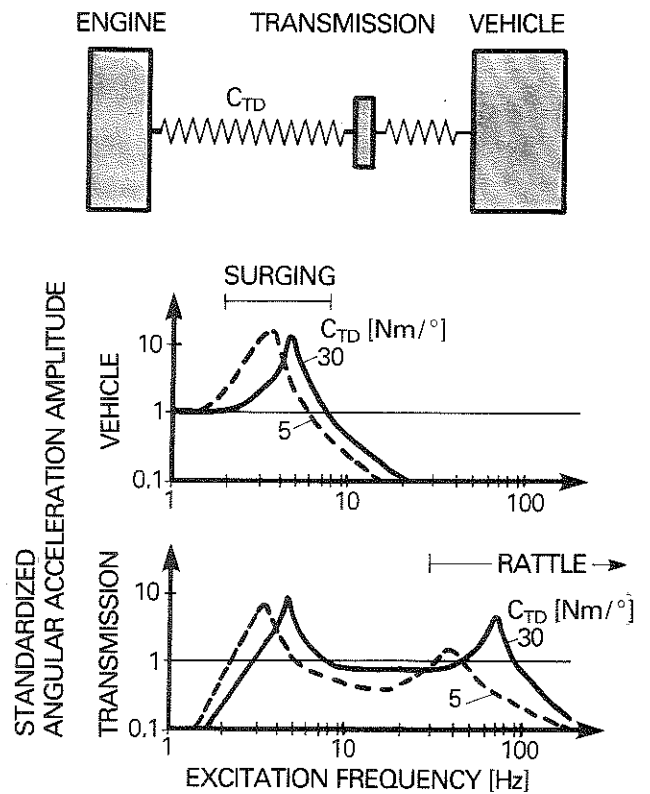
Gear rattle can be anticipated at frequencies over 30 Hz, and the resonance point is located in precisely this range. This point is significantly influenced by the torsion damper characteristic.

Figure 2 also shows the influence of the damper hysteresis on transmission acceleration. A high hysteresis prevents any significant resonance. However, it diminishes vibration isolation at higher frequencies. The hysteresis has virtually no influence on vehicle acceleration or surging.

The resonance range with amplification is typical for spring-coupled systems. To combat resonance amplification, high damping is necessary, which will cause the acceleration amplitude to approach the value of 1 at high frequencies, thus approximating rigid performance.

Figure 3 shows the influence of the spring rate on the vibration performance of the drive train for a linear torsion damper rate. In the rattle range, a lower rate has a favorable effect. It shifts the resonance to lower frequencies and reduces the amplitude at the transmission. It has hardly any effect on vehicle vibration. Only the resonance frequency is shifted, and it is scarcely perceptible from a subjective standpoint.

This changes, however, if we use multi-stage characteristics such as those used to combat gear rattle in idle mode. The extremely low rate for the idle stage acts similar to lash in the drive train and can cause tip-in/back-out performance to deteriorate.



**Figure 3:**  
System response with conventional clutch disc

### Dual Mass Flywheel

If we take the flywheel inertia, which is normally attached to the engine, and divide it into a primary and a secondary inertia, we can achieve a marked shift in the resonance at the transmission input (Figure 4). The secondary inertia increases the effective inertia of the transmission. This is particularly effective – as demonstrated in one of the previous presentations – if a very low spring rate is used between the two flywheel inertias. This is a primary feature of modern dual mass flywheels.

The transmission features excellent vibration isolation at all critical rattle frequencies above 30 Hz. For lower excitation frequencies, for instance those that occur during engine start-up and shut-off, the low spring rate of 2 Nm/° is clearly superior to the spring rate of 10 Nm/°. Vehicle vibration can also be reduced by a low spring rate and the appropriate damping value. As a result, modern DMFWs promise improvements with respect to surging as well.

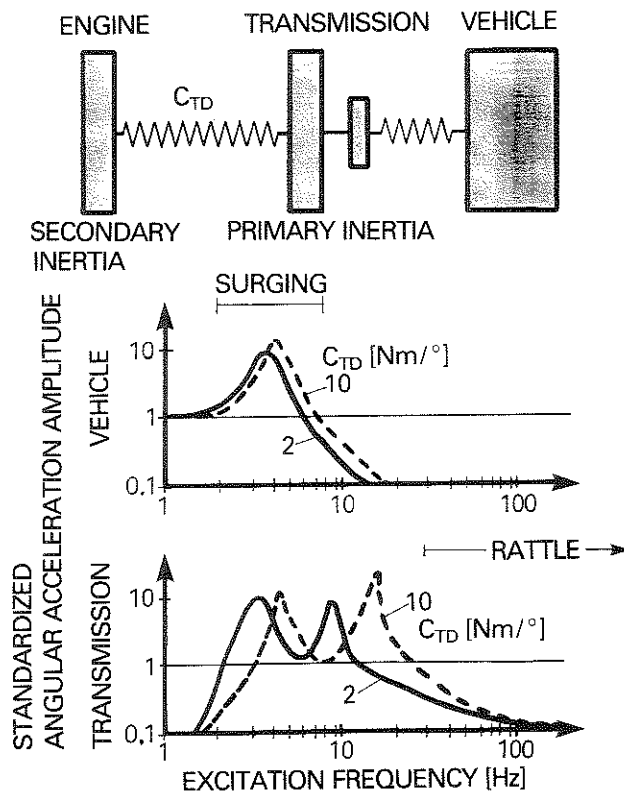


**Figure 4:**  
System response with  
spring-coupled dual mass  
flywheel

### Prop Shaft Dampers

Prop shaft dampers represent a totally different option for eliminating torsional vibrations. These dampers are occasionally attached to the transmission output for rear-wheel drive vehicles. They are capable of decreasing the amplitude of torsional vibrations in the transmission at excitation frequencies corresponding to the frequency of the prop shaft damper (Figure 5).

In operation, the prop shaft damper generates a vibration opposing that of the engine in the effective speed range and can thus compensate for at least part of the irregularity transmitted to the transmission via the torsion damper. In favorable cases, the torque generated by the prop shaft damper is precisely the opposite and equal to the oscillating torque transmitted by the torsion damper. The resulting oscillating torque at the transmission is completely neutralized and the oscillating accelerations disappear.



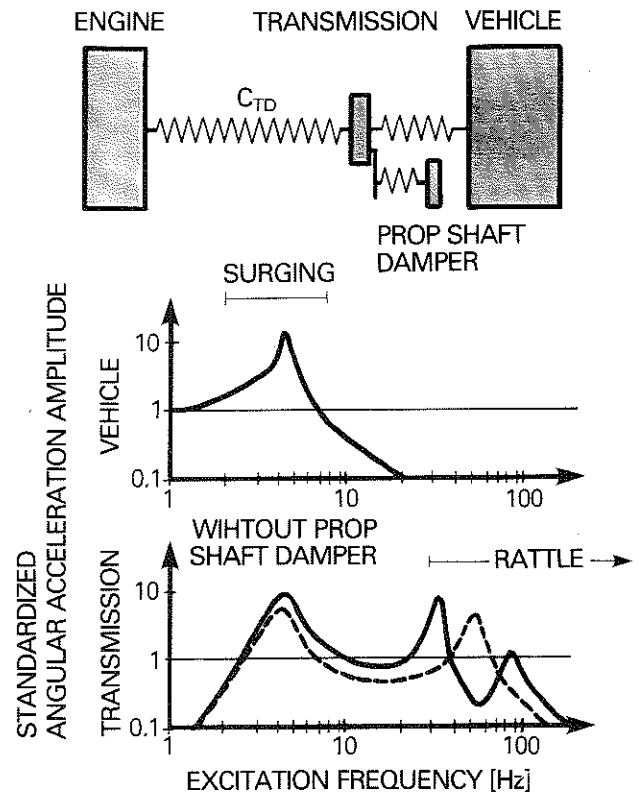


**Figure 5:**  
System response with prop shaft damper

Unfortunately, this damping effect is limited to a narrow speed range. On either side of this range an equiphase vibration can even occur in the prop shaft damper itself. This vibration is associated with an amplification that can only be diminished somewhat by appropriate damping in the prop shaft damper, which reduces its effect at the tuned frequency. The prop shaft damper has no effect on surging.

### Centrifugal Pendulum

The ideal prop shaft damper ought to possess a normal frequency that would change with the excitation frequency in order to overcome the disadvantage of its narrowly limited range of effectiveness. Theoretically, the prop shaft damper frequency would have to adjust to the excitation frequency. This would require that the prop shaft damper have a torsional

spring rate that would increase with the square of the excitation frequency. This is impossible with the springs that are commonly used for this purpose.

However, there are ways to create a vibrating system without using springs. Instead of briefly storing energy in springs, it is possible to transform it into potential energy. The simple mathematical pendulum of length  $l$  is an example of this principle. The resonance frequency is represented by

$$f = 2 \pi \sqrt{g/l}$$

where  $g$  is the acceleration due to gravity.

If this kind of pendulum is attached to a rotating disc, the acceleration due to gravity must be replaced by the centrifugal acceleration  $r\Omega^2$  (see Figure 6, top), where  $r$  is the radius on which the pendulum mass is located and  $\Omega$  is the angular acceleration of the disc. The natural frequency of this kind of rotating pendulum is

$$f = 2\pi \Omega \sqrt{r/l}$$

and is thus proportional to the speed. Values of  $r$  and  $l$  can be selected to achieve a precisely defined order. To be able to damp the main excitation in four cylinder engines, we select

$$\sqrt{r/l} = 2.$$

With this kind of properly tuned centrifugal pendulum attached to the clutch disc torsion damper, it is possible to completely damp excitation frequencies with two full vibration phases per revolution (Figure 6). All other orders remain virtually unaffected. Unfortunately, it is impossible to effect surging tendencies with this kind of centrifugal pendulum because surging excitation is usually broad-band and is not proportional to speed. Hence it cannot be assigned to a single order.

Many studies have examined the option of using a centrifugal pendulum (sometimes called a Taylor or Sarazin pendulum) [see 3 – 8]. Obviously, many developers were attracted by the possibility of completely eliminating an entire order for a broad frequency range, but no one has arrived at any practically applicable solution. LuK has also studied this option closely [9]. Numerous difficulties, for instance tolerance problems, overly large pendulum mass and very high vibration amplitudes at low speeds, hampered any success.

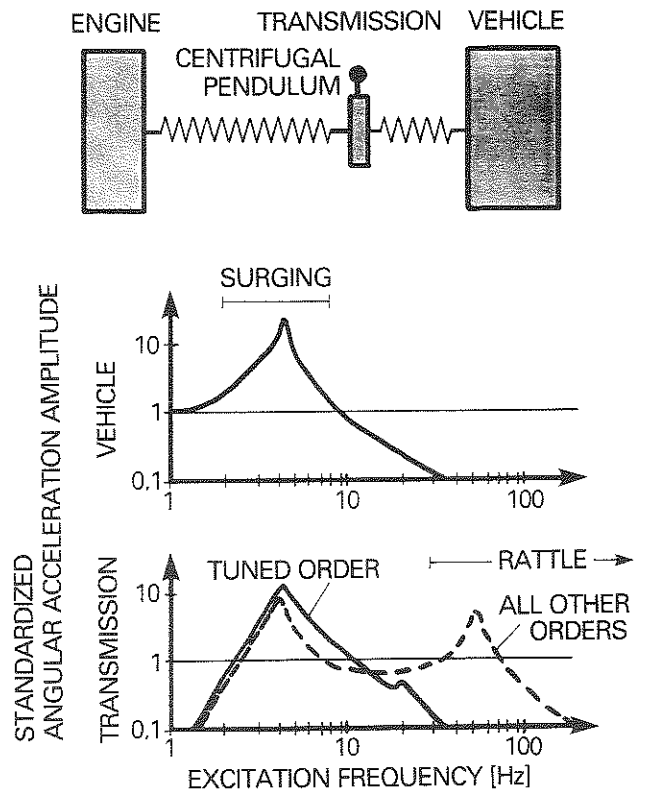


**Figure 6:**  
System response with centrifugal pendulum

### Hydrodynamic Torque Transmission

The hydrodynamic coupling – sometimes called the Föttinger coupling – and torque converters represent a completely different kind of coupling between the engine and the transmission. No spring mechanism is present to serve as a short-term energy store, a requirement for vibrations. Consequently, resonance between the engine and the transmission is impossible. However, since there is no torsional elasticity whatsoever, with which vibration isolation might be achieved, the transmission component must permit slip between the engine and the transmission.

Automatic transmissions use torque converters or hydrodynamic couplings to isolate vibration. Their behavior with respect to vibration excitation has been described in the literature [10 – 13]. Because the torque converter becomes increasingly stiffer with increased speed,

vibration isolation is strongly dependent on speed. Figure 7 shows a typical example. Low impeller speeds produce particularly good vibration isolation. However, this solution exacts a trade-off in the form of a high slip, which results in high energy loss.

Figure 7 also reveals that not only is the high rattle frequency isolated, low-frequency surging is also significantly reduced.

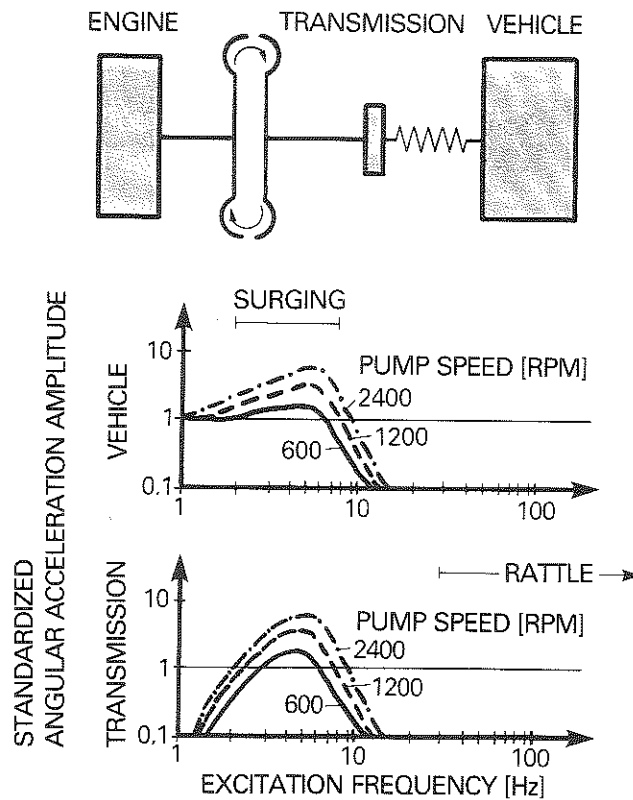


**Figure 7:**  
System response with hydrodynamic coupling

### Hydrostatic Torque Transmission

Instead of being hydrodynamic, the coupling between the engine and the transmission can also be hydrostatic [14]. This system uses a pump featuring a hydraulic flow control valve that transmits the torque from the pump unit to the drive shaft. In the LuK design shown in Figure 8, several parallel gear pumps are situated between the primary and secondary

flywheel inertias. Slip can be varied using flow control valves that are controlled by centrifugal force. These valves are not shown in this drawing. Figure 9 shows the acceleration amplitudes of the transmission and the vehicle. Here as well, vibration isolation improves at higher slip speeds, that is, at wider valve openings.

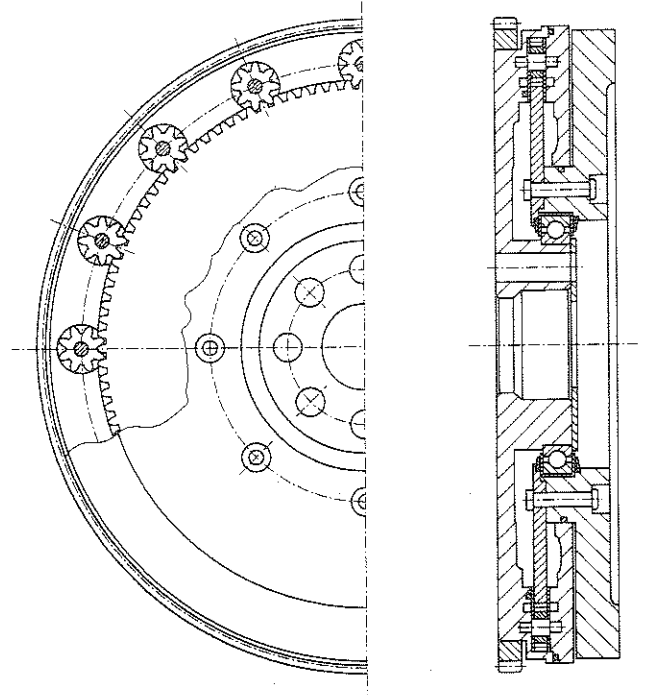


**Figure 8:**  
Hydrostatic dual mass  
flywheel

In comparison to torque converters (Figure 7), it is obvious that the isolating effect on the transmission is still relatively poor at high frequencies. Furthermore, vehicle surging vibrations are only eliminated at the cost of very high slip. Tip-in/back-out measurements taken using a hydrostatic dual mass flywheel like the one shown in Figure 8 confirm these observations (Figure 10). The speed curves for the engine and the transmission after a tip-in are plotted as a function of time. The pump is blocked in the top graph in Figure 10. Consequently, the engine and the transmission speed have an identical curve. After the tip-in, there is a strong surging vibration that then decays gradually.

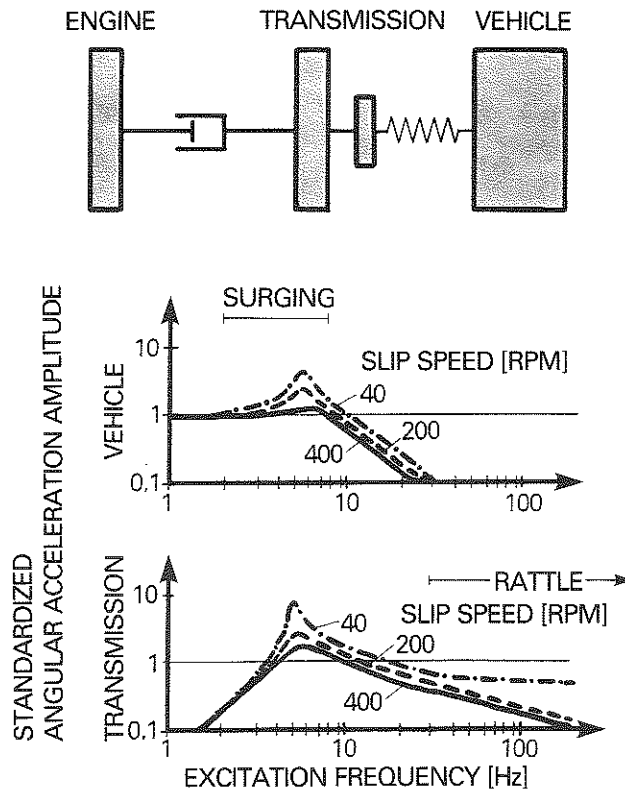


**Figure 9:**  
System response with hydrostatic dual mass flywheel

In contrast, the bottom graph in Figure 10 reflects the same process using a relatively high slip of 200 rpm. To be sure, the surging vibration is significantly damped, but falls far short of being eliminated. Nor was this to be anticipated based on Figure 9.

The high slip factor required for efficient operation causes thermal problems that are made even worse as a result of the frictional heat generated by the clutch. As we all know, at high temperatures, for instance under extreme driving conditions, the viscosity of all oils decreases drastically. This increases slip even more and can lead to thermal destruction. As a result, LuK has discontinued any efforts to develop a purely hydrostatic DMFW.

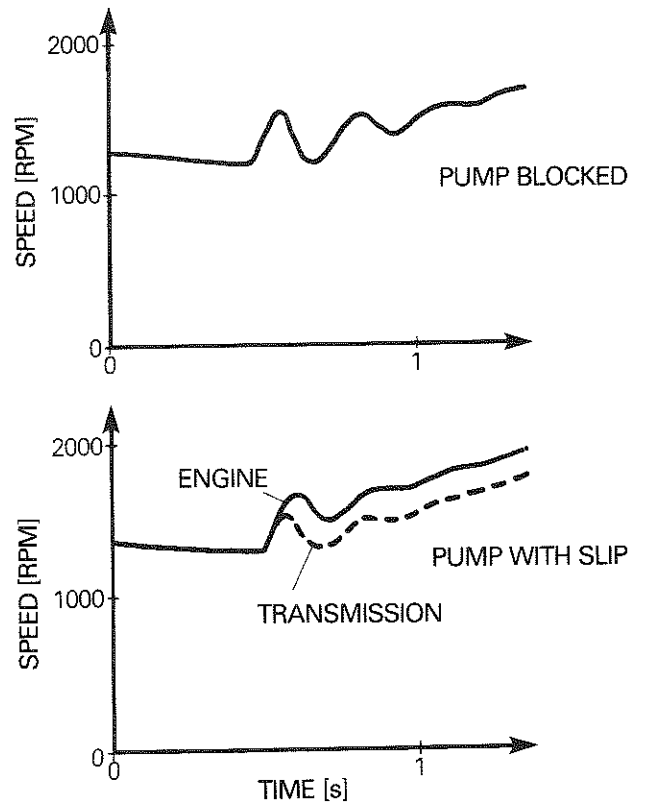


**Figure 10:**  
Tip-in for hydrostatic dual mass flywheel

### Viscous Coupling

In addition to the hydrostatic pump, a viscous coupling can be used in a dual mass flywheel. At first glance, the mathematical derivation of vibration performance reveals surprising results. We observe exactly the same performance as with hydrostatic load transmission. The reason for this similarity is that in both cases load is transmitted using fluid shear. This is not readily apparent in the case of the pump because the actual shear occurs in the hydraulic flow control valve. The pump itself just converts torsional movement into hydraulic flow. In the case of the viscous coupling, on the other hand, the fluid transmission medium is sheared directly between rotating plates.

If we don't use the viscous coupling or the hydrostatic pump in a DMFW and employ a clutch disc instead – that is, if we do not use a secondary inertia between the engine and the transmission – vibration isolation is considerably worse (Figure 11). It is scarcely possible to eliminate gear rattle with an acceptable amount of slip. However, similar to the situation with the hydrostatic DMFW, high slip improves vehicle surging.

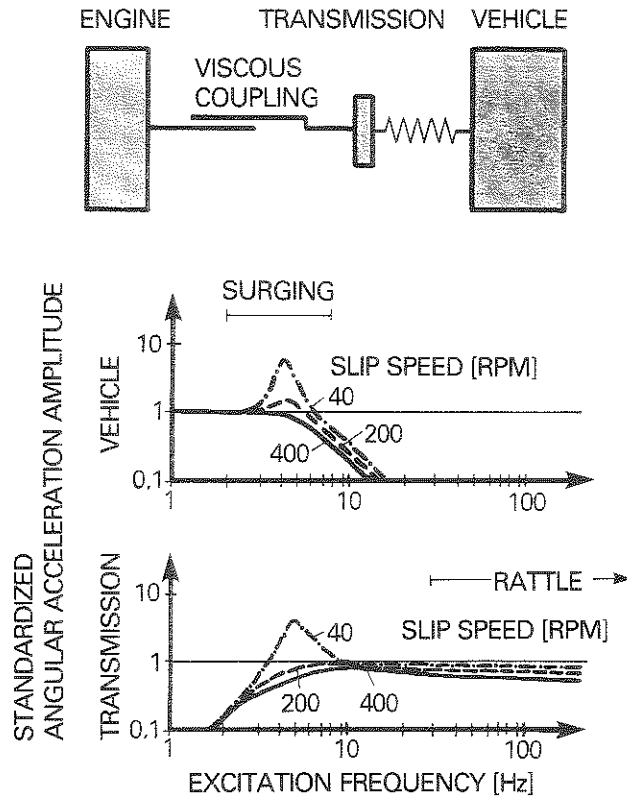


**Figure 11:**  
System response with viscous coupling

### Torque Control Isolation

Torque control isolation, which is the topic of one of the presentations in this series, offers totally new options. An electronic control loop allows us to change drive train vibration performance over wide ranges. With optimum tuning – see Figure 12 – isolation is achieved at excitation frequencies as low as 5 Hz. Both rattle and surging can be completely eliminated.



However, it would be inappropriate to demand isolation at even lower excitation frequencies because this would introduce a delayed vehicle response to drivers' acceleration needs. Therefore, at very low excitation frequencies, the standardized amplitude of the vehicle angular excitation must approach 1 in order to transmit constant torque. The limiting frequency, at which the steep decrease in the transmitting function occurs, should therefore lie between approximately 2 to 5 Hz.

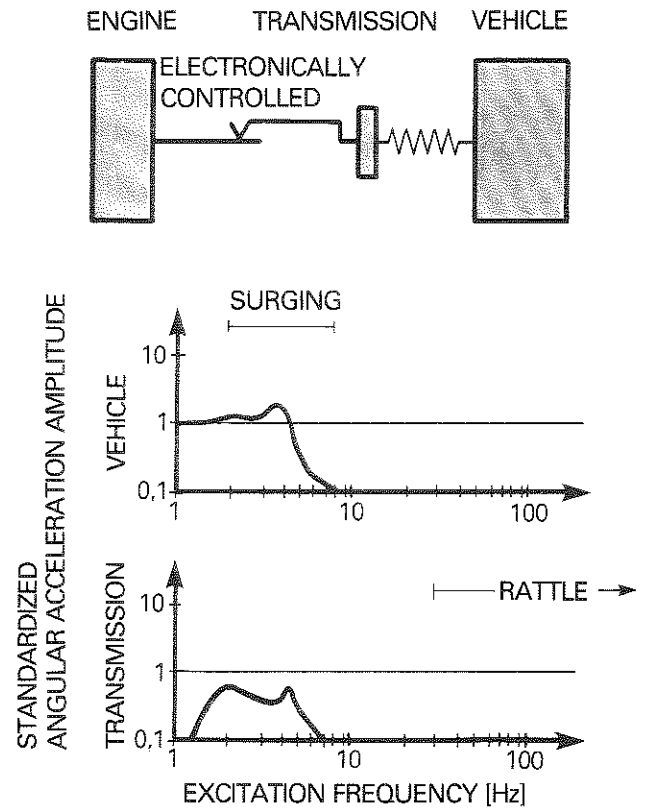


**Figure 12:**  
System response with torque control isolation

### Vibration Damping Procedures: A Comparison

The current options for producing vibration isolation between the engine and the transmission can be divided into three major groups. With the first group, the engine and the transmission are connected by an elastic coupling. As shown in Figure 13, this group can be further subdivided into conventional torsion dampers and spring-coupled dual mass flywheels. Several strong peak resonance points are characteristic. Vibration isolation is not clearly evident until we reach a range above the highest resonance frequency.

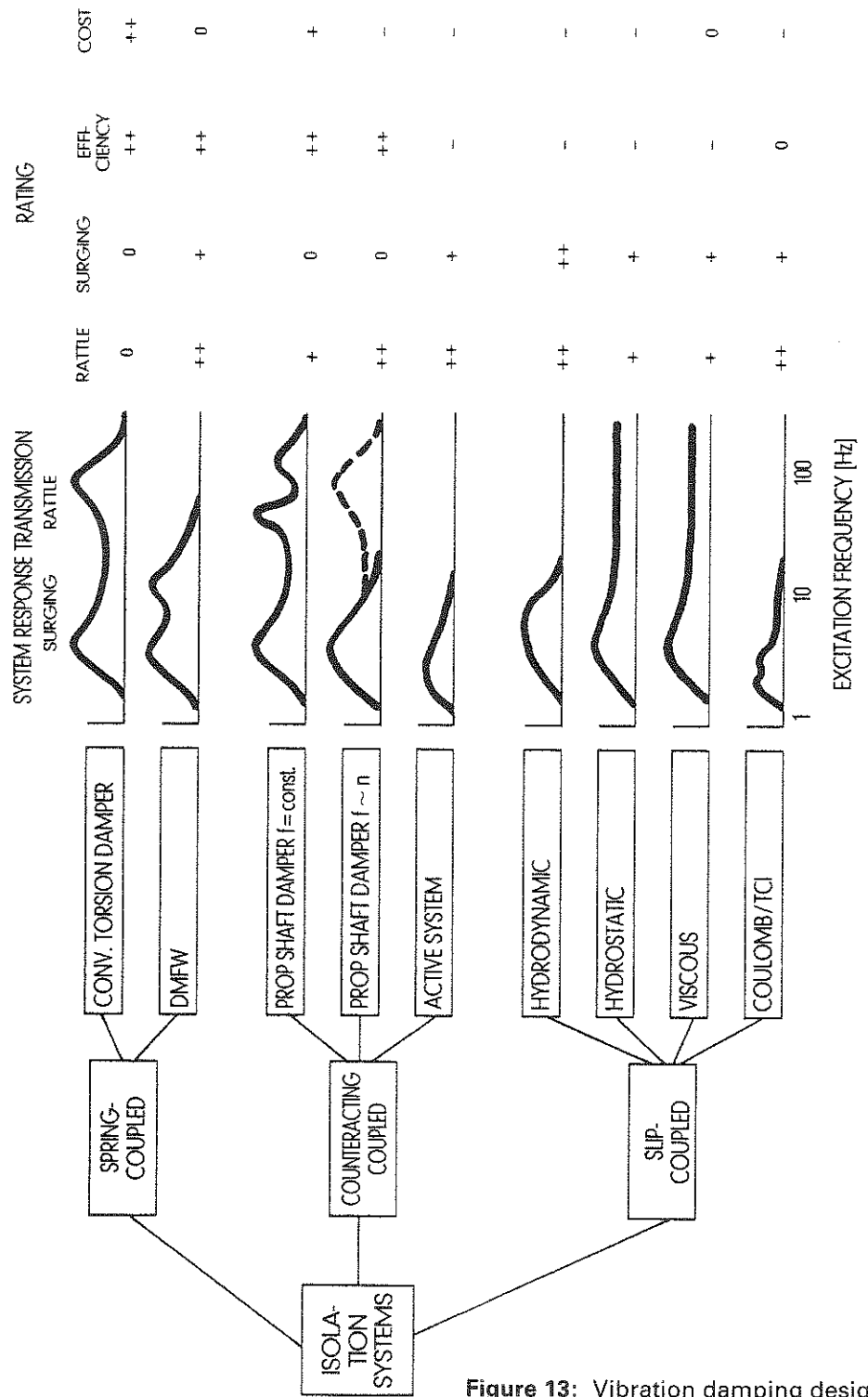


Figure 13: Vibration damping designs

The advantage of the dual mass flywheel lies in the fact that transmission isolation starts at a much lower speed. Moreover, it is possible to improve surging with very flat spring rates and appropriate damping values. All spring-coupled systems have a high degree of efficiency. Minimal losses resulting from damping are insignificant.

For the next major group, the counteracting coupled systems, vibration isolation between the engine and the transmission is not of primary importance. With these systems, a counteracting torque is introduced at the transmission. This torque is designed to neutralize the oscillating torques generated by the engine. Generally speaking, however, prop shaft dampers are attached to the transmission output shaft. They are capable of neutralizing vibration and eliminating rattle, but only for a fixed frequency.

The centrifugal pendulum would provide some improvement in this regard. With this design, the damper frequency is proportional to speed, so an entire order of excitation can be completely canceled out. This solution provides an almost ideal transmitting function. However, other orders are not affected. At the moment, this design poses unsolved problems and is associated with high costs.

Both options, the prop shaft damper and the centrifugal pendulum, are actually passive systems. But truly active, counteracting coupled systems are also conceivable. In such systems, the counteracting torque would not just be an attached, elastic mass, but would instead be generated by an actuator or supplemental motor. An electronic control would generate a counter-phase torque in opposition to the measured transmission acceleration and would then be able to neutralize torsion vibrations completely over a wide frequency range. This design would entail high technical expenditure and would exhibit poor efficiency because of the energy required to operate the extra motor, both of which factors represent definite disadvantages.

To our knowledge, this kind of expensive, active compensation system has not yet been developed for a motor vehicle drive train. Isolated designs have been implemented for suspension systems, machine tools, and structures [15 – 17].

In the case of the third group, the slip-controlled systems, no additional resonance occurs. This is an exceptional advantage, but it must be bought with energy loss.

A comparison shows the advantages of the hydrodynamic torque converter and the electronically controlled friction clutch, particularly at the higher rattle frequencies. Low surging frequencies can be damped with high slip values in all systems.

As already noted with respect to torque control isolation, slip and the associated efficiency loss can be minimized using appropriate characteristic fields. However, the costs for such a system are high.

## **Combined Systems**

None of the systems illustrated in Figure 13 is able to rack up plus points in all categories. However, a skillful combination of systems can be used to counteract weak points. Such combinations can feature either serial or parallel designs. In some cases, individual systems are activated in certain speed ranges.

An example of this kind of hybrid design is the torque converter with a lock-up clutch. At low speeds, the system utilizes the vibration isolating capability of the torque converter. At high speeds, a lock-up clutch with a conventional torsion damper acts parallel to the torque converter to provide complete torque transmission without any slip, while at the same time filtering out vibrations at high excitation frequencies. This arrangement permits the elimination of energy-consuming slip, at least in the high speed range.

For the same reasons, it is advisable to use a standard, serial torsion damper design with torque control isolation. Low excitation frequencies are filtered out via TCI, and the torsion damper takes care of the high frequency components. In this range, the clutch can be locked up to avoid slip.

Figure 14 shows an additional combination option involving elements of both a spring and a slip control system. A hydrostatic pump in a DMFW is situated in series with an elastic component. At first glance this doesn't appear to make much sense, because neither system provides adequate protection against low-frequency surging vibrations, at least not with an acceptable degree of slip. However, we can use the following trick. The pump flow control valve is closed during normal operation and the slip factor is reduced to a minimum of approximately 10 rpm. The elastic torsion damper provides vibration isolation to completely absorb engine irregularity. During tip-ins, for instance when the driver suddenly steps on the gas, pressure builds up in the throttled pump system. This pressure

triggers the flow control valve to open briefly, thus providing for increased slip in order to prevent surging vibrations. Because this valve recloses automatically within a few seconds, the total energy loss is limited.

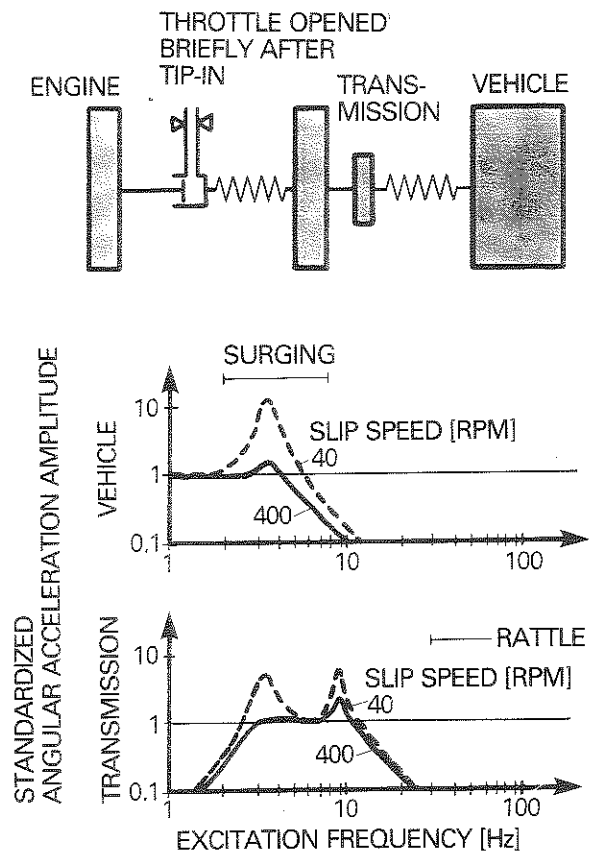


**Figure 14:**  
System response with hydrostatic pump and spring

Figure 15 shows this kind of design. The gear pump is located on the outer diameter, and the serial springs are arranged around the inner diameter. However, this kind of combination is hardly ready for production and may prove to be very expensive to build.

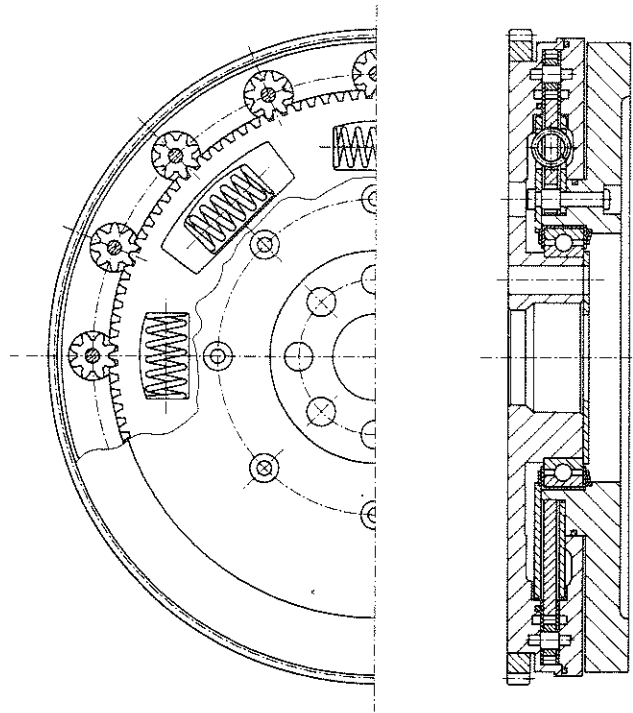


**Figure 15:**  
Dual mass flywheel with serial design featuring a hydrostatic pump and springs

### Summary

Systems for isolating torsional vibrations in motor vehicle drive trains can be divided into three groups:

- spring-coupled systems, for instance conventional torsion dampers and spring-coupled dual mass flywheels
- counteracting systems, for instance prop shaft dampers or centrifugal pendulums
- slip-coupled systems, such as torque converters, torque control isolation or viscous couplings.

In the case of spring-coupled systems, engine excitation is absorbed by torsional elasticity. There is virtually no energy loss involved because the energy stored in the springs is later returned to the system. The additional resonance associated with the energy store can lead to gear rattle. By optimizing the inertial relationships and introducing an extremely reduced

spring rate in association with a modern, long-travel DMFW, we can shift these additional resonance points out of the driving range, thus eliminating gear rattle.

Counteracting systems generate a counter-torque at the transmission. Technically practical prop shaft dampers have a narrow, limited efficiency range and are only capable of improving gear rattle in individual cases.

In the case of slip-coupled systems, engine irregularity is compensated with slip. No resonance can occur between the engine and the transmission. High slip can be used to damp low-frequency surging vibrations effectively. The unavoidable disadvantages include energy loss and high cost.

Consequently, in the future appropriate combinations will be developed joining slip- and spring-coupled systems in which the slip system is only engaged as long as necessary to combat low-frequency vibrations.

#### **Bibliography**

- [1] Jürgens, G. and Fischer, R.  
Vergleich verschiedener Systeme zur Verringerung von Triebstrangschwingungen [Comparison of Various Systems for Decreasing of Drive Train Vibrations], VDI-Berichte Nr. 697 (1988), p. 233
- [2] Schöpf, H-J., Jürgens, G. and Fischer, R.  
Optimierung der Komforteigenschaften des Triebstranges von Mercedes-Benz-Fahrzeugen mit Schaltgetriebe [Optimizing Drive Train Comfort Characteristics in Mercedes Benz Vehicles with Manual Transmissions], Automobiltechnische Zeitschrift 91 (1989), p. 568
- [3] Wilson, W.  
Practical Solution of Torsional Vibration Problems, Chapman & Hall 1963
- [4] Rosean, M.  
Vibration in Mechanical Systems, Springer Verlag
- [5] Klotter, K.  
Technische Schwingungslehre [Technical Vibration Theory], Springer Verlag 1978
- [6] Kammerer, H.  
Die Eigenfrequenzen bei Drehschwingungssystemen mit Fliehkraftpendeln [Natural Frequencies in Torsional Vibration Systems with Centrifugal Pendulums], Dissertation, München 1941

- [7] Kraemer, O.  
Schwingungstilgung durch das Taylor-Pendel [Vibration Damping Using the Taylor Pendulum], VDI-Zeitschrift, Vol. 82, Nr. 45 (1938)
- [8] Schick, W.  
Wirkung und Abstimmung von Fliehkraftpendeln am Mehrzylinderomotor [Effect and Tuning of Centrifugal Pendulums on Multi-cylinder Engines], In.-Archiv, Vol. X, 5. Heft (1939), p. 303
- [9] Ganghoff, P.  
Untersuchung des Fliehkraftpendels als Schwingungstilger am Beispiel eines Fahrzeugantriebsstranges [Study of a Centrifugal Pendulum Used as a Vibration Damper on a Sample Vehicle Drive Train], Studienarbeit, Karlsruhe 1985
- [10] Condray, P. and Guesdon, M.  
Determination of the Transfer Matrix of a Fluid Coupling, ASME Conference on Mechanical Vibration and Noise, Cincinnati, September 1985
- [11] Rohne, E.  
Verhalten von Föttinger-Wandlern bei Laständerungen und Schwingungsvorgängen [Behavior of Hydrodynamic Converters during Tip-in/Back-out and Vibration Phases], Antriebstechnik 11 (1983) Nr. 12, p. 37
- [12] Herberitz, R.  
Untersuchung des dynamischen Verhaltens von Föttinger-Getrieben [Study of the Dynamic Performance of Hydrodynamic Transmissions], Dissertation, Hannover, 1973
- [13] Niikura, Y. and Takemura, T.  
An Analysis of the Torque Transfer Characteristics of Viscous Couplings, JSAE Review Vol 10 (1989), No. 3, p. 30
- [14] Petri, H. and Heidingsfeld, D.  
The Hydraulic Torsion Damper, SAE-Congress, 1989
- [15] Soong, T. and Natke, H.  
From Active Control to Active Structures, VDI-Berichte Nr. 695 (1988), p. 1
- [16] Janocha, H. and Gosebruch, H.  
Aktive Dämpfung dynamischer Wechselwirkungen an Außenrundscheifmaschinen [Active Damping of Dynamic Oscillating Effects on Cylindrical Surface Grinders], VDI-Berichte Nr. 695 (1988), p. 105
- [17] Meller, I.  
Elektronisch gesteuerte Dämpfung im Kraftfahrzeug [Electronically Controlled Damping in Motor Vehicles], VDI- Berichte Nr. 695 (1988) p. 171